NTNU – Trondheim
Norwegian University of
Science and Technology

Once-Through Gas-to-Liquid Process Concept for Offshore Applications

Kristin Dalane

Chemical Engineering and Biotechnology
Submission date: June 2015
Supervisor: Magne Hillestad, IKP

Norwegian University of Science and Technology
Department of Chemical Engineering

Abstract

The worlds energy demand is increasing, and at the same time the amount of easily accessible oil is reduced. Associated gas for most offshore applications are flared or injected in the reservoir due to transportation challenges. A gas-to-liquid (GTL) process for offshore applications could be a solution to make valuable products of the associated and remote natural gas resources.

GTL is a process that converts carbon based feedstock to more valuable liquid products. One of the main technologies used are the Fischer-Tropsch synthesis.

A new process design for a GTL process for offshore applications are proposed. The syngas is produced with an autothermal reformer (ATR) with enriched air as oxidant. The process design is a once-through, to prevent accumulation of nitrogen. Once-through means that no unconverted syngas is recycled in the process. In order to maximize the conversion and production of higher hydrocarbon the Fischer-Tropsch synthesis are staged. Three multitubular fixed bed stages are used with product separation and hydrogen added between each step. Two Fischer-Tropsch reactors in parallel are used for the two first reactor stages. The hydrogen is produced by steam methane reforming in a heat exchanged reformer, where heat needed for reaction is provided from the hot outlet stream from the ATR. The tail gas in the process is used for power production in a gas turbine. The hot effluent gas from the gas turbine is used for pre-heating of the natural gas.

The process design is modelled and optimized with the use of Aspen HYSYS V8.6, with some use of Aspen Custom Modeler and MATLAB programming. The kinetic model used for the Fischer-Trospch reactors are proposed by Todic *et al.* [1, 2], with a product distribution model proposed by Hillestad [3].

There are several parameters in the process that could be optimized. Optimizing in this master thesis are focused on obtaining the maximum production of C_{5+}, which means hydrocarbons with five carbon atoms or more. The optimal distribution of the natural gas in the process was found to be 90% to the autothermal reformer and 10% to the heat exchanged reformer.

With a natural gas feed amount of 120 MMSCF or 6,000 kmole/h the total production in the process are found to be 53.9 tonne/h or approximately 10,000 bbl/day. The carbon efficiency in the process is 57% and the energy efficiency is 45%. The process is self-supported with utilities and produces 36.4 MW of external power and 501 tonne/h of medium pressure steam. The total investments cost for the plant is estimated to 543.7 million$.

Sammendrag

Verdens energibehov er økende, samtidig som mengden av lett tilgjengelig olje ressurser er redusert. Assosiert gass for de fleste offshore applikasjoner fakles eller injisert i reservoaret som følge av utfordringer med transport. En gass-til-væske prosess (GTL) for offshore bruk kan være løsningen for å produsere verdifulle produkter av assosiert gas og natur gass ressurser som ligger langt fra eksisterende infrastruktur.

GTL er en prosess som omdanner karbonbasert råmateriale til mer verdifulle flytende produkter. En av de viktigste teknologiene som brukes er Fischer-Tropsch syntese.

Et nytt prosessdesign for et GTL anlegg til offshore applikasjoner er foreslått. Syntesegassen produseres ved bruk av en autotermisk reformer (ATR) med anriket luft som oksidasjonsmiddel. For å unngå akkumulering av nitrogen i prosessen er en gjennomstrømmning foretrukket. Det betyr at uomsatt syntesegass ikke blir resirkulert i prosessen. For å maksimere omsettningen og produksjon av høyere hydrokarboner er Fischer-Trospch syntesen delt opp i flere steg. Tre multitubular "fixed bed" reaktor steg er brukt, med produkt separasjon og hydrogen tilførsel mellom hvert steg. To Fischer-Tropsch reaktorer er brukt i parallel for de to første reaktortrinnene. Hydrogen blir produsert ved dampreformering av metan i en varmevekslet reformer (HER), hvor nødvendig varme til reaksjonen blir gitt fra den varme ATR utløpsstrømmen. Uomsatte reaktanter blir brukt til kraftproduksjon i en gassturbin. Den varme eksosgassen fra gasturbinene blir brukt til å forvarme naturgassen.

Prosess designet er modellert og optimalisert ved bruk av Aspen HYSYS V8.6, med noe bruk av Aspen Custom Modeler og MATLAB programmering. Den kinetiske modellen brukt for Fischer-Tropsch reaktorene er foreslått av Todic *et al.* [1, 2], med produktfordelings modell foreslått av Hillestad [3].

Det er flere parametre i prosessen som kan optimaliseres. I denne oppgaven har fokuset vært på optimaliseringen for maksimal produksjon av C_{5+}, som betyr hydrokarboner med fem eller flere karbonatomer. Den optimale fordelingen av naturgass føde i prosessen ble funnet til å være 90% til ATR og 10% til HER.

Med en naturgass føde på 120 MMSCF eller 6 000 kmole/h er den totale produksjonen i prosessen 53,9 tonne/h eller ca. 10 000 fat/dag. Karboneffektiviteten i prosessen er 57% og energieffektiviteten er 45%. Prosessen er selvforsynt med hjelpesystemer og produserer 36,4 MW energi til eksport og 501 tonne/h av medium trykk damp. Den totale invisteringskostnaden for prosessen er estimert til 543,7 millioner$

Preface

This report describes my thesis work for my Master of Science degree in Chemical Engineering at the Norwegian University of Science and Technolgy (NTNU). The work has been carried out at the researcher group of Environmental Engineering and Reactor Technology at the Department of Chemical Engineering (IKP) during the spring semester of 2015.

This work consist of modelling, design and optimization of a gas-to-liquid process for offshore applications. The modelling is made mainly with the use of Aspen HYSYS, and partly also Aspen Custom Modeler and MATLAB programming.

I will use the opportunity to thank my supervisor Professor Magne Hillestad for guidance and good advice during this work. Our meetings during the semester have been both inspiring and educational.

Further more, I will thank my two co-supervisors Erling Rytter and PhD student Mohammed Ostadi. Thanks to Erling Rytter for giving good advice during the work, based on industrial experience, and PhD student Mohammed Ostadi for good discussions during the work and for helping me when simulation problems occurred.

I would also like to thank May-Britt Hägg and Arne Linbråthen for providing me with information about a hydrogen selective carbon membrane, Svein G. Norland from Air Product that have given me information about air membranes, and Sandra Winter-Madsen from Haldor Topsøe for information about the autothermal reformer technology.

"*I declare that this is an independent work according to the exam regulations of the Norwegian University of Science and Technology (NTNU).*"

Kristin Dalane
Trondheim, June 2015

Contents

List of Figures

List of Tables

Acronyms

ACCR	Annual Capital Charge Ratio
ASF	Anderson-Schulz-Flory
ASU	Air Separation Unit
ATR	Autothermal Reformer
FPSO	Floating, Production, Storage and Offloading
FT	Fischer-Tropsch
FTS	Fischer-Tropsch Synthesis
GHSV	Gas Hourly Space Velocity
GTL	Gas-to-Liquid
HER	Heat Exchanged Reformer
HI	Heat Integration
HTFT	High Temperature Fischer-Tropsch
ISBL	Inside Battery Limits
LTFT	Low Temperature Fischer-Tropsch
SCR	Steam Carbon Reforming
SMR	Steam Methane Reforming
SRK	Soave-Redlich-Kwong
TIT	Turbine Inlet Temperature
TOT	Turbine Outlet Temperature
WGS	Water Gas Shift

Nomenclature

Chapter 1

C_{i+}	Hydrocarbon chain with i carbon atoms or more

Chapter 2

C_{i+}	Hydrocarbon chain with i carbon atoms or more
CP	Heat capacities
T_{act}	Actual temperature
T^*	Shifted temperature
α	Chain growth probability
ΔH_i	Heat required in interval i
ΔT_{min}	Minimum temperature difference between hot and cold stream
ΔT_i	Interval temperature difference
w_i	Weight fraction of component i

Chapter 3

a	Area per volume
C_i	Hydrocarbon chain with i carbon atoms
C_{i+}	Hydrocarbon chain with i carbon atoms or more
J_i	Flux of component i
k_i	Reaction rate constant
K_i	Equilibrium constant
n_i	Molar flow of component i
p_i	Partial pressure of component i
P	Pressure
y_i, x_i	Mole fraction of component i
α_1,α_2,α_M	Growth probability factors
ν	Stoichiometric coefficient

Chapter 4

C	Total ISBL cost
C_{fc}	Fixed capital cost
C_{i+}	Hydrocarbon chain with i carbon atoms or more
C_{inv}	Total membrane cost
C_y	Annual capital charge
OS	Offsite
D	Diameter
$D\&E$	Design and engineering
i	Interest rate
n	Membrane lifetime
P	Pressure
$T_{average}$	Average radial temperature
T_{cw}	Cooling water temperature
T_{max}	Maximum radial temperature
U	Overall heat transfer coefficient
X	Contingency
α	Chain growth probability
ΔT	Temperature difference
ΔT_{min}	Minimum temperature difference between hot and cold stream
λ	Effective radial conductivity

Chapter 5

C_{i+}	Hydrocarbon chain with i carbon atoms or more

Appendix B

n	Number of mole

P	Pressure
R	Gas constant
T	Temperature
V	Volume

Appendix E

$Im\%$	Imbalance
$\dot{m}$	Mass flow
Q	Total heat flow
$\dot{Q}$	Heat flow in streams
W	Power

Appendix F

E	Thermal energy
P	Mechanical energy
T	Temperature
α_{iH}	Upper limit for growth probability factor i
α_{iL}	Lower limit for growth probability factor i
C_{i+}	Hydrocarbon chain with i carbon atoms or more
ΔH_c	Heat of combustion
η	Carnot efficiency

Appendix G

CP	Heat capacities
ΔH_i	Heat required in interval i
ΔT_{min}	Minimum temperature difference between hot and cold stream
ΔT_i	Interval temperature difference

Appendix H

a	Membrane packing density
A	Heat transfer area
A_s	Surface area
A_c	Cross section area
D	Diameter
f	Fraction of empty space
F_t	Correction factor
H	Height
H_h	Height of vessel head
h_v	Liquid height
m	Mass
$\dot{m}$	Mass flow

N	Number of reactor tubes
N	Number of membrane units
N_t	Number of membrane tubes
$\dot{n}$	Molar flow
P	Pressure
Q	Heat transferred per unit time
R	Correction factor parameters
S	Allowable stress
S	Correction factor parameters
$S.F$	Straight flange
t_w	Wall thickness
U	Overall heat transfer coefficient
u_s	Settling velocity
V	Volume
$\dot{V}$	Volumetric flow
ρ	Density
τ	Residence time
ΔT_{lm}	Logarithmic mean temperature
ΔT_m	Mean temperature difference

Appendix I

a	Cost constant
b	Cost constant
C_e	Purchased equipment cost
f_{el}	Cost factor electrical
f_{er}	Cost factor equipment erection
f_i	Cost factor instrument and control
f_l	Cost factor lagging and paint
f_m	Cost factor material
f_p	Cost factor piping
I	Cost index
L	Length
n	Cost constant
N_t	Number of reactor tubes
S	Size cost parameter

Appendix J

T_R	Temperature at tube wall
R	Radius of reactor tubes
U'	Heat transfer through the wall
T_{cw}	Temperature of cooling water
$T_{average}$	Average radial temperature

T_{max}	Maximum radial temperature
λ	Effective radial conductivity
D	Diameter

Chapter 1

Introduction

Gas-to-liquid (GTL) is a process that converts natural gas or other gaseous carbon based feedstock to more valuable liquid products. One of the main technologies used are the Fischer-Tropsch synthesis (FTS). This process is named after the German coal researchers, F. Fischer and H. Tropsch. They discovered in 1923 that synthesis gas (syngas) can be converted to a large range of hydrocarbons by the use of a catalyst [4].

The worlds energy demand is increasing, while the amount of easily accessible oil is reduced. As a consequence investigations on untapped resources, like associated and stranded gas reserves, which currently are not used due to technical or economical reasons are increased. The main challenge for remote natural gas is transportation, and therefore associated gas for most offshore applications are flared or injected in the reservoir. The regulations of flaring has over time become more stringent. There are several reasons for this like protecting the environment and also the fact that much energy is lost by flaring big amounts of gas [5, 6]. A GTL process for offshore applications could be a solution to make valuable products of the associated and remote natural gas resources. Then existing infrastructures could be used for the transportation of the produced hydrocarbon products. If the GTL plant is integrated with oil production, the GTL products could be blended with the conventional oil before shipping.

There are several aspects that needs to be considered when evaluating a GTL process with a floating production, storage and offloading vessel (FPSO). The equipment used needs to be robust for marine motion, with respect to inclination and inertia effect. This can be a problem with the use of high columns with liquid inventory. The design need to be compact as there are limitations in space and weight. The use of a cryogenic air separation unit (ASU) to produce pure oxygen for the syngas production may be problematic on a FPSO due to safety challenges. Pure oxygen in the vicinity of hydrocarbon has fire and explosion possibilities. At last the process need to be autonomous in the sense that all utilities are supplied on-board.

Investigation on a GTL-FPSO has been done and is reported in the literature. Kim *et al.* [7] investigated a GTL-FPSO plant where syngas is produced with steam carbon reforming (SCR) technology. When using SCR the need of pure oxygen is eliminated due to external heating. In addition, this technology is capable to handles natural gas feeds with high CO_2 content. For the

FTS a slurry-phase reactor was used due to small size and weight, even though it is less robust for marine motion compared to the multitubular fixed bed. A simple once-through GTL-FPSO process was evaluated by Van Loenhout *et al.* [8]. In their process the syngas is produced with an air-blown autothermal reformer (ATR) and for the FTS two three-phase slurry reactor in series were used. The use of air-blown ATR will reduce the capital cost and space for the syngas production due to the elimination of the ASU. However, the concentration of inert in the system would be increased and the downstream equipments need to be bigger. Masanobu *et al.* [9] used an oxygen-blown ATR, which requires an ASU onboard, and can give safety challenges. Fonseca *et al.* [10] considered syngas production with the use of steam methane reforming (SMR). Both the SMR reactor and the Fischer-Tropsch (FT) reactors considered in this process design were catalytic compact mini-channel reactors. On of the pioneers of commercializing microchannel technology are Velocy. They proposed the use of microchannel technology on a FPSO [11].

For the process design in this master thesis a multitubular fixed bed reactor is used. The result from this work is used in a paper to compare with the use of a microchannel fixed bed reactor, performed by Ostadi. The paper is planed submitted to Fuel and Processing Technology (Draft version in Appendix A). The use of a fixed bed reactor is decided due to the robustness for marine motions.

The production of syngas is the most energy intensive part of the GTL process and accounts for around half of the plant capital cost. This is due to the high cost of an ASU needed for an oxygen-blown ATR [12, 13]. However, the ATR is preferred for syngas production for GTL application as it gives a syngas with H_2/CO ratio in the favourable region [14]. In the process design proposed in this master thesis a ATR is used for the production of syngas. Enriched air is used as oxygen feed to the ATR. The use of enriched air instead of normal air reduces the inert concentration in the syngas and the size of the downstream equipment. The use of enriched air instead of pure oxygen is due to safety, and the elimination of having an ASU onboard. The syngas production cost for this process will be reduced as no ASU is needed.

One important factor in the FTS are the H_2/CO ratio, as it effects the reaction rate and the selectivity towards higher hydrocarbons. A reduction in H_2/CO ratio gives a reduced reaction rate, however, the selectivity towards higher hydrocarbons is increased [15]. With a understoichiometric or close to stoichiometric H_2/CO ratio in the feed to the FT reactor the ratio is decreased along the reactor. As the consumption ratio is around 2, to convert as much as possible of the CO hydrogen should be added [16]. Evaluation of staging the reactor with addition of hydrogen has been evaluated, indicating a higher C_{5+} production [15–18]. In this process several FT reactors is used with product separation and addition of hydrogen between each reactor.

The hydrogen used in the proposed process design is produced with SMR in a heat exchanged reformer (HER), followed by a water gas shift (WGS) reactor and a hydrogen selective carbon membrane to separate H_2 from CO_2. A HER is a heat-exchanged based steam reformer with catalyst filled tubes for SMR. The possibility of using a heat exchanged reformer for syngas

production in parallel or series with an ATR is reported several places in literature [12, 19–22]. The main challenge with the use of a HER is the risk of metal-dusting corrosion [12]. However, many of this corrosion problems is resolved. In the proposed process design in addition to hydrogen production, the HER provides efficient heat recovery from the ATR outlet and eliminates the need for a waste heat boiler.

The proposed capacity for the GTL plant is to utilize 120 MMSCFD (million standard cubic feet per day) of natural gas, giving a production of hydrocarbon of about 53 tonne/h or approximately 10,000 bbl/day. In the process due to the use of enriched air and to avoid accumulation of nitrogen in the system the design is once-through. The tail gas from the process is used in a gas turbine to produced power needed in the process. For some applications the capacity of this process may be to big and need to be scaled down.

1.1 Objective

The goal for this master thesis is to evaluate a new GTL process design for offshore applications. Different parameters in the process should be optimized, where the main goal is to achieving highest possible C_{5+} production. C_{5+} indicates hydrocarbons with five or more carbon atoms. In addition to decide optimal process conditions for the process heat integration should be included to increase the energy efficiency of the plant. Finally, the size of the equipment and investment cost for the plant should be evaluated.

1.2 Declaration of Contribution

The process structure for the new design was proposed by my supervisor Professor Hillestad [23]. The Fischer-Tropsch reactor and the heat exchanger reformer are both programmed in Aspen Custom Modeler and implemented to Aspen HYSYS. These models are made by respectively Ostadi [24] and Falkenberg [25]. All the other work reported in this master thesis, is what I have done.

My main contributions are:

1. Made a simulation model of the process design in the simulation tool Aspen HYSYS V8.6.

2. Made a MATLAB model for the hydrogen selective carbon membrane, where the results are implemented in the HYSYS simulation.

3. Evaluated the process to find optimal operation conditions, for different parameters.

4. Evaluated some of the assumptions made for the process.

5. Contributed to a paper (Appendix A) planed submitted to Fuel and Processing Technology. My contribution for this article are;
   (a) All the results for the process design with use of multitubular fixed bed reactor.
   (b) My HYSYS model has been used in the paper (first author have had full access to all simulation files).
   (c) Discussion related to structure and content of paper.
   (d) Discussion related to the documented findings.
   (e) Provided all information and results about the two membranes used in the process design.

1.3 Thesis Structure

Chapter 2 gives a detailed description of the different process steps in a GTL process and the reason for using specific equipments. This provides the background information to understand the different steps in a GTL process with information about what reactions that takes place.

Chapter 3 gives information about how the HYSYS simulation was performed, with the given input parameters. The reactor models programmed in Aspen Custom Modeler an MATLAB will also be explained in this chapter.

Chapter 4 gives the result from the simulation of the final process design, together with the equipment size and investment cost. The evaluation of the different parameters and background for the chosen values are given. The last part of this chapter includes an evaluation of some of the assumptions used in the process.

Chapter 5 gives a conclusion to the work performed and recommendations for further work.

Chapter 2

Gas-to-Liquid Process Steps

In this chapter a more detailed description of the GTL plant is given and the reason for using specific equipments is presented. The process design consist of three main parts; synthesis gas (syngas) production, hydrogen production, and Fischer-Tropsch syntesis (FTS). Background information for each of the process parts are given, with equipments used and the reactions that takes place. If several possibilities are given, the chosen solution for the proposed process design are stated at the end of the section.

A detailed block diagram of a the GTL plant is given in Figure 2.1. In the following section a description of the most important features of each of the steps in the process will be given.

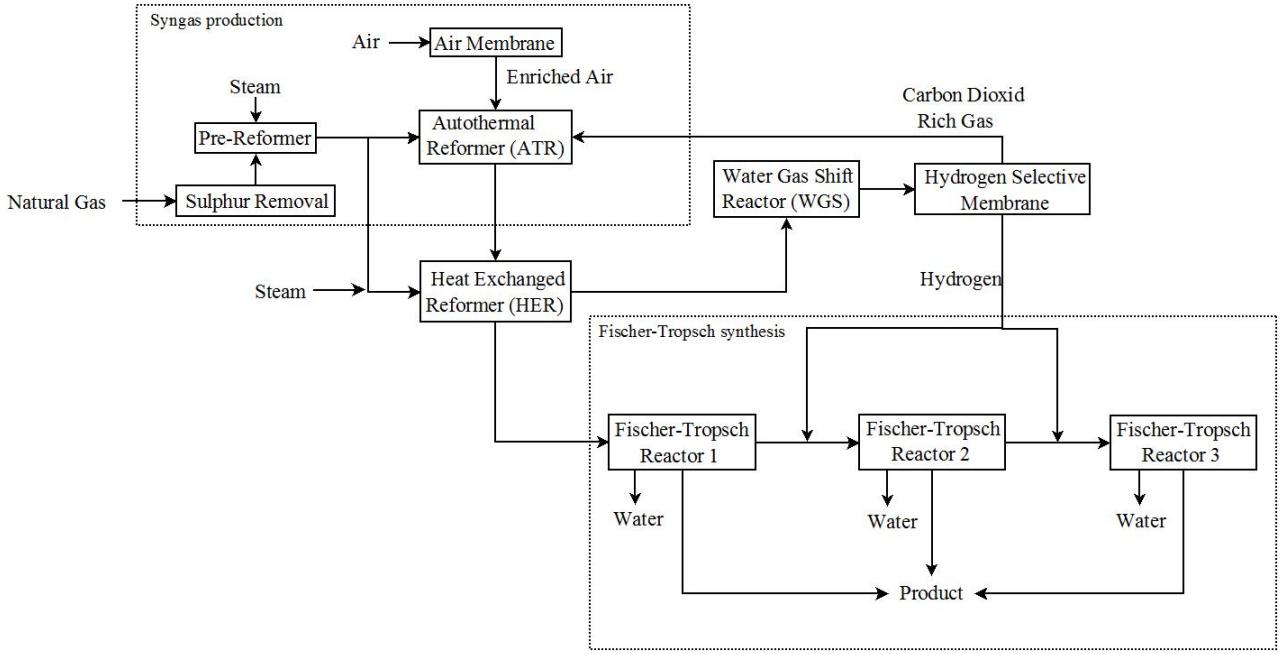

Figure 2.1: An overview over the different steps in the proposed GTL process design.

2.1 Syngas Production

The main step in syngas production is; sulphur removal, adiabatic pre-reforming and auto thermal reforming (ATR). Syngas can be produced from any hydrocarbon feedstock, ranging from natural gas to coal. Which feedstock to be used is dependent on price and availability. For GTL applications the main feedstock is natural gas [26].

A GTL-FPSO gives the possibility to use the associated gas and remote natural gas reserves as feedstock for the syngas production. By using associated gas it is possible to make valuable products from gas that elsewhere is flared or injected in the reservoir.

2.1.1 Sulphur Removal

The first step in the syngas production is sulphur removal. This is an important step to protect the gas reforming nickel-based catalyst. Sulphur- and halogen-containing compounds can block active site and poison the catalyst. The removal is performed in two steps; hydrotrating and quantitatively removing.

Hydrotrating is a process where hydrogen is used to brake the bonds between C-S and C-X (X=halogen) making hydrogen sulphide (H_2S) and hydrogen acid (HX). These components are then quantitatively removed [4, 27]. Some examples of mechanisms used for this process are adsorption on activated carbon, reaction with zinc oxide, or scrubbing with a solvent. After sulphur-removal the sulphur content in the feed should not exceed 1 ppm [4]

In this master thesis the process is considered to start after the sulphur removal part. Sulphur removal is therefore not included in the simulation and calculations and it is assumed a sulphur free feed to the process.

2.1.2 Pre-reformer

The pre-reformer is an adiabatic catalytic fixed bed reactor with a highly active steam reforming catalyst, usual a nickel based catalyst [28]. The natural gas feed mainly consist of methane, but it could also include small amounts of higher hydrocarbons. Higher hydrocarbons could easily form carbon (reaction 2.1.1) at higher reforming temperatures. To prevent this it is recommended to include a pre-reformer [27].

$$\mathrm{C}_n\mathrm{H}_{2n+2} \rightarrow n\mathrm{C} + (n+1)\,\mathrm{H}_2 \tag{2.1.1}$$

Before entering the pre-reformer the feed is mixed with steam and preheated to around 500 °C. In the pre-reformer heavier hydrocarbons is converted into a mixture of methane and carbon dioxide according to reaction 2.1.2 [27, 29].

$$\mathrm{C}_n\mathrm{H}_{2n+2} + \frac{1}{2}(n-1)\mathrm{H}_2\mathrm{O} \rightarrow \frac{1}{4}(3n+1)\mathrm{CH}_4 + \frac{1}{4}(n-1)\mathrm{CO}_2 \tag{2.1.2}$$

The reforming reaction are endothermic and are usually followed by the exothermic methanation (2.1.3), and water gas shift (WGS) reaction (2.1.4) [27, 29].

$$3H_2 + CO \leftrightarrow CH_4 + H_2O \tag{2.1.3}$$
$$CO + H_2O \leftrightarrow H_2 + CO_2 \tag{2.1.4}$$

The implementation of a pre-reformer allows a higher pre-heat temperature to the ATR. A higher feed temperature to the ATR gives a reduction of oxygen consumption and increases the production capacity [28, 29]. After the higher hydrocarbons are removed the stream is pre-heated to 650°C.

The outlet flow of the pre-reformer is divided into two streams with different flow amount. One stream is mixed with a CO_2 rich stream, recycle from the process, and fed to the ATR. The other stream is mixed with steam and fed to the heat exchanged reformer (HER).

2.1.3 Autothermal Reforming

The ATR is the main part of the syngas production, and a sketch is shown in Figure 2.2. It consist of a burner, a combustion chamber and a catalytic bed placed in a refractory-lined pressure vessel [28].

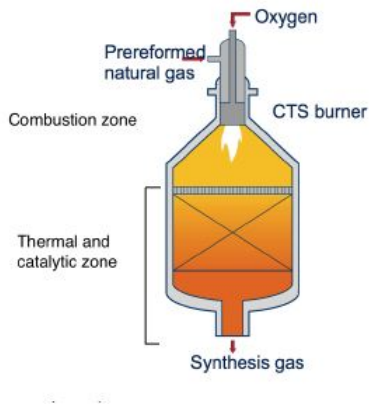

Figure 2.2: Sketch of an autothermal reformer (ATR) with markings for the combustion zone and thermal and catalytic zone [30].

In the combustion chamber the feed reacts with oxygen and steam in a sub-stoichiometric flame according to reaction 2.1.5 [4].

$$CH_4 + \frac{3}{2}O_2 \rightarrow CO + 2H_2O \tag{2.1.5}$$

In the catalytic bed in the thermal and catalytic zone the feed is catalytic reformed according to reaction 2.1.6 and 2.1.7 [28]. A nickel supported catalyst is used as it is stable at the high

temperature and steam partial pressure that occur in the ATR. The composition of the syngas is determined by the thermodynamic equilibrium [31]. The oxidation is exothermic and provides heat to the endothermic reforming reactions [4].

$$CH_4 + H_2O \leftrightarrow CO + 3H_2 \tag{2.1.6}$$

$$CO + H_2O \leftrightarrow H_2 + CO_2 \tag{2.1.7}$$

The steam to carbon ratio (S/C) is important both in the pre-reformer and in the ATR. In the pre-reformer it is important to prevent carbon formation and in the ATR it is to prevent soot formation [32]. A steam to carbon ratio of 0.6 is commercialised by Holdor Topsøe [12]. For FT applications the desired H_2/CO ratio in the syngas is about 2. With the use of an ATR this low value are only achieved with a very low S/C value. However, a low S/C ratio increase the risk for soot formation in the ATR and carbon formation in the pre-reformer. Operation with a lower S/C ratio has been investigated, however, it is not industrially proven [31,32]. With higher values of S/C the best way to reached the wanted composition is to recycle CO_2. According to WGS reaction (2.1.7) introduction of CO_2 shifts the reaction towards left giving an increased production of H_2O and CO. This will give more CO in the syngas and less H_2 giving a lower H_2/CO ratio. It also gives CO_2 reforming or "dry reforming", that follow reaction 2.1.8 [4].

$$CH_4 + CO_2 \leftrightarrow 2CO + 2H_2 \tag{2.1.8}$$

The major types of ATR are air-blown or oxygen-blown. Air-blown ATR is only possible in once-through processes due to high accumulation of nitrogen in the system. The use of air will also increase the downstream equipment and the power consumption will be increased due to a higher volume flow with a large fraction of inert [14]. For an oxygen-blown ATR pure oxygen is needed, which requires an air separation unit (ASU), which is the main cost for the syngas production [14]. In addition to large cost and space required for an ASU the use of pure oxygen on a FPSO can be a safety challenge, due to fire and explosion possibilities.

For the proposed process design it is decided to use enriched air as oxidant to the ATR. This is decided to keep downstream equipment size low and respect safety challenges. A kinetic study of the FTS with nitrogen rich syngas indicates that nitrogen only dilutes the syngas and has no influence on the kinetic as long as the partial pressure of carbon monoxide and hydrogen are kept constant [33].

2.1.4 Air Membrane

To produce enriched-air a nitrogen selective polysulphone PRISM membrane separator from Air Products were considered. The membrane produces a permeate with a high purity of nitrogen and gives enriched-air in the retentate. Permeate is the flow that passes through the membrane, while retentate is what is retained.

This type of membrane exist with many different feed capacities. The oxygen content of the enriched-air is decided based on what unit is used and the operating conditions, as feed pressure

and permeate purity, for the membrane.

The lifetime of the membrane is set to 10 years with a capacity reduction of around 2% per year. The reduction in capacity is compensated by increased feed temperature [34].

2.1.5 Other Alternatives

There are several possible syngas production processes, like catalytic steam methane reforming (SMR) and partial oxidation. The different process makes syngas with different compositions and H_2/CO ratio. And for the FTS it is required to have a ratio of about 2.

In SMR, methane and steam are catalytically converted to a mixture of hydrogen, carbon dioxide and carbon monoxide. Due to high stability of methane both a high temperature and a nickel-based catalyst is required for the endothermic reforming reaction (2.1.6) to occur. [4,27]. In this process no oxygen is needed and an air separation unit (ASU) would not be required, which is good according to cost and space. For the use on a FPSO it is also favourable due to safety challenges with the use of pure oxygen.

Another alternative is partial oxidation. In this process methane and oxygen reacts exothermic to a mixture of hydrogen, carbon dioxide and carbon monoxide without the use of catalyst.

Howevere, the syngas produced from SMR has a H_2/CO ratio much higher than what is required for the FTS, and the ratio from partial oxidation has a lower value [26]. As non of this methods gives the required ratio, it is more favourable to use an ATR where partial oxidation is combined with catalytic reforming. Due to the high H_2/CO ratio, from SMR it is an advantage to use this process for hydrogen production.

2.2 Hydrogen Production

Hydrogen is needed in several steps of the process. It is needed in the sulphur removal part (which is not included in this master thesis), as feed between the Fischer-Tropsch reactors, and for hydrocracking of the wax product before transportation. However, the amount of H_2 needed to upgrading in this process is much less than what would have been required if a full upgrading unit was included.

With a near stoichiometric or under-stoichiometric H_2/CO ratio in the feed to the FT reactors the ratio will decrease along the reactor. If the ratio is over stoichiometric the ratio will increase along the reactor. The stoichiometric consumption H_2/CO ratio can be calculated as described by Hillestad [3]. A syngas feed to the FT reactor with a low H_2/CO gives a reduction in reaction rate, however, it increase the selectivity to C_{5+} products. To keep the decreasing ratio to the same value at each reactor inlet H_2 needs to be added. Process design with several reactor steps and distribution of hydrogen has been evaluated an indicates higher production of C_{5+}

products [16–18]

2.2.1 Heat Exchanged Reformer

To produce the hydrogen a heat exchanged reformer (HER) is used, which is a compact alternative to the fired steam reformer. There are several other name used for this compact convective steam reformer, some names are; gas heated reformer, reforming exchanger, and compact reformer.

The design of the HER is similar to a heat exchanger, illustrated in Figure 2.3.

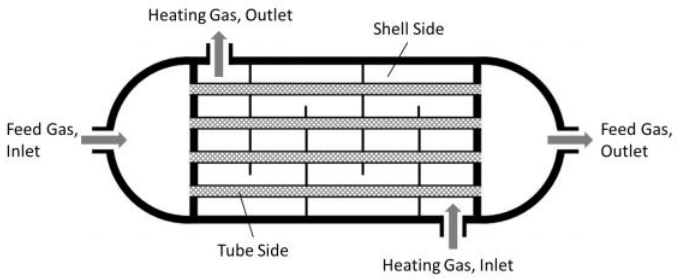

Figure 2.3: An illustration of the heat exchange reformer (HER) [25].

The SMR takes place in the catalyst filled tubes, according to reaction 2.1.6 and 2.1.7 [19–22]. As earlier mentioned is the H_2/CO ratio in the syngas produced from SMR high. It is therefore favourable to use SMR for hydrogen production.

The reaction is endothermic and the heat required for the reforming is provided from the hot outlet stream from the ATR. Apart from being a hydrogen generator, the HER reactor provides efficient heat integration and avoids using a waste heat boiler after the ATR.

There are two main challenges with the use of a HER; coke formation that deactivates the catalyst and metal dusting [12, 35]. To prevent these challenges a high steam to carbon ratio is needed. In this process the steam to carbon ratio in the feed to the HER is 2.

2.2.2 Water Gas Shift Reactor

The outlet of the HER is cooled to 350°C before entering the high temperature water gas shift (WGS) reaction. The reactor operating temperature variates in the range of 310-450°C, however, to prevent catalyst damage due to high temperature the inlet temperature are usually around 350°C [36]. The WGS reactor is a fixed bed reactor with catalyst based on Fe_2O_3-Cr_2O_3 [27]. In the WGS reactor CO reacts with H_2O to produce CO_2 and H_2 according to

equation 2.1.7. This is done to convert as much as possible of the CO.

The flow from the WGS reactor, mainly containing H_2, CO_2 and H_2O, is cooled down to 30°C and water is knocked out before it enters the membrane.

2.2.3 Hydrogen Selective Membrane

The hydrogen selective membrane considered in the process is a molecular sieve carbon membrane. The membrane unit consist of ceramic tubes with a carbon membrane surface and tailored pores with a size so only H_2 passes though the membrane. The membrane is design with counter-current flow, and to keep the H_2 flow as clean as possible no sweep gas is used. The membrane used in the design is not a commercialised membrane [37].

2.3 Fischer-Tropsch Synthesis

After the syngas is produced it is cooled down to knock out water before it enters the FTS. In the FTS syngas is converted to long chained hydrocarbons, syntetic crude oil. The syngas is converted to alkanes and alkenes with hydrogenation according to reaction 2.3.1-2.3.2 [38]

$$n\mathrm{CO} + (2n+1)\mathrm{H_2} \rightarrow \mathrm{C}_n\mathrm{H}_{2n+2} + n\mathrm{H_2O} \tag{2.3.1}$$

$$n\mathrm{CO} + (2n)\mathrm{H_2} \rightarrow \mathrm{C}_n\mathrm{H}_{2n} + n\mathrm{H_2O} \tag{2.3.2}$$

An illustration of the chain growth of the hydrocarbons without considering reaction mechanism is given in Figure 2.4. α is the growth probability, while $1-\alpha$ is the probability for chain termination.

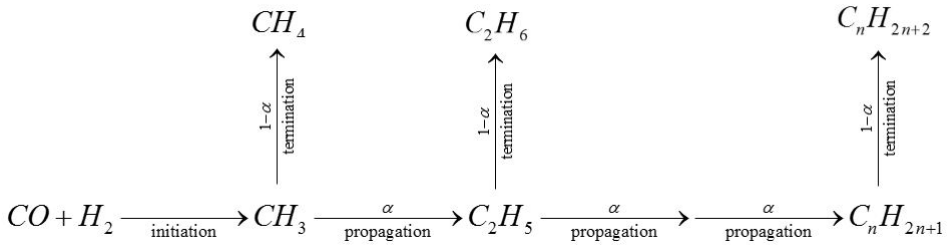

Figure 2.4: Chain growth mechanism for Fischer-Tropsch synthesis, with Anderson-Schulz-Flory (ASF) distribution.

The product from the FTS has a large range from methane to heavy waxes, depending on operation condition and catalyst. The distribution of the products can be explained with the statistic model, called Anderson-Schulz-Flory (ASF) distribution [3, 38], given in equation 2.3.3.

$$w_i = i(1-\alpha)^2\alpha^{i-1} \tag{2.3.3}$$

where w_i is the weight fraction and i is the number of carbon.

An illustration of the product selectivity as a function of the chain growth probability factor, α, is given in Figure 2.5 [4, 38, 39].

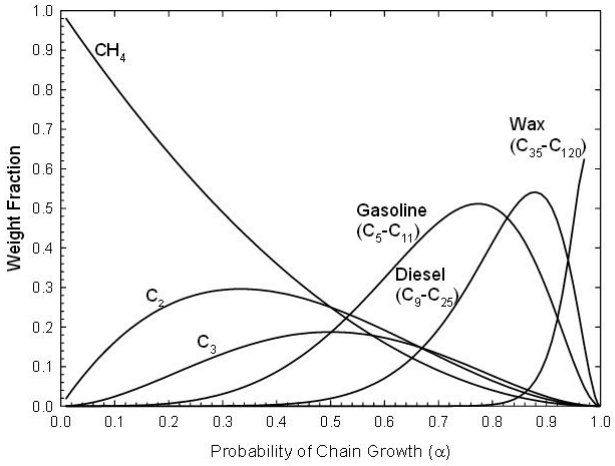

Figure 2.5: Anderson-Schulz-Flory (ASF) Fischer-Tropsch product selectivity as a function of the chain growth probability factor α [39].

However, there are some deviation from this model, probably related to the difficulty to find an exact FTS mechanism. The actually methane selectivity in the process is usually higher than predicted from the ASF. And the ethylene selectivity is predicted to a higher value [27]. More information about the kinetic and product distribution used in this master thesis is given in section 3.2.1.

The chain growth probability factor, α, is dependent on operation conditions like temperature, pressure, and H_2/CO ratio. [4, 38]. An increase in H_2/CO ratio will increase the probability factor and decrease the selectivity towards higher hydrocarbon. If the temperature is increased the α value will be reduced and the selectivity toward lower hydrocarbons is increased [4].

There are three main reactor types used for the FTS; fixed bed, slurry-phase and fluidized bed. For low temperature Fischer-Tropsch synthesis (LTFT) the fixed bed and slurry-phase reactors are most used (a comparison is given in Table 2.1), while fluidized bed is used at high temperature (HTFT). An important factor for the design of the reactor is heat removal due to the exothermic reaction. The operating temperature effects the FTS product, as a higher temperature will lead to chain termination. The main product from HTFT is gasoline and chemicals, while from LTFT the product is wax [27,38]. For GTL processes where the goal is to have high production of C_{5+}, the FTS is at low temperature.

Table 2.1: Comparison of the multitubular fixed bed and the slurry phase reactor.

	Multitubular fixed bed	Slurry phase
Catalyst location	Placed in tubes	Dispersed in liquid
Catalyst replacement	Batch	In operation
Product separation	No need for separation of wax and catalyst	Need separation of wax and catalyst
Heat removal	Through the tube walls	Cooling coils
Temperature	Axial and radial temperature gradients	Well mixed, almost isothermally

When selecting reactor type for a GTL-FPSO process it is important to consider robustness to marine motion, with respect to inclination and inertia effect. The reactor chosen for the proposed process is therefore a fixed bed reactor. Two different types of fixed bed reactors can be used; multitubular and microchannel. In this thesis the multitubular fixed bed reactor is used.

The main catalyst used for FTS are iron (Fe) and cobalt (Co) catalyst. Iron is used for HTFT, however, both the catalysts can be used for LTFT. Cobalt catalyst are more active than the iron catalyst giving a larger chain growth probability. An important difference between the cobalt and iron catalyst is that cobalt catalyst do not promote WGS reactions. Cobalt catalyst is therefore operating at higher H_2/CO ratios than the iron catalyst. This makes cobalt suitable for syngas production from natural gas. While iron is more suitable for processes with syngas obtained form coal gasification. [4, 27]. Based on this the use of cobalt catalyst is chosen for the process in this master thesis.

The FT reactor has two outlet streams; one liquid stream and one vapour stream. The liquid stream consist mainly of wax, while the vapour stream consist of lighter syncrude components and unconverted syngas. The vapour stream is cooled down, and sent to a three phase separator where light syncrude is separated from water and tail gas [27].

2.4 Product Upgrading

For GTL plant onshore wax and cold condensate is further treated to produce high quality products. For an offshore application a fully upgrading of the product would not be included. The FT products would be shipped as feed to a refinery, where upgrading would take place. To stabilize the products for shipping some upgrading may be needed. This upgrading is done with hydrocracking, which requires some hydrogen.

In this master thesis the process is evaluated from sulphur free natural gas to FT products. The upgrading and stabilizing of the products are not included in the simulation and calculations.

2.5 Heat Integration

Heat integration is a way to improve the energy efficiency of a process by recovering available heat. In heat integration available energy in high-temperature process streams are used to heat up cold streams. To evaluate possible external energy savings for the process a heat integration network must be designed. The most commonly used method for designing a heat integration network is to use the "pinch-analysis". For the analysis it is required to decide a minimum temperature difference between the hot and cold streams, ΔT_{min}. For the design to be functional a temperature of 10°C or higher is required [40, 41].

For the hot and the cold streams included in the heat integration network the temperature can be plotted as a function of enthalpy (H) also called composite curve. Usually the minimum temperature difference for a network only occurs at one point in the composite curve. This point is called the heat recovery pinch and divides the system in two distinct thermodynamic regions. The region above pinch is considered as a heat sink with external heat. While the region below is considered as a heat source with external cooling. The composite curve can be used to graphically evaluate the heat recovery pinch. One method to calculated the heat recovery pinch temperature without the use of graphically illustrations is called "The Problem Table Algorithm" [40, 41]. The method follows the steps given below;

1. The actual temperature (T_{act}) is converted to shifted temperatures (T^*) by adding $\Delta T_{min}/2$ to the cold streams and subtracting $\Delta T_{min}/2$ from the hot streams.

2. Arrange the different temperatures in order. If several stream has the same temperature it is only given ones.

3. Calculate the energy balance for each heat interval from:

$$\Delta H_i = \left[\sum CP_C - \sum CP_H\right] \Delta T_i$$

   where ΔH_i is the heat required in interval i, CP is the heat capacities for the hot (H) and the cold (C) streams, and ΔT_i is the interval temperature difference.

4. Cascade the heat surplus from one interval to the next down the column of temperature intervals. Cascading the heat from one interval to another implies that the given heat amount can be transferred from the hot to the cold streams in the given temperature interval.

5. Introduce the smallest amount of external heat needed to the top of the cascade to eliminate negative values.

The heat recovery pinch temperature occurs where the heat flow in the cascade is zero. To make the heat integration network design evaluation from pinch is done. To make sure that the minimum temperature difference is maintained the pinch heat exchangers need to fulfil the given heat capacities criteria given below [40, 41].

$$\text{Above pinch:} CP_H \leq CP_C$$

$$\text{Below pinch:} CP_H \geq CP_C$$

Some heat integration network may not have a heat recovery pinch to divide the process into two parts. In these cases only one hot or cold utility is needed. This type of problem is called threshold problem. To design the heat integration network for a threshold problem it is normal to start in the most constrained part.

For a process with multiple hot and cold streams the heat integration design is more complex and several network design could be feasible. For the heat integration network for a GTL-FPSO plant it is important to achieve large temperature driving forces, as this reduces the heat transfer area needed.

Chapter 3

Simulation and Modelling

This chapter will give information about how the simulation was performed and how different process equipments was modelled. First the HYSYS model will be explained and the given input parameters will be presented. Some of the units in the simulations are programmed with the use of Aspen Custom Modeler and MATLAB. After the HYSYS model is presented the modelling of these units will be described. At the end, information about the utility systems used for the process are given. Only the input values for the simulation are given in this chapter. All the results are given in Chapter 4.

The simulations of the GTL plant were performed using Aspen HYSYS V8.6. Chemical properties were provided by Aspen properties and Soave-Redlich-Kwong (SRK) equation of state was used to calculate thermodynamic properties.

Assumptions and parameters used in the process design are decided in collaboration with my supervisor Professor Hillestad [23].

3.1 HYSYS Simulation

In this section information of how the process was modelled in Aspen HYSYS are given, with the given input parameters (Table 3.1 and Table 3.2). A flow sheet of the process is given in Figure 3.1, and a picture of the simulation flow sheet is given in Appendix B.

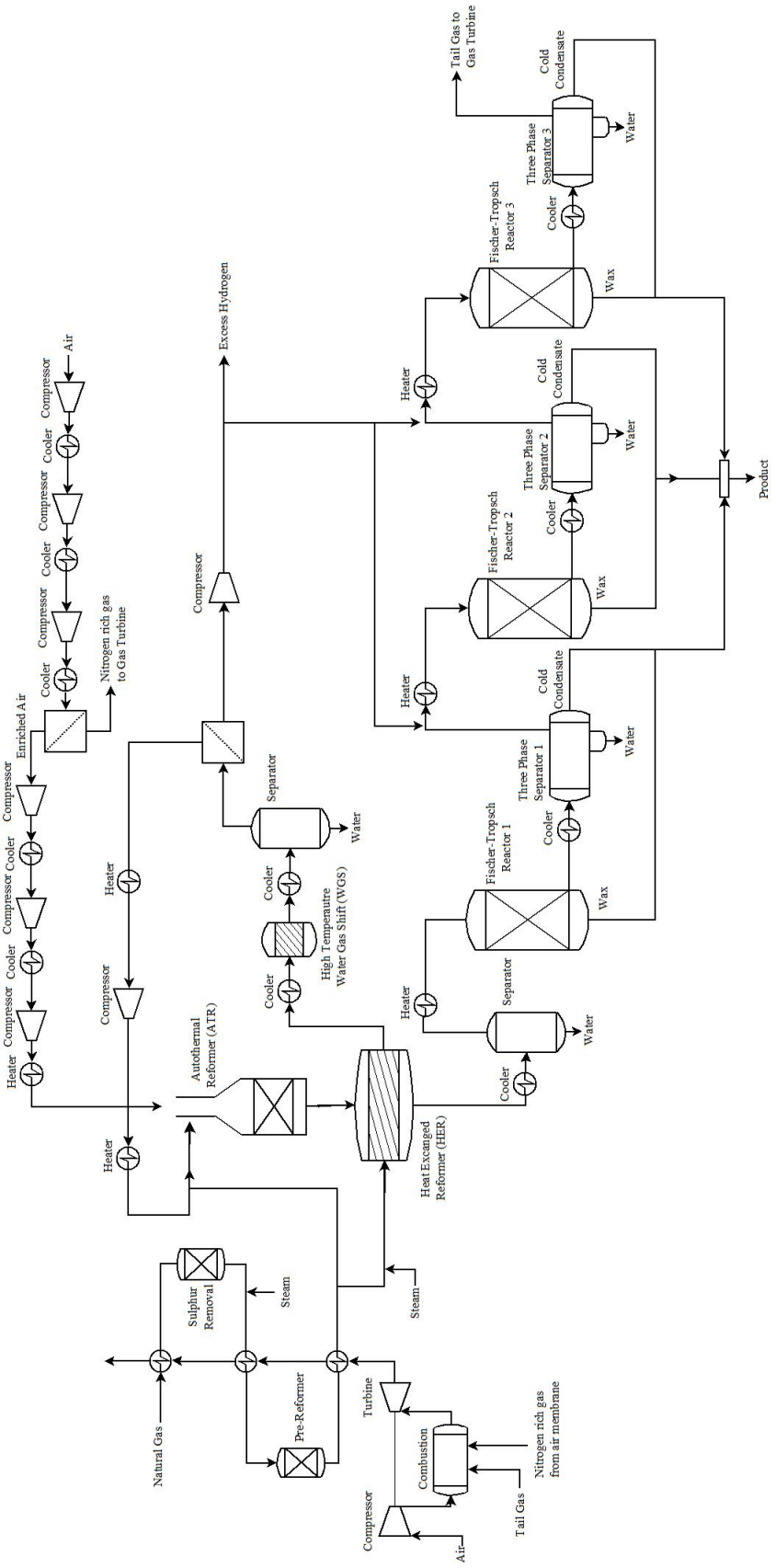

Figure 3.1: Flow sheet of the propose GTL process, with synthesis gas production and Fischer-Tropsch synthesis. The heat integration and steam cycle is not illustarded in this flow sheet.

The feedstock in the process is natural gas with the composition given in Table 3.1. The amount of natural gas feed to the process is 6,000 kmole/h, with a temperature of 50°C and 30 bar.

Table 3.1: Composition of the natural gas feed.

Component	Mole fraction [-]
Methane	0.950
Ethane	0.020
Propane	0.015
n-Butane	0.010
n-Pentane	0.005

As mentioned in section 2.1.1, is the sulphur removal part not included in the simulations. It is therefore assumed that the feed to the process is sulphur free. This is reasonable assumption as the feed after sulphur removal should have a sulphur content lower than 1 ppm. Before the natural gas feed enters the pre-reformer it is mixed with steam and pre-heated to 480°C. In the pre-reformer the small amount of higher hydrocarbons in the natural gas feed is converted to methane. The pre-reformer is simulated as a Gibbs reactor.

The outlet stream for the pre-reformer is further heated to 650°C before it is divided into two streams; one flow to the ATR and one to the HER. The natural gas in the syngas production is pre-heated by heat exchanging with the effluent gas from the gas turbine.

The stream to the ATR is mixed with CO_2 rich gas from the hydrogen selective membrane before entering the ATR together with enriched air. A Gibbs reactor is also used for the autothermal reformer. The enriched air fed to the ATR is produced with the use of a nitrogen selective PRISM membrane. In the simulation the membrane is simulated as a component splitter. The feed to the membrane is compressed air with a temperature of 55°C. The enriched air after the membrane has a pressure of 1 bar, and is further compressed and pre-heated before entering the ATR. The ATR outlet temperature is adjusted with the amount of enriched air feed to the system.

The flow to the HER is mixed with steam, to a steam to carbon ratio of 2 before entering the HER. In the heat exchanged reformer the endothermic steam methane reforming (SMR) takes place inside the tubes. While the heat required for the reforming is provided from the hot outlet flow from the ATR that passes through the shell side. The outlet flow from the HER is cooled down to 350°C before entering the high temperature water gas shift (WGS) reactor. In the WGS reactor the remaining CO in the flow is shifted toward CO_2. An equilibrium reactor is used for the WGS reactor only including the WGS reaction. After the WGS reactor the flow is cooled down to 30°C to knock out water before entering the the hydrogen selective membrane. In the simulation the membrane is simulated as a component splitter. The CO_2 rich stream (retentate) is compressed and pre-heated before it is recycled to the ATR as earlier mentioned. This is done as CO_2 reduces the H_2/CO ratio in the produced syngas from the ATR, as mentioned in

section 2.1.3. The hydrogen stream is used for hydrogen supply between each reactor step.

The hot syngas from the ATR gives heat to the HER, before it is further cooled down to knock out water. Before entering the first FT reactor the flow is heated to 210°C. In the process it is desirable to have a CO conversion of around 90%. To achieve this three FT reactor stages in series are required for the FTS. Between each stage product is separated out and hydrogen is injected. The reactor outlet consist of one vapour stream and one liquid stream. The liquid stream consist mainly of wax. The vapour stream is cooled down to 30°C and sent to a three phase separator. Here, water and cold condensate are separated out from the tail gas. The tail gas is mixed with hydrogen to obtain the same H_2/CO conditions as the first reactor and heated to 210°C before entering the next FT reactor.

To increase the carbon efficiency of the plant the tail gas from the last reactor, consisting of unconverted syngas could be recycle back in the process. However, in this design with enriched air in the ATR, recycle would lead to accumulation of nitrogen. The tail gas in this process design is therefore used as fuel for a gas turbine producing the power needed in the plant.

All the coolers and heaters included in the simulation, with exception of the air compression inter cooling, is assumed to have a pressure drop of 0.5 bar.

Table 3.2: Boundary and inputs for the process design.

Parameter	Value
Natural gas feed [kmole/h]	6,000
Natural gas feed temperature [°C]	50
Natural gas feed pressure [bar]	30
Pre-reformer inlet temperature [°C]	480
ATR natural gas inlet temperature [°C]	650
Air membrane inlet temperature [°C]	55
Steam to carbon ratio HER inlet[-]	2
Water gas shift reactor inlet temperature [°C]	350
Separator after WGS reactor inlet temperature [°C]	30
Fischer-Tropsch reactor inlet temperature [°C]	210
Three-phase separator inlet temperature [°C]	30
Number of Fischer-Tropsch reactor stages [-]	3

3.2 Aspen Custom Modeler Models

Two of the process units used in the simulation are modelled in Aspen Custom Modeler and implemented to Aspen HYSYS. The two units are the Fischer-Tropsch fixed bed reactor and the heat exchanged reformer. In this section these models will be explained.

3.2.1 Fischer-Tropsch Fixed Bed Reactor

The FTS reactor model used in the simulation was made by PhD student Ostadi [24], in Aspen Custom Modeler. The reactor is assumed as a two-dimensional homogeneous plug flow reactor (PFR) with no axial/radial dispersion. Boiling water is used as cooling medium and it is assumed constant temperature along the reactor.

There are several kinetic models proposed in the literature for the FTS. However, in the reactor model used in this simulation the kinetic model proposed by Todic *et al.* [1, 2] was used. This kinetic model was developed by experiment with a stirred tank slurry reactor with cobalt catalyst over a range of operating conditions. The operating conditions used in this process is in the same range as the kinetic mode was tested.

The CO-insertion mechanism used in the derivation of the kinetic is given in Table 3.3, where S is the active site of the catalyst. The mechanism can be divided into four steps; adsorption of the reactants (CO and H_2), chain initiation, propagation and termination.

Table 3.3: The elementary steps used in the derivation of the kinetic model proposed by Todic et al. [1,2]. RDS is the rate determining step.

No.	Elementary step	Rate and equilibrium constant
(1)	$CO + S \leftrightarrow CO - S$	K_1
(2)	$H_2 + 2\,S \leftrightarrow 2H - S$	K_2
(3^{RDS})	$CO - S + H - S \rightarrow CHO - S + S$ $CO - S + CH_3 - S \rightarrow CH_3CO - S + S$ $CO - S + C_nH_{2n+1} - S \rightarrow C_nH_{2n+1}CO - S + S \quad n = 2, 3, ...$	K_3
(4)	$CHO - S + H - S \leftrightarrow CH_2O - S + S$ $CH_3CO - S + H - S \leftrightarrow CH_3CHO - S + S$ $C_nH_{2n+1}CO - S + H - S \leftrightarrow C_nH_{2n+1}CHO - S + S \quad n = 2, 3, ...$	K_4
(5)	$CH_2O - S + 2H - S \leftrightarrow CH_3 - S + OH - S + S$ $CH_3CHO - S + 2H - S \leftrightarrow CH_3CH_2 - S + OH{-}S + S$ $C_nH_{2n+1}CHO - S + 2H - S \leftrightarrow C_nH_{2n+1}CH_2 - S + OH - S + S \quad n = 2, 3, ...$	K_5
(6)	$OH - S + H - S \leftrightarrow H_2O + 2S$	K_6
(7^{RDS})	$CH_3 - S + H - S \rightarrow CH_4 + 2S$ $C_nH_{2n+1} - S + H - S \rightarrow C_nH_{2n+2} + 2S \quad n = 2, 3, ...$	K_{7M} K_7
(8^{RDS})	$C_2H_5 - S \rightarrow C_2H_4 + H - S$ $C_nH_{2n+1} - S \rightarrow C_nH_{2n} + H - S \quad n = 3, 4, ...$	K_{8E} K_8

For the product distribution the model proposed by Hillestad [3] was used. The model gives a realistic and consistent product distribution from the FTS with the Anderson-Schultz-Flory distribution as basis. In the model it is assumed that there are no chain limitations giving an infinite of component. To implement this product distribution model in the reactor model it is necessary to make lumps of higher hydrocarbons.

In the reactor model two lumps were made. One for alkanes higher than C_{10} named C^p_{11+} and one for the alkenes higher than C_4, named C^o_{5+}. p denotes paraffins also known as alkanes and o denotes olefins also known as alkenes. The alkenes is lumped from a lower hydrocarbon number as the production is smaller, and a larger lump would make a more efficient and easy solved reactor model, because of less equations to solve.

The production of methane and ethylene deviates from the ideal ASF distribution. In reality there are a higher selectivity for methane then expected from ASF and there are a lower selectivity for ethylene [27]. Two extra equations are included to correct for the deviation; the methanation reaction (Eq. 3.2.3) and cleavage of ethylene (Eq.3.2.4). The FTS reaction with component lumps are given below [3].

$$\mathrm{CO} + U_1\mathrm{H}_2 \xrightarrow{r_1} \sum_{i=1}^{10} \nu_{i,1}\mathrm{C}_i\mathrm{H}_{2i+2} + \nu_{[11,\infty],1}\mathrm{C}^p_{11+} + \mathrm{H}_2\mathrm{O} \tag{3.2.1}$$

$$\mathrm{CO} + U_2\mathrm{H}_2 \xrightarrow{r_2} \nu_{1,2}\mathrm{CH}_4 + \sum_{i=1}^{4} \nu_{i,1}\mathrm{C}_i\mathrm{H}_{2i} + \nu_{[5,\infty],1}\mathrm{C}^o_{5+} + \mathrm{H}_2\mathrm{O} \tag{3.2.2}$$

$$\mathrm{CO} + 3\mathrm{H}_2 \xrightarrow{r_3} \mathrm{CH}_4 + \mathrm{H}_2\mathrm{O} \tag{3.2.3}$$

$$\mathrm{C}_2\mathrm{H}_4 + 2\mathrm{H}_2 \xrightarrow{r_4} 2\mathrm{CH}_4 \tag{3.2.4}$$

The growth factor for alkane, α_1, and for alkenes, α_2, is given in Equation 3.2.5 - 3.2.6. α_M is the growth factor for methane. It is not a part of the product distribution, however, it is included in the reaction rates [3].

$$\alpha_1 = \frac{1}{1 + \frac{k_7\sqrt{K_2 p_{\mathrm{H}_2}}}{k_3 K_1 p_{\mathrm{CO}}}} \tag{3.2.5}$$

$$\alpha_2 = \alpha_1 e^{-0.27} \tag{3.2.6}$$

$$\alpha_M = \frac{1}{1 + \frac{k_{7,M}\sqrt{K_2 p_{\mathrm{H}_2}}}{k_3 K_1 p_{\mathrm{CO}}}} \tag{3.2.7}$$

$$\tag{3.2.8}$$

The reaction rate for the reactions are given in Eq.3.2.9 - Eq.3.2.12 [3].

$$r_1 = k_7 \sqrt{K_2 p_{\mathrm{H}_2}} [S]^2 \frac{\alpha_M}{(1-\alpha_1)^2} \tag{3.2.9}$$

$$r_2 = k_8 [S] \frac{\alpha_M}{(1-\alpha_2)^2} \tag{3.2.10}$$

$$r_3 = k_{7,M} \sqrt{K_2 p_{\mathrm{H}_2}} [S]^2 \alpha_M - r_1 \nu_{1,1} - r_2 \nu_{1,2} - 2r_4 \tag{3.2.11}$$

$$r_4 = r_2 \nu_{2,2} - k_{8,E} [S] \alpha_M \alpha_2 \tag{3.2.12}$$

$$[S]^{-}1 = 1 + K_1 p_{\mathrm{CO}} + \sqrt{K_2 p_{\mathrm{H}_2}} + \left(\frac{1}{K_2^2 K_4 K_5 K_6} \frac{p_{\mathrm{H}_2\mathrm{O}}}{p_{\mathrm{H}_2}^2} + \sqrt{K_2 p_{\mathrm{H}_2}} \right) \frac{\alpha_M}{(1-\alpha)} \tag{3.2.13}$$

where k_i is reaction rate constants, K_i is the equilibrium constants and p_i is the partial pressure of component i.

The reaction rate constants is calculated with the us of Arrhenius equation with the estimated values from Todic *et al.* [1, 2]. And the pressure drop in the reactor is calculated with the use of Ergun equation.

The oxygenates produces in the FTS is neglected in the model. This is a good assumption as the production of these components are small. Table 3.4 gives the main design parameters for the FT fixed bed reactor.

Table 3.4: Reactor design parameters for the Fishcer-Tropsch fixed bed reactor.

Parameter	Value
Diameter of tubes [mm]	25
Length of tubes [m]	12
Catalyst bulk density [kg/m^3]	1,200
Catalyst diameter [mm]	3
Catalyst Voidage [%]	40
Coolant temperature [°C]	220

3.2.2 Heat Exchanged Reformer

The heat exchanged reformer (HER) was made by Falkenberg [25] with modifications made by Ostadi.

The HER is a baffled multitubular steam methane reforming reactor. The design is similar to a shell and tube heat exchanger, where the endothermic SMR reaction takes place inside the tubes. And the heat provided for the reforming is given by the flow passing though the shell. In the model counter-current flow is assumed, however, due to the baffles the flow would be a

mixture of cross-flow and counter-current flow. Homogeneous phase is assumed on the shell side, while at the tube side pseudo-homogeneous phase is assumed [25].

The SMR reaction considered in the model is given in Eq.3.2.14 - Eq.3.2.16, with the use of kinetic expressions for a Ni/$MgAl_2O_4$ catalyst reported by Xu and Froment [42].

$$CH_4 + H_2O \leftrightarrow CO + 3H_2 \tag{3.2.14}$$
$$CO + H_2O \leftrightarrow CO_2 + 3H_2 \tag{3.2.15}$$
$$CH_4 + 2H_2O \leftrightarrow CO_2 + 4H_2 \tag{3.2.16}$$

The pressure drop in the tube side is calculated from the Erguns equation, while for the shell side the Kern method reported by Sinnott and Towler [40] is used.

In Table 3.5 the main design parameters for the HER is given.

Table 3.5: Heat exchanged reformer design parameters.

Parameter	Value
Diameter of tubes [mm]	100
Length of tubes [m]	10
Catalyst bulk density [kg/m^3]	2,355.2
Catalyst diameter [mm]	5.6
Catalyst Voidage [%]	54.5
Effectiveness factor [-]	0.03

3.3 MATLAB Model

Two different membranes are included in the process design, one nitrogen selective membrane separator to produce enriched-air and a hydrogen selective membrane to separate H_2 from CO_2. In the HYSYS simulations these membranes are included as component splits.

For the air membrane, a data sheet is received from Air Products [43]. From the information given in the data sheet, the split factor used in the simulation was calculated. The calculations to decide the split factor is given in Appendix C.

3.3.1 Hydrogen Selective Carbon Membrane

To decide the split factors to be used for the hydrogen selective carbon membrane, a MATLAB model was made, given in Appendix D. This section explain how the model are made, and what is the input. The model is solved using orthogonal collocation.

The code is based on one ceramic tube with a diameter of 4 mm and a length of 1 m, illustrated in Figure 3.2.

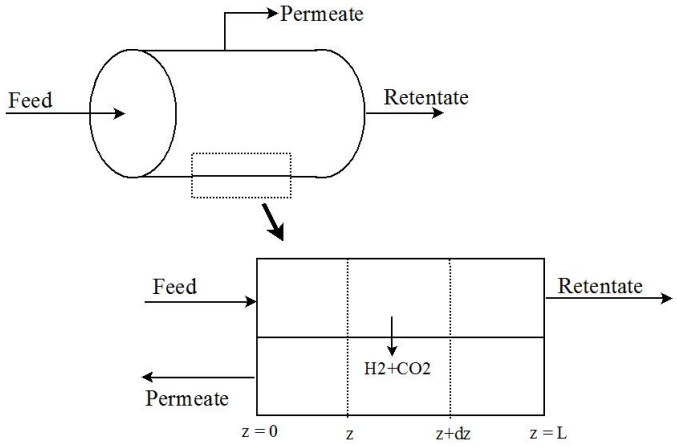

Figure 3.2: A sketch of one ceramic tube, and how the model is made.

Assumptions used for the membrane model

- Only H_2 and CO_2 passes though the membrane.
- No diffusion is included, assuming that all gas flow is in contact with the membrane.
- Constant pressure and concentration on each side of the membrane.

The permeance is a measure of gas transportation rate through the membrane, and is defined as flux per unit driving force. The permeance values used in the model for the different components is given in Table 3.6 [37]. In reality small amount of the other components would probably pass though, however, as the amount in the feed is so small it will not have a very big effect.

Table 3.6: The permenace of the different component in the membrane feed used in the MATLAB code for membrane split deciding [37].

Component	Permeance [GPU]
H_2	200
CO_2	2
CO	0
H_2O	0
CH_4	0

The feed flow is decided to be located to the tubes. This gives feed flow in the direction of the membrane, an no area will be lost due to changes in flow direction. However, when having the feed in the tubes the tube design needs to handle the high feed pressure. With the feed

flow in the tubes the assumption of full contact for the flow with the membrane is more realistic.

If the tube is divided into small segments the flux change over each segment is describes as:

$$\frac{dn_{R,i}}{dz} = -J_i a \tag{3.3.1}$$

$$-\frac{dn_{P,i}}{dz} = J_i a \tag{3.3.2}$$

where $n_{R,i}$ is the flow of component i in the retentate, $n_{P,i}$ is the flow of component i in the permeate, J_i is the flux of component i from retentate to permeate, and a is the membrane area per volume in $\frac{m^2}{m^3}$.

The flux is given in equation 3.3.3

$$J_i = k_i(P_h\frac{n_{R,i}}{n_{R,i}+n_{P,i}} - P_l\frac{n_{P,i}}{n_{R,i}+n_{P,i}}) = k_i(P_h y_i - P_l x_i) \tag{3.3.3}$$

where k_i is the permeanc of component i for the membrane, P_h is the pressure on high pressure side (retentate), P_l is the pressure on low pressure side (permeate), y_i is the mole fraction of component i in the retentat and x_i is the mole fraction of component i in the permeate.

The boundary conditions for the counter-current membrane is given in the equations below.

$$n_{R,i}(\xi = 0) = n_{R0,i} \tag{3.3.4}$$

$$n_{P,i}(\xi = L) = n_{P0,i} \tag{3.3.5}$$

where $n_{R0,i}$ is the feed flow of component i, and $n_{P0,i}$ is the feed flow on permeate side of component i.

Before the split factors to be used in the simulation were found an evaluation on the membrane to decide the gas velocity and permeate pressure was done, with the results given in section 4.2.6.

3.4 Heat Integration

To reduce the amount of external heating and cooling duties needed in the process a heat integrating network is designed. The theory behind heat integrating is given in section 2.5.

There are several hot streams in the process that could be used. However, for the heat integration on a GTL-FPSO plant it is important to achieve small heat exchangers. To obtain this high driving forces are needed, meaning having as high temperature differences as possible. Due to this some hot streams are more sufficient for the integration. The chosen hot streams are;

1. The cold side outlet flow from the HER tubes.

2. The hot side outlet flow from the HER coming from the ATR.

The cold streams which needs heat are;

3. Pre-heat of feed to FT reactor 1
4. Pre-heat of feed to FT reactor 2
5. Pre-heat fo feed to FT reactor 3
6. Heating of CO_2 rich gas from hydrogen selective membrane to evaporate H_2O before compression.
7. Pre-heat of CO_2 rich gas before ATR.
8. Pre-heat of enriched air

The effluent gas from the gas turbine after pre-heating the natural gas feed has still more heat that could be used. However, this flow is not included in the heat integration network as it is assumed to be used for heating in the steam cycle. More information about this is given in section 3.5.2.

3.5 Utility System

The utility systems in the process has not been designed in detail, however, some assumptions are done and a design is suggested for the different utility systems.

3.5.1 Reactor Cooling Cycle

As coolant in the FT reactors boiling water at 220°C is used. To keep this water clean, it is considered as a closed cycle as illustrated in Figure 3.3.

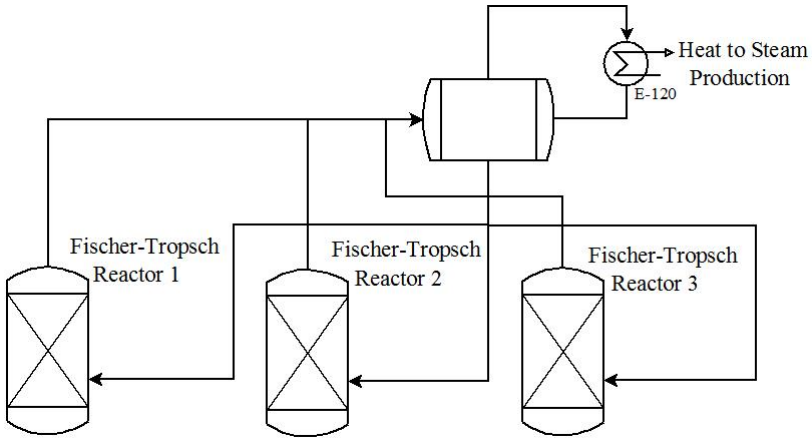

Figure 3.3: An sketch of the cooling cycle of the Fischer-Trospch reactors with steam drum and heat exchanger for steam production.

The heat released from condensing the steam before the steam drum inlet is used to produce medium pressure (MP) steam. The MP steam has a temperature of 210°C and a pressure of 19.07 bar and is produced from water with a temperature of 20°C and a pressure of 19.07 bar.

3.5.2 Steam Cycle

The water from the three phase separator can contain some hydrocarbons and alcohols and it is therefore favourable to reuse the water in the process. If this water is reused in the process the ATR would treat the water, instead of needs for external water treatment system.

The steam cycle in the process is designed as illustrated in Figure 3.4.

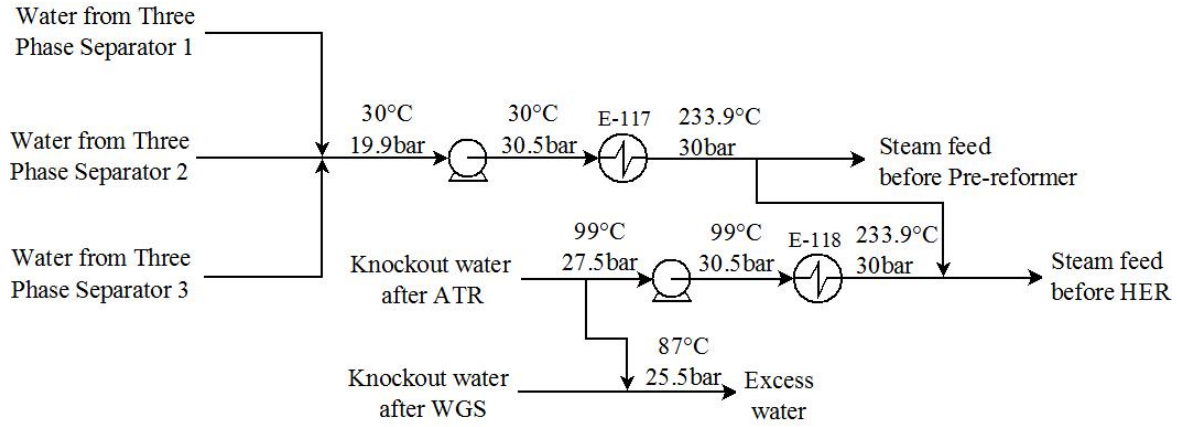

Figure 3.4: A sketch of the steam cycle in the process, giving an overview over where the different water flows are used.

The heat needed to evaporate the water is supplied by heat exchanging with the effluent gas from the gas turbine after the pre-heating of natural gas, as illustrated in Figure 3.5.

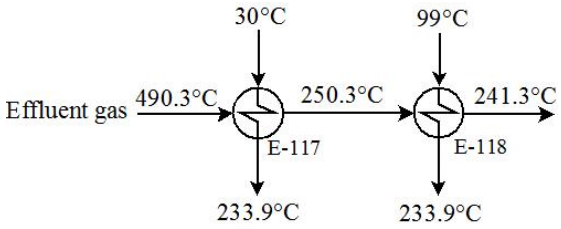

Figure 3.5: Heat integration of the effluent gas from the gas turbine after preheating of natural gas with the steam cycle.

3.5.3 Power Production

The tail gas from the process is sent to a gas turbine for power production. In this master thesis the design of the gas turbine has not been detailed evaluated. It is assumed that the gas turbine

unit consist of air compression, the combustion chamber, the turbine and a exhaust gas duct for heat integration to pre-heat the natural gas feed. For the air compression it is assumed one stage compressing from 1 atm to 16 bar with no inter-cooling.

Chapter 4

Results and Discussion

The simulation was performed as described in Chapter 3. This chapter will present and discuss the result from the simulation of the final process design, the background and optimizing of the parameter used, and an evaluations of the assumptions. First a presentation of the parameters used for the final design is given, than the results from the simulation are presented. Section 4.2 will give the evaluation of the different parameters and the background for the use of specific values. At the end of this chapter some of the assumptions used will be evaluated.

The total production in the process is reported as two values; total production and C_{5+} production. The total production is the total flow amount in the product stream. However, when the value is given as C_{5+} production it only includes the amount of hydrocarbons with five carbon atoms or more.

4.1 Simulation Results for the Final Process Design

In the final process design the hydrogen selective carbon membrane (section 4.2.1.1) and FT Reactor B (section 4.2.1.2) with a catalyst effectiveness factor of 0.08 are used. A flow sheet of the process is given in Figure 4.1, and a table over operating conditions and composition for the numbered streams in the flow sheet is given in Table 4.1. A table with the composition in mass fraction is given in Appendix E.

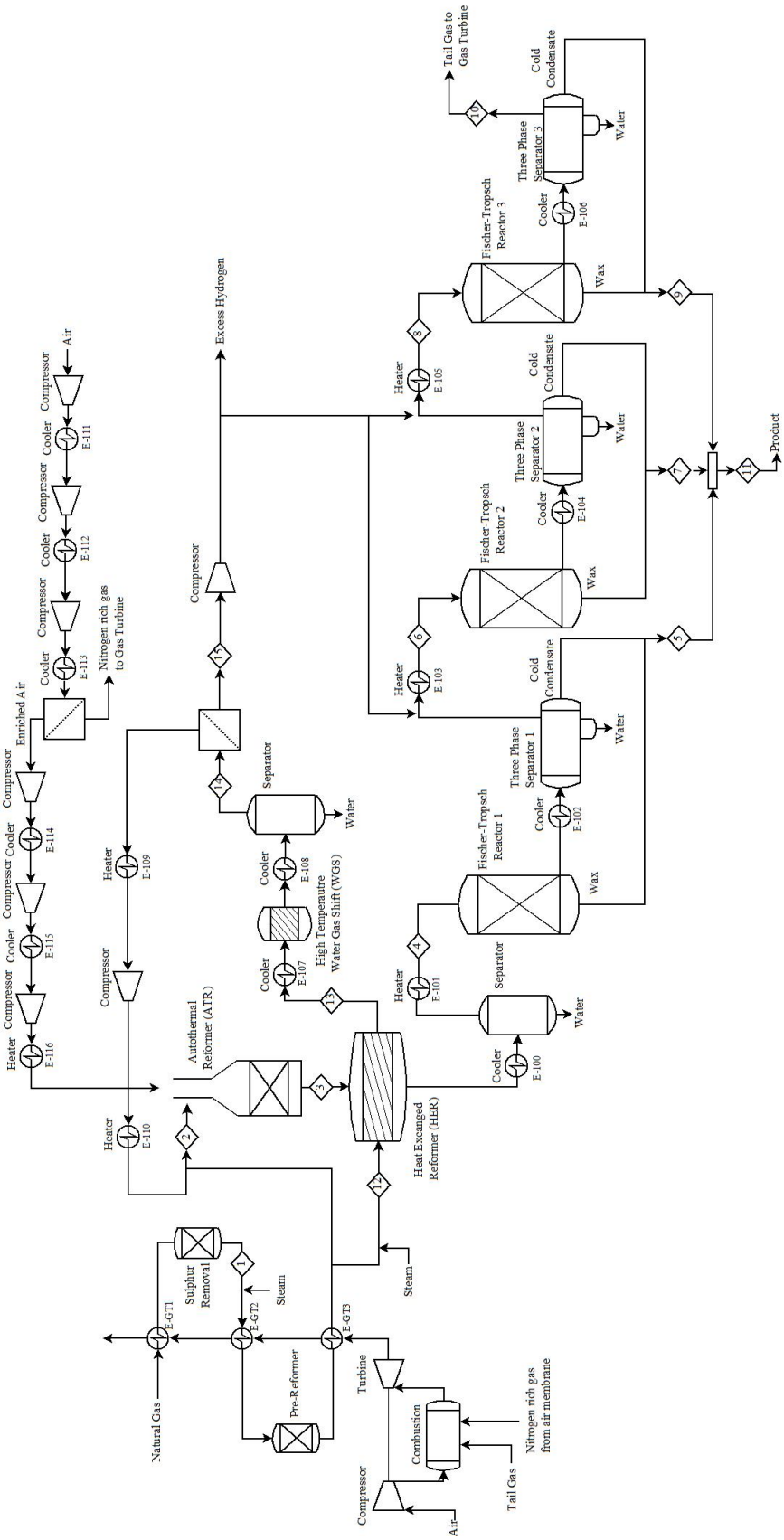

Figure 4.1: Flow sheet of the propose GTL process. The heat integration and steam cycle is not illustarded in this flow sheet.

Table 4.1: Specification of temperature, pressure, molar flow and mass flow for the numbered streams in the process flow sheet. The compositions is given in mole fraction.

Stream Number	1	2	3	4	5	6	7	8	9	10	11	12	13	14
Temperature [°C]	350.0	649.9	1,060.1	210.0	189.9	210.0	171.4	210.0	135.6	30.0	174.7	440.5	1,050.0	30.0
Pressure [bar]	30.0	28.5	28.5	27.0	25.1	24.6	22.6	22.1	19.9	19.9	19.9	28.5	26.5	25.5
Molar Flow [kmole/h]	6,000	11,084	28,787	24,681	80	17,668	68	12,735	42	10,038	190	2,440	3,671	2,993
Mass Flow [tonne/h]	104.7	193.5	485.3	411.3	26.2	340.5	18.7	292.1	9.0	266.9	53.9	42.4	42.4	30.2
Mole fraction [-]														
Carbon monoxide	0	0.019	0.188	0.219	0.007	0.178	0.004	0.116	0.002	0.058	0.005	0	0.142	0.068
Hydrogen	0	0.088	0.393	0.459	0.009	0.372	0.005	0.243	0.002	0.112	0.006	0.028	0.547	0.778
Water	0	0.318	0.151	0.010	0.040	0.001	0.030	0.001	0.017	0.001	0.031	0.701	0.273	0.002
Carbon dioxide	0	0.064	0.038	0.045	0.014	0.063	0.022	0.087	0.029	0.110	0.020	0.013	0.034	0.148
Nitrogen	0	0	0.227	0.265	0.014	0.369	0.019	0.512	0.020	0.650	0.017	0	0	0
Methane	0.950	0.511	0.003	0.003	0.001	0.013	0.002	0.030	0.004	0.051	0.002	0.257	0.003	0.004
Ethane	0.020	0	0	0	0	0	0	0.001	0.001	0.002	0	0	0	0
Ethylene	0	0	0	0	0	0.001	0.001	0.003	0.001	0.004	0.001	0	0	0
Propane	0.015	0	0	0	0	0	0.001	0.001	0.002	0.002	0.001	0	0	0
Propylene	0	0	0	0	0	0.001	0.002	0.002	0.003	0.003	0.001	0	0	0
n-Butane	0.010	0	0	0	0.001	0	0.003	0.001	0.005	0.001	0.002	0	0	0
1-Butene	0	0	0	0	0.001	0	0.003	0.001	0.006	0.002	0.003	0	0	0
n-Pentane	0.005	0	0	0	0.002	0	0.008	0.001	0.014	0.001	0.007	0	0	0
n-Hexane	0	0	0	0	0.006	0	0.019	0.001	0.034	0.001	0.017	0	0	0
n-Heptane	0	0	0	0	0.014	0	0.39	0	0.059	0.001	0.033	0	0	0
n-Octane	0	0	0	0	0.027	0	0.055	0	0.070	0.	0.047	0	0	0
n-Nonane	0	0	0	0	0.038	0	0.57	0	0.63	0	0.051	0	0	0
n-Decane	0	0	0	0	0.044	0	0.052	0	0.054	0	0.049	0	0	0
C^{p}_{11+}	0	0	0	0	0.519	0	0.420	0	0.324	0	0.440	0	0	0
C^{o}_{5+}	0	0	0	0	0.261	0	0.258	0	0.290	0	0.266	0	0	0

The parameters used in the process (Table 4.2) are decided based on parameter optimizing and the evaluation of the parameters and background for the choice are given in section 4.2.

Table 4.2: An overview of decided operating conditions based on evaluations for the process design.

Parameter	Value
Amount of natural gas to ATR [%]	90
Amount of natural gas to HER [%]	10
Steam to Carbon ratio [-]	0.6
H_2/CO ratio [-]	2.097
Air feed temperature [°C]	550
ATR outlet temperature [°C]	1,060
Gas turbine inlet pressure [bar]	16
Air membrane;	
Air feed pressure [barg]	15
Split fraction permeate, N_2 [-]	0.545
Split fraction permeate, O_2 [-]	0.108
Hydrogen selective membrane;	
Pressure ratio [-]	3.6
Split fraction permeate, H_2 [-]	0.845
Split fraction permeate, CO_2 [-]	0.037

A simulation tool as Aspen HYSYS calculates each unit individual and add all the values together instead of evaluating the whole process as one unit. It is therefore important to check that the overall mass and energy balance is conserved in the process. This is controlled and found to be acceptable, and the evaluation is given in Appendix F.

The feed streams to the process are natural gas, air and steam. With the given natural gas feed amount, approximately 31,600 kmole/h air and 5,900 kmole/h of steam are needed (Table 4.3). The steam temperature is given by HYSYS for steam at the given pressure.

Table 4.3: An overview of the total amount of the different feed needed in the process together with the temperature and pressure.

Feed	Amount [kmole/h]	Temperature [°C]	Pressure [bar]
Natural gas	6,000	50.0	30
Air to process	18,168	10.0	1.013
Air to gas turbine	13,428	10.0	1.013
Steam	5,868	233.9	30

The total production from the process is 53.9 tonne/ h with a CO conversion of 89.23% (Table 4.4). The total product consist mainly of C_{5+}, however it contains some amount of lighter hydrocarbons (Table 4.5).

Table 4.4: An overview of the production, CO conversion, and CH_4 selectivity for each reactor and for the total process.

	Reactor 1	Reactor 2	Reactor 3	Total Process
Product amount [tonne/h]	26.2	18.7	9.0	53.9
C_{5+} product amount [tonne/h]	26.0	18.5	8.9	53.4
CO conversion [%]	41.93	52.92	60.63	89.24
CH_4 selectivity [%]	6.91	9.29	14.09	9.06

Table 4.5: The final amount of hydrocarbons in the product from the process. The list is divided in alkanes and alkenes with the total amount of alkanes and alekens at the end.

Component	Alkanes [tonne/h]	Component	Alkenes [tonne/h]
C_1	0.01	C_1	-
C_2	0	C_2	0
C_3	0.01	C_3	0.01
C_4	0.03	C_4	0.03
C_5	0.09	C_{5+}	5.39
C_6	0.28		
C_7	0.63		
C_8	1.01		
C_9	1.24		
C_{10}	1.33		
C_{11+}	43.39		
Total amount	48.02	Total amount	5.44

The gas velocity through the reactor and the effectiveness factor are kept constant for all the FT reactors. With these values kept constant the CO conversion is increased for the different reactors, with the lowest conversion for the first. CO conversion is defined as the amount of CO in to the reactor minus the amout out divided on the inlet flow. Because of a lower feed amount of CO to the second and third reactor the relative conversion for each reactor is increased. However, the total amount of CO converted ($CO_{inn} - CO_{out}$) from the first to the last reactor is reduced. However, the production of C_{5+} is reduced for the second and third reactor, as the gas feed amount is reduced.

The methane selectivity is increased for the reactor stages. This can be explained from the kinetic model used [1, 2] which predicts a reduction in the growth probability factor as the

pressure is reduced. A reduced chain growth probability factor increases the selectivity towards lighter hydrocarbons.

4.1.1 Carbon and Energy Efficiency

Carbon efficiency is defined as the amount of carbon present in the products divided by the amount of carbon in the natural gas feed. The carbon efficiency for the final design is 57% (Figure 4.2). For a onshore GTL plant with recycle the carbon efficiency is around 70-80% [44], and for a once-through GTL process it is therefore expected a lower carbon efficiency, and a value around 60% could be reasonable. The rest of the carbon ends up in the tail gas where 8% is methane, 17% is CO_2, and 3% of higher hydrocarbon, C_{5+}.

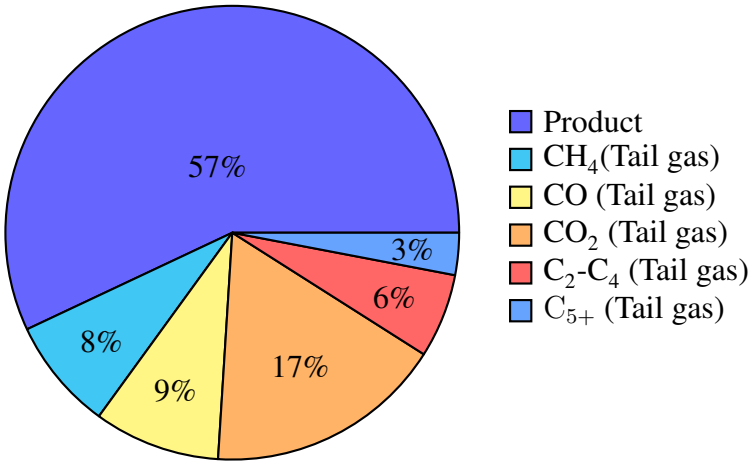

Figure 4.2: Overview of where the carbon in the natural gas feed ends up.

Energy efficiency is defined in many different ways in the literature. But, here it is defined as the lower heating value of the products divided by the lower heating value of the natural gas feed. The mechanical work for the compressor are covered by the power produced in the gas turbine, and the energy input and output of the process is illustrated in Figure 4.3.

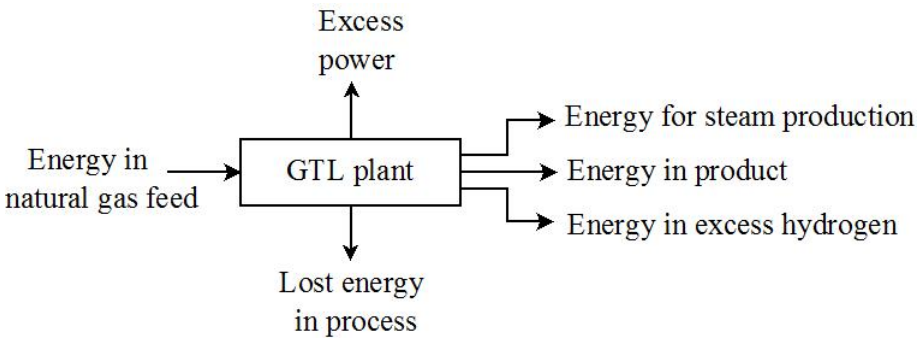

Figure 4.3: Illustration of energy input and output for the GTL plant

In the process, 45% of the energy in the natural gas ends up in the FT product, 9% in excess hydrogen, 26% is used for steam production, 6% goes to power export and 15% is lost in the process (illustrated in Figure 4.4). The values used to calculate the energy efficiency are given in Appendix G.

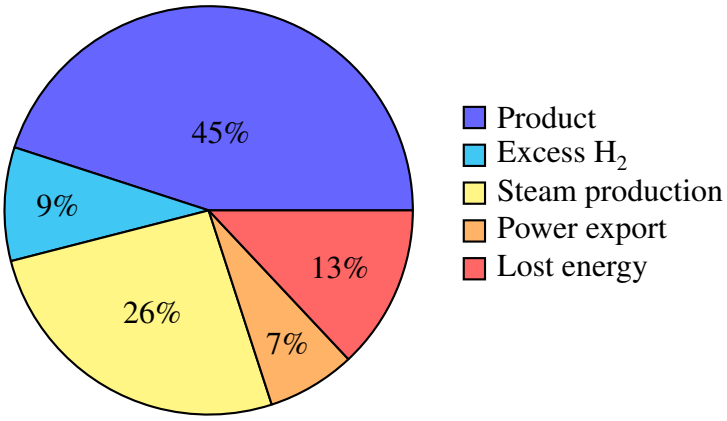

Figure 4.4: Overview of where the energy in the natural gas feed ends up.

Excess power is the amount produced from the gas turbine, that are not used for compression in the process. The power is converted to thermal energy with the use of Carnot efficiency, and is reported as power export. Energy used for the steam production is the heat removed from the FT reactors, in addition to some steam produced from cooling the hot synthesis gas, more information is given in section 4.1.2. Some of the excess hydrogen would be used for upgrading of products and increase the efficiency of the products. However, the amount of hydrogen available is probably more than needed and the extra hydrogen could have been used for power production in the gas turbine. Lost energy includes the external cooling and the lost thermal energy in the exhaust gas from the gas turbine, in addition to energy lost from the compressors and turbine.

The energy efficiency in commercialised GTL plants are usually about 60-65% on a lower heating value basis [45]. In this process the energy efficiency to the FT product are some reduced, however, in this process design hydrogen and power are produced in addition to the FT products and the total efficiency would be in the same range as commercialised GTL plants.

4.1.2 Heat Integration

A heat integration network was conducted for the final process design (illustrated in Figure 4.5). The stream included in the heat integrating is given in section 3.4, and overview of the temperatures, the heat flow and heat capacities (CP) for the different streams are given in Table 4.6.

The process was found to be a threshold problem with use of the composite curve, and there are no heat recovery pinch in the process. Calculations and the composite curve are given in Appendix H.

Table 4.6: Overview of the hot and the cold streams for the heat integration.

Stream nr.	Supply temp. [°C]	Target temp. [°C]	Heat Load [MW]	CP [MW/°C]
1	1050	350	24.6	0.32
2	854	99	243.4	0.04
3	99	210	23.1	0.21
4	30	210	27.3	0.15
5	31	210	20.2	0.11
6	30	85	0.6	0.01
7	106	650	5.8	0.01
8	188	550	31.3	0.09

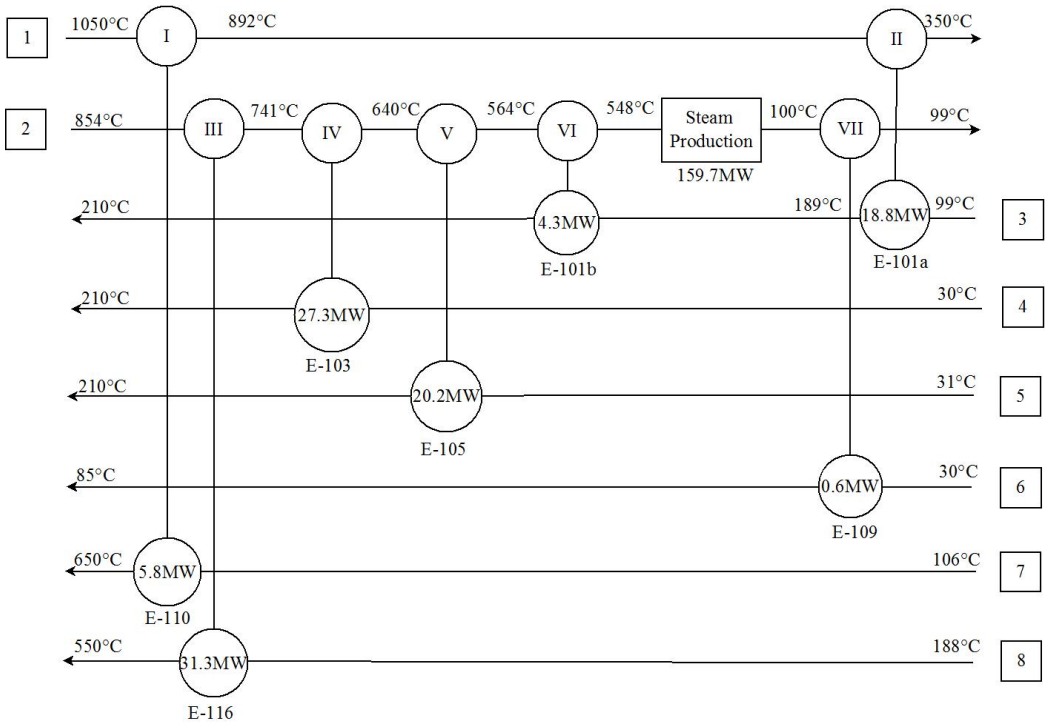

Figure 4.5: The proposed heat integration network for the final process design.

When the heat integration network was developed, one important aspect was to connect streams to get the highest possible driving force. With high driving forces the heat transfer area needed is reduced giving smaller heat exchanger which is important due to space limitations on a FPSO. In addition it is favourable to keep the number of units to as few as possible. This means that if a hot stream can provide all the duty needed to heat a cold stream only one heat exchanger is used for the stream.

4.1.2.1 Heat Exchanger I

The outlet flow from the HER tubes (stream 1) is connected with the pre-heat of the CO_2 rich gas from the hydrogen selective carbon membrane after the compressor (stream 7). The heat amount transferred is sufficient to cover the heat need for stream 7. This connection was decided as stream 7 is the cold stream which is pre-heated to the highest value and stream 1 is the hot stream with the highest temperature giving the largest temperature difference and driving force for the heat exchanger.

4.1.2.2 Heat Exchanger II

The stream from the HER after heat exchanger I is still at a high temperature and has heat that can be utilised. There are several possibilities for the use of the heat. One possibility is to heat exchange with the CO_2 rich gas from the carbon membrane before the compressor (stream 6), however, steam 1 needs more cooling than stream 6 can provide. Another possibility is to use the heat to pre-heat one of the reactor inlets, however, there is not enough heat to complete any of the other streams. Pre-heating of any of the rector inlet streams would give a large temperature difference and the choice of stream is therefore based on the one with the highest heat capacity.

4.1.2.3 Heat Exchanger III

Pre-heating of the air (stream 8) was connected to the HER outlet from the ATR (stream 2). Stream 1 after heat exchanger 1 have a higher temperature than stream 2. However, the heat amount in stream 1 is not enough to complete the need for stream 8. As stream 2 has the second largest temperature this stream was used.

4.1.2.4 Heat Exchanger IV

The reactor inlet to FT reactor 2 (stream 4) is pre-heated with stream 2 outlet of heat exchanger II. The same driving forces were achieved for heat exchanging between the inlet to reactor 2 or reactor 3 (stream 5). However, as the heat capacity of stream 4 is higher than stream 5 the pre-heat of the reactor inlet to reactor 2 was done before reactor 3.

4.1.2.5 Heat Exchanger V

The third heat exchanger on the stream from the ATR, is providing the heat needed for pre-heating of the feed to FT reactor inlet 3.

4.1.2.6 Heat Exchanger VI

The inlet flow to FT reactor 1 still needs some pre-heating after heat exchanger II. The needed heat is given from the hot outlet stream from heat exchanger V.

4.1.2.7 Heat Exchanger - Steam Production

Even after four heat exchangers the stream from the ATR (stream 2) still has a lot of energy. Some of this energy is used for steam production. 212 tonne/h of medium pressure (MP) steam at 210°C and 19.07 bar is produced, from water at 20°C and 19.07 bar.

4.1.2.8 Heat Exchanger VII

The CO_2 rich gas from the membrane, contains some small amount of H_2O that needs to be vaporized before the compressor. The heat duty for this exchanger are small and the temperature driving forces are still sufficient with the heat exchanger places after the steam production. This is the reason why it is not placed before the steam production and it gives more duty to be used to produce steam.

At an earlier stage it was decided to cool down the syngas to 30°C to knock out water before the FTS. After the heat integration the temperature of stream 2 is 99 °C. Further cooling of the stream requires external cooling duty and more energy for pre-heating after the separator. An evaluation of using 99°C instead of 30°C was done with the result in Table 4.7.

Table 4.7: A comparison of syngas cooling to two different temperatures.

Cooling temperature [°C]	30	99
Mol fraction H_2O in syngas [-]	0.002	0.010
Cooling duty needed [MW]	22.4	0
Pre-heating FT reactor 1 [MW]	37.0	23.2
C_{5+} product [tonne/h]	53.53	53.36

It is decided to not include any further cooling of stream 2 as the C_{5+} production is only reduced with 170 kg/h, while the external cooling duty demand is reduced with 22.4 MW and the external heating with 13.8 MW.

When heat integration (HI) is included in the process no external heating is required, and the external cooling demand is reduced with 268.1 MW (Table 4.8).

Table 4.8: An comparison of the total external cooling and heating demand for the process with and without heat integration.

	Without HI	With HI
Cooling demand [MW]	504.6	236.5
Heating demand [MW]	108.4	0

4.1.3 Utility Systems

4.1.3.1 Process Cooling Cycle

There are several coolers in the system that needs external cooling (an overview is given in Table 4.9) and many possibilities for cooling cycle design. For an onshore GTL plant air cooling is used, due to limitations in water supply [8]. However, for offshore applications water cooling is more sufficient, as air cooling requires more space and the availability of water is high.

One possibility is to use sea water directly in the cooling cycle. If sea water is used directly some treatment of the water is needed like chlorination [46]. However, this is a good possibility as the plant is located offshore.

Another alternative is to have a closed fresh water cooling cycle. Where the temperature is kept low by rejecting heat to the sea water. With the use of fresh water problems with corrosion that may occur with the use of sea water is eliminated, however, an extra heat exchanger for heat rejection to the sea is needed.

Without deciding which alternative to use it is assumed in this master thesis that the water used has a feed temperature of 10°C with a ΔT of 15 °C.

Table 4.9: The external cooling duty needed in the process.

Cooler		Duty [MW]
Air compression	E-111	17.3
inter-cooling	E-112	22.1
	E-113	7.1
	E-114	14.8
	E-115	12.1
FTS coolers	E-102	64.6
	E-104	45.6
	E-106	30.8
Carbon membrane cooler	E-108	22.1
Total cooling duty		236.5

The amount of cooling water needed is found from a simple HYSYS simulation. A water stream is heated from 10°C to 25°C with the total cooling duty needed. The amount is found to 13,580 tonne/h.

4.1.3.2 Reactor Cooling Cycle

The amount of cooling water needed in the reactor cooling cycle is found from HYSYS in a simple simulation. A water stream with vapour fraction of 1 and a temperature of 220 °C was heated with the amount of heat released from the three reactor to vapour fraction of 1 and temperature of 220°C. From, this simple simulation the amount of cooling water needed is given to 422 tonne/h.

As illustrated in section 3.5.1 the cooling cycle is assumed to be a closed cycle where the heat to condense the steam is used to produce steam at 210°C and 19.07 bar. The amount of steam each reactor can produce and the total amount is given in Table 4.10.

Table 4.10: Overview over the amount of steam produced from the Fischer-Tropsch reactors.

	Steam produced [tonne/h]
Reactor 1	135.4
Reactor 2	99.8
Reacotr 3	53.9
Total	289.1

Given in section 4.1.2 MP steam is also produced from a process stream. The total amount of MP steam produced in the plant is 501 tonne/h.

The steam produced in the process is not decided for specific use. In the process it is assumed that all the compressors are electrical driven. However, a possibility could be to us some of the steam produced in the process to have steam driven compressors. Other alternatives are to have a steam turbine to produce electricity, or use the steam in other processes on the FPSO.

4.1.3.3 Steam Cycle

An illustration of the steam cycle is given in section 3.5.2, and a water balance is given in Table 4.11.

All the water from the three phase separators are used in the process. Some of the knock out water from the ATR separator is also used in the process. However, there are a surplus of water inn the system of 71.3 tonne/h.

The knock out water from the syngas process separators can contain small amount of CO_2. However, if the quality of the excess water is satisfied to be injected back into the oil reservoir the water could be used for this purpose. Injection of water is done to maintain the pressure in

the oil reservoir [8]. If the quality is not satisfied some water treatment may be required in the process.

Table 4.11: Water balance in the process.

		[tonne/h]
Water sources	Knock out water before Fischer-Tropsch synthesis	74.0
	Knock out water before hydrogen selective membrane	12.2
	Water from three phase separator 1	44.8
	Water from three phase separator 3	29.9
	Water from three phase separator 2	16.1
Water consumers	Steam demand before pre-reformer	81.9
	Steam demand before heat exchanged reformer	23.8
Excess water		71.3

4.1.3.4 Power Production

To determine if the process is self sufficient with power, a power balance was made (Table 4.12).

Table 4.12: Power balance in the process.

		Power [MW]
Power sinks	Air compression to process	90.4
	Air compression to gas turbine	49.1
	H_2 compression	3.0
	CO_2 recycle compression	0.2
Power source	Gas turbine	179.0
Excess power		36.4

The main power sink in the process is compression of air to the process. However, in the process there are an excess of power of 36.4 MW. Some external power generation is good for a FPSO design, to supply energy to other parts of the FPSO.

4.1.4 Equipment Sizing

For a GTL-FPSO plant it is important to considered the space and weight of the equipments. The size and weight of different equipments were calculated, with the result given in Table 4.13. A detailed calculation for the different equipments are given in Appendix I. It is assumed that all equipments are made with stainless steel, with a density of 8,000 kg/m^3 [47]. The weight given in this table is only the equipment weight, the catalyst in the reactors are not included.

Table 4.13: An overview over sizes of different equipments in the plant.

Equipment	Outer Size			Weight [tonne]
	Diameter [m]	Height/ Length [m]	Volume [m^3]	
Pre-reformer	3.9	8.1	86.4	62.2
ATR	6.8	14.1	455.1	307.7
HER	2.9	18.0	111.9	96.0
Syngas separator	4.3	10.3	137.1	70.6
Membrane separator	1.5	4.7	8.1	2.9
WGS reactor	2.3	4.8	18.4	11.2
Carbon membrane	0.3*	1.2*	13.2	0.03
Air membrane	0.2*	1.6*	241.8	211.7
FT reactor 1a/1b	6.6	20.0	593.4	367.9
FT reactor 2a/2b	5.8	20.0	475.2	290.5
FT reactor 3	7.4	20.0	733.0	460.3
Steam drum	3.1	13.8	88.5	46.3
Three phase separator 1	2.6	11.5	54.1	18.5
Three phase separator 2	2.3	10.3	39.0	12.5
Three phase separator 3	1.9	8.6	22.7	6.2

*Size of one membrane unit

The FT reactor is the most important equipment to evaluate as it counts for a large part both of the volume and the weight. In the table above the first and second FT reactors are divided in two shells in parallel. By having one reactor the diameter is increased giving a shell with a thicker wall. A comparison of having two reactor shells in series and having one reactor is given in Table 4.14.

Table 4.14: Comparison of FT reactor size and weight, if first and second reactor stages are divided in to shells in parallel or not.

	Reactor 1		Reactor 2	
	Two shells	One shell	Two shells	One shell
Diameter [m]	6.4	9.1	5.7	8.0
Outer volume [m^3]	1,187	1,114	950	900
Weight [tonne]	736	726	581	575
Weight with catalyst [tonne]	1,079	1,069	851	845

By dividing the reactors in two shells in parallel, the total weight of reactor 1 is reduced with 10 tonne and reactor 2 reduced with 4 tonnes. The outer volume of the reactor 1 and 2 when changing from one shell to two are reduced with respectively 73 m^3 and 50 m^3. As the weight and volume are reduced it is decided to have two shells in parallel for reactor 1 and 2. Another

reason for dividing the reactors into two is to reduce the shell diameter to ensure that the weigh on the tube distribution plat in the reactor is not to big.

4.1.5 Cost Estimations

A cost estimate of the equipments for the GTL plant was made and the result are given in Table 4.15. The catalyst cost is included in the cost for the reactors. The equation used and detailed calculations are given in Appendix J. To calculate the installed cost a factorial method given in Appendix J was used. The factors included are piping, equipment erection, instrumentation and control, electrical, and lagging and paint. Factors like civil and structure and buildings are not included in the equipment installation cost as it is assumed to be a part of the ship.

All the equipment is assumed to be in stainless steel. However, when calculation the purchased equipment cost for some of the equipments, the cost correlations used gives the value in carbon steel. This is also the reason for different installation factors used for the cost calculations.

Table 4.15: An estimation of equipments cost for the process.

Equipment	Equipment cost [million$]	
	Purchased	Installed
Pre-reformer	1.3	2.8
ATR	8.7	20.4
Air membrane**	18.8	37.5
HER	2.1	6.6
WGS reactor	0.3	0.7
Separators	1.2	3.1
Compressors*	9.3	30.2
Carbon membrane**	2.6	5.1
FT reactors	42.6	100.9
Steam drum	0.7	1.8
Three phase separator	0.7	1.8
Heat exchangers*	7.4	24.1
Gas turbine	40.4	43.1
Total	136.2	278.1

* purchase equipment cost in carbon steel

** installation factor of 2 are used

The cost of the FT reactor without the catalyst has been estimated with the use of several different methods, giving a wide range of results (Table 4.16). The method used are listed below:

1. The cost is calculated based on a cost correlation for a shell and tube heat exchanger given by Walas [48].

2. The cost is calculated based on a U-tube shell and tube heat exchanger with correlations given by Sinnott and Towler [40].

3. The FT reactor cost is calculated based on cost correlations for a pressure vessel given by Sinnott and Towler [40]. The cost of the reactor tubes were calculated in two different ways. The first method is based on a correlation found in literature [49] given an approximately price of 0.5 $/feet of tube (1991 price) (3a). In the second method the reactor tubes is calculated based on tube prices given online to 4,000 $/tonne [50] (3b).

4. The last method used was by calculating the cost of the material needed for the unit, with material cost found from two different sources online. The cost used was 2,762 $/tonne [51](4a) and 2,899 $/tonne [52](4b).

Table 4.16: Estimation on Fischer-Tropsch reactor cost with the use of different cost estimate methods.

Method	Equipment cost [million$]	
	Purchased	Installed
1	402.8	765.4
2	46.9	152.0
3a	19.5	48.7
3b	19.6	48.8
4a	4.9	12.2
4b	5.2	12.8

The correlation used for 1 and 2 is giving cost estimates for a given region for heat transfer area. However, the heat transfer area in the reactors are much larger than the correlation is made for. This gives an over estimation of the cost, due to extrapolation errors.

Method 4a/b is clearly underestimating the cost and gives the lower limit for FT reactor cost. As it only gives the cost of the material used for producing the reactor and do not include the price of making the reactor.

The last method used (3a/b) gives also an underestimation of the cost, due to only including the cost of the pressure vessel and the tubes. The work to connect the parts is not included. To decide a cost estimate for the FT reactor it is assumed that method 3a/b gives the best result. However, it is assumed that the cost of the equipments parts counts for 50% of the total cost. This will give purchased equipment cost for the reactor of 39.1 million$ and installed cost of 97.4 million$ without catalyst.

The FTS counts for 37.6% of the total equipment cost (ISBL), and the syngas production counts for 32.0% (Figure 4.6). For a normal GTL plant the syngas normally counts for around 60% of the total capital investment for the plant [28, 53]. However, for this design as the ASU is removed from the syngas production this plant has a more economically syngas production.

And due to the use of enriched air in the process the FT reactor size and other equipments in FTS is increased giving a larger cost for the FTS.

Figure 4.6: Illustration of the contribution different parts of the process has to the total investment cost.

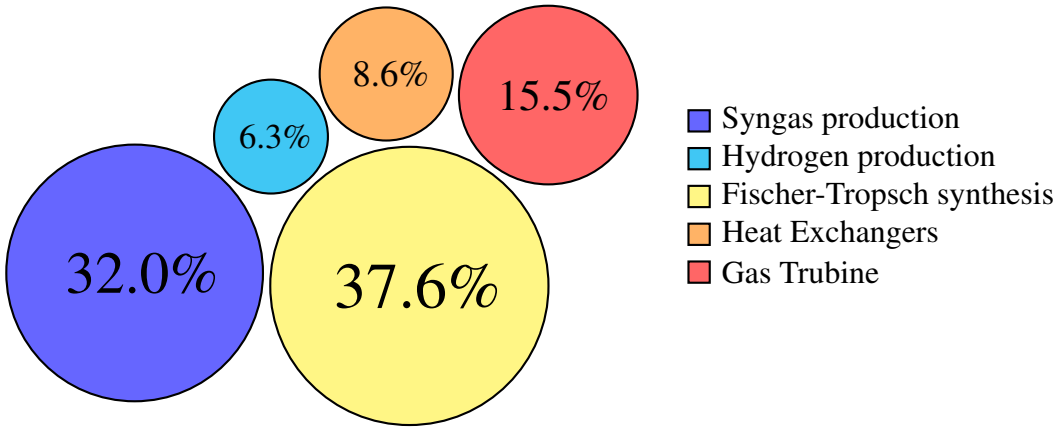

The equipment included in the syngas production part is the ATR, the pre-reformer, air compression and air membrane. The hydrogen production part includes HER, WGS reactor, carbon membrane and the two separators. The FT reactors, the steam drum and the three phase separators are included in the FTS part. The gas turbine part consist of the air compression to the combustion, the turbine and the three heat exchangers for pre-heating of natural gas. All the other heat exchangers in the process are included in the heat exchanger part.

The total investment cost is the sum of the total fixed capital cost and the working capital and is found to be 543.7 million$ (Table 4.17). Working capital is the cost needed to start up and run the plant before it produces it own income and is set to 15% of the fixed investment cost [40].

Table 4.17: Total investment, including installed equipment cost, offsite cost, design and engineering cost, contingency cost, working capital costs and fixed capital investment for the process.

Cost	million$
Total ISBL cost	278.1
Offsites	83.4
Engineering and design	83.4
Contingency	27.8
Fixed capital investment	472.8
Working capital	70.9
Total investment cost	543.7

In the literature total investment cost of existing onshore GTL plants are given as investment cost per barrel per day (bpd) produced of FT product with value of around 100,000 $/bpd or above [54,55]. An evaluation of a once-through GTL process with slurry reactor was evaluated

to have a investment cost of approximately 84,900 $/bpd (2014 price) [56].

For this process the investment cost is approximately 54,400 $/bpd. It is expected that the cost of this process should be lower than for commercialised GTL plants, as it is a simple process design with a low cost syngas production. When calculating the installation cost for this process some factors, as mentioned earlier, is not included. Therefore comparison with values from literature is not that easy as not all the same values are used. However, it gives an indication that the process is cheaper than commercialized design.

4.2 Parameter Optimizing

In a GTL process there are many degrees of freedom, and many parameters that can be optimized. In this master thesis the optimizing was towards getting highest possible C_{5+} production.

This section gives the background and evaluation of the different parameters used in the final process design (Table 4.2 in section 4.1). For the evaluations the number of tubes in the FT reactor is changed to keep the gas space velocity constant to 0.43 m/s. This is done to keep the residence time in the reactor constant for all the evaluations.

4.2.1 Simulation Improvements

During the work, improvements of the process have been included. This results in different operation conditions under evaluation of different parameters. The two main changes that has been done is the use of another type of hydrogen selective membrane, and change of effectiveness factor in the FT reactor.

4.2.1.1 Hydrogen Selective Membrane

In the beginning of the work a hydrogen selective polymer membrane was used in the simulation [57]. For this type of membrane, the separation of H_2 from CO_2 was low, and much of the CO_2 passed through the membrane. The effect of recycle CO_2 is mentioned earlier in section 2.1.3, and it is favourable to recycle as much as possible of the CO_2. Because of this result, other membrane alternatives was evaluated. The membrane used in the final process design is a carbon membrane.

The split factors for the permeate side (H_2 rich stream), for both the polymer membrane and the carbon membrane is given in Table 4.18.

During the work the main evaluation for some of the parameters, that will be discussed in the following sections, are preformed with the hydrogen selective polymer membrane. However,

values are tested for the carbon membrane to check that the optimal point is not completely changed.

Table 4.18: The split factors used in the component splitter in the simulation for the hydrogen selective membrane, for both polymer membrane and carbon membrane.

	Split fraction Permeate [-]	
Component	Polymer membrane	Carbon membrane
CO_2	0.490	0.037
H_2	0.840	0.845
CO	0.140	0
H_2O	0	0
CH_4	0.050	0

4.2.1.2 Effectiveness Factor in Fischer-Tropsch Reactor

The effectiveness factor for a catalyst is defined as the ratio of the actual overall rate of reaction to the rate of reaction if entire interior surface were exposed to the external pellet surface conditions [58].

In the beginning of the work it was assumed a 100% catalyst loading on the pellet. The effectiveness factor was then calculated including concentration gradient and diffusion through the catalyst pellets. The first reactor used in the work has therefore different effectiveness factor for the different reactions (3.2.1 - 3.2.4). The calculated values was reduced with 50%, due to unexpected high conversion. However, during the work new information about the catalyst was found, and an egg-shell catalyst type were used. This mean that catalyst pellets only has a thin layer of active catalyst, giving constant equal effectiveness factor for all the reactions. It was assumed a catalyst loading of 8%. The effectiveness factors for the two reactors are given in Table 4.19. In this mater thesis the first reactor will be called Reactor A, while the final reactor used is called reactor B.

Table 4.19: Overview of the effectiveness factors for the different reactors.

	Reactor A	Reactor B
Effectiveness factor 1 [-]	0.1	0.08
Effectiveness factor 2 [-]	0.175	0.08
Effectiveness factor 3 [-]	0.5	0.08
Effectiveness factor 4 [-]	0.025	0.08

Some of the parameter evaluations where performed in more detailed for the Reactor A, then for the reactor B. However, simulations are repeated with reactor B to check the results.

4.2.2 Flow Distribution to ATR and HER

As mentioned earlier is hydrogen needed several places in the process. The flow amount to the heat exchanged reformer decide how much hydrogen is produced in the plant. However, more natural gas feed to the HER gives less syngas produced in the ATR, resulting in a lower feed flow to the FTS. Different split ratios for ATR and HER was evaluated to find the optimal distribution of natural gas.

This evaluation was performed for both the reactors and the different hydrogen selective membranes, however only the results with the use of hydrogen selective carbon membrane (Table 4.18) is reported in this section. In the evaluation of split factor the temperature out of the ATR was kept at a constant value of 1060°C by adjusting the enriched air feed. As mentioned in section 2.2 is the H_2/CO ratio decreased over the reactor if the ratio in the feed is under-stoichiometric and decreased if the feed has a over-stoichiometric ratio. In the simulation when the ratio is decreased hydrogen is added to maintain the same ratio for each reactor inlet. However, it the ratio is increased no hydrogen is added or removed and the ratio is not the same for each reactor inlet.

The result of changing the flow split between ATR and HER with the use of Reactor A (Table 4.19), and a steam to carbon ratio to the ATR of 0.3 is given in Figure 4.7. The results indicates an increase in production with more flow to the HER. This will also give a higher production of H_2 (illustrated in Figure 4.8), which is higher than needed in the process. These results led to a lot of time spent on evaluations performed with Reactor A with 85% of the natural gas feed to the ATR and 15% to the HER. However, only the results from evaluation of oxidant feed to the ATR is included (section 4.2.4.1 and section 4.2.4.2). The other values are not reported as Reactor B altered the results.

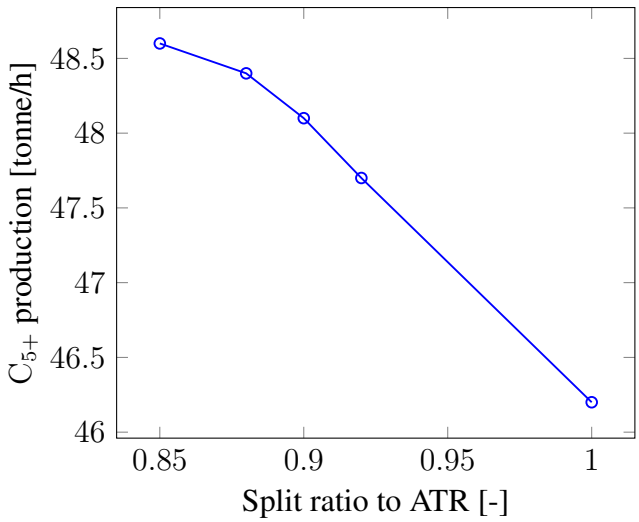

Figure 4.7: C_{5+}production as a function of split ratio to the ATR, with S/C=0.3 and Reactor A.

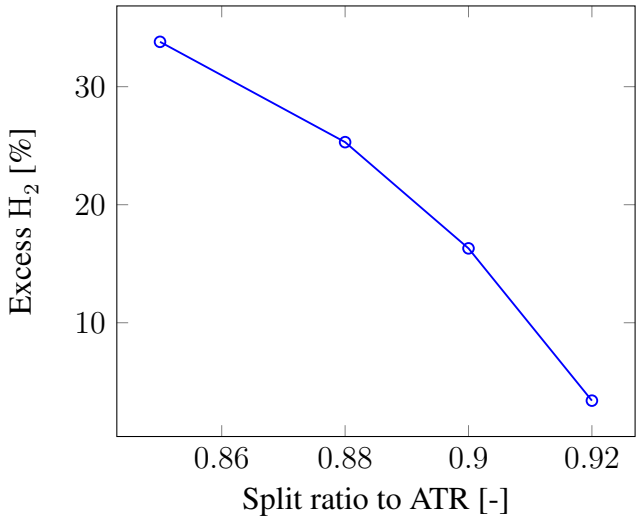

Figure 4.8: Excess H_2 in the process as a function of split ratio to the ATR, with S/C=0.3 and Reactor A.

By changing the effectiveness factors for the FT reactor the result for C_{5+} production as function of flow to ATR was changed. The evaluation was therefore repeated for Reactor B with a steam to carbon ratio of 0.6 (Table 4.20).

Table 4.20: Result of changing the split of feed to ATR and HER with S/C=0.6 and Reactor B.

Split ratio to ATR [-]	0.85	0.9	0.92	0.95	0.97	1.0
H_2/CO ratio [-]	2.00	2.10	2.13*	2.18*	2.22*	2.28*
CO conversion [%]	88.92	89.47	89.87	90.49	91.03	90.64
C_{5+} product [tonne/h]	53.34	53.52	53.53	53.34	53.23	52.84
CH_4 selectivity, reactor 1 [%]	6.44	6.88	7.11	7.38	7.57	7.66
CH_4 selectivity, reactor 2 [%]	8.70	9.32	9.75	10.38	10.80	11.02
CH_4 selectivity, reactor 3 [%]	13.12	14.18	14.86	16.92	18.39	19.41

*H_2/CO ratio is increased over the reactor

As mentioned earlier, when the feed is over-stoichiometric the ratio will increase, this happens for a split ratio higher than 0.9. The H_2/CO ratio is increased with more flow to the ATR. This is expected as less flow to the HER will give less recycle of CO_2. A higher recycle flow of CO_2 will give a lower H_2/CO ratio, according to the water gas shift reaction.

The CO conversion is increased with higher split. This can be explained from the kinetic model [1, 2] that dictates enhanced reaction rates for higher H_2/CO ratio. However, the chain growth probability, α is decreases, giving less selectivity towards higher hydrocarbons, C_{5+}.

The reason for the increased methane selectivity in the process is because of the reduction in pressure and increased amount of inter. This gives an reduction in the H_2 partial pressure lead-

ing to a lower α value and therefore higher selectivity to lower hydrocarbons, due to the applied kinetic model [1, 2].

The production of C_{5+} is dependent on several parameters like temperature, pressure, steam to carbon ratio and H_2/CO ratio. An illustration of the production of C_{5+} for different split ratio to ATR is given in Figure 4.9.

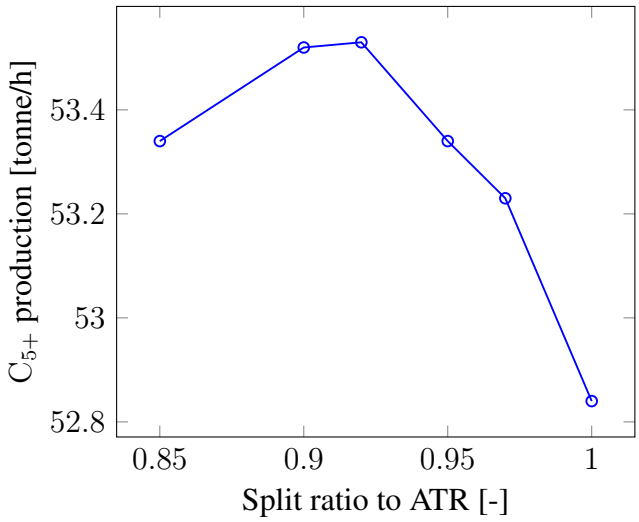

Figure 4.9: C_{5+} production as a function of split ratio to the ATR, with S/C=0.6 and Reactor B.

The curve has a maximum production point with a split around 90-92%. The difference in production for these two split is small, and as the H_2/CO ratio is increased over the reactors with 92% split, the optimal point is decided to be 90% split.

The production of C_{5+} with the decided split of 90% is increased with 0.5 tonne/h compared to a process design with no heat exchanged reformer. Even though the production is not increased with a very high amount the introduction of the HER is favourable. In addition to producing the required hydrogen needed in the process the heat exchanged reformer provides efficient heat integration and avoids the use for a waste heat boiler downstream the ATR. Further, the HER gives possibilities for recycle of CO_2 rich gas that reduced the H_2/CO ratio in the syngas increasing the selectivity towards C_{5+} production.

4.2.3 Steam to Carbon Ratio

Steam to carbon ratio (S/C) is defined as the steam amount divided on the total amount of carbon atoms in all hydrocarbons and CO [28, 32]. As earlier mentioned is the ATR commercialized with a steam to carbon ratio of 0.6 by Haldor Topsøe. The effect of using a lower steam to carbon ratio was evaluated, for the process design with Reactor B and hydrogen selective carbon membrane.

The H_2/CO ratio is changed with the steam to carbon ratio and an illustration is given in Figure 4.10.

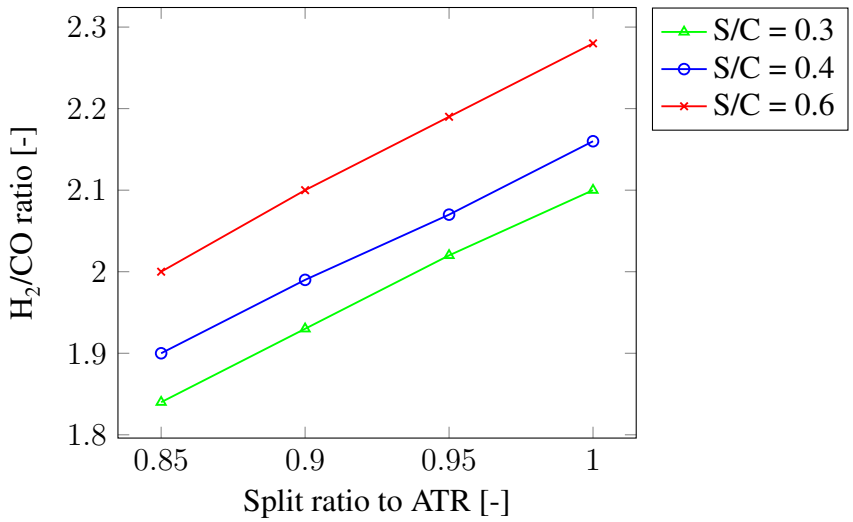

Figure 4.10: The effect of changing the steam to carbon ratio in the feed to the ATR on the H_2/CO ratio.

The reduction in H_2/CO ratio with reduced S/C ratio can be explained from the WGS reaction (2.1.7). With less addition of H_2O the reaction would be shifted towards left according to Le Chatelier's principle. This gives an increased production of CO giving a lower H_2/CO ratio.

The steam to carbon effect on the production of C_{5+} with different flow amount to the ATR is illustrated in Figure 4.11 and a comparioson of the result from a design with 90% flow to the ATR and different steam to carbon ratios is given in Table 4.21.

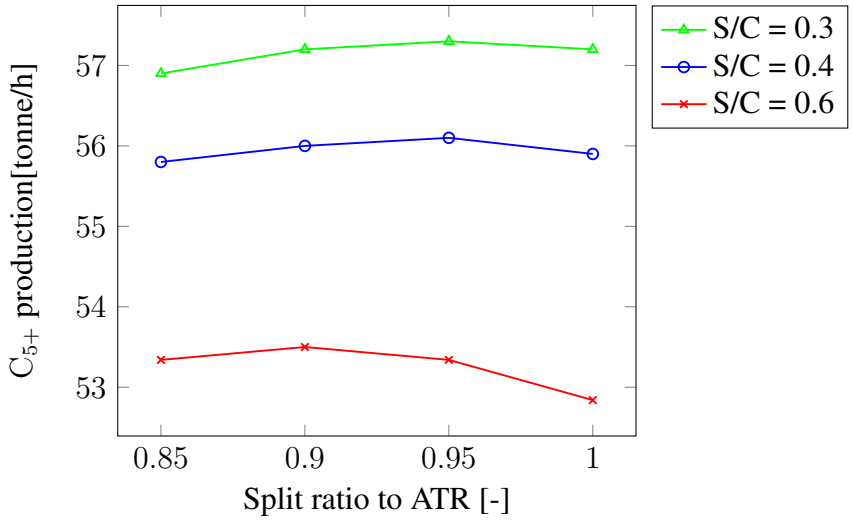

Figure 4.11: The effect on changing the steam to carbon ratio in the feed to the ATR on the production of C_{5+}.

Table 4.21: The effect of changing the steam to carbon ratio in the feed to the ATR, in a process design where 90% of the natural gas goes to the ATR and 10% to the HER.

Steam to carbon ratio [-]	0.3	0.4	0.6
H_2/CO ratio to first reactor [-]	1.93	1.99	2.10
CO conversion [%]	87.9	88.6	89.6
C_{5+} product [tonne/h]	57.2	56.0	53.5
CH_4 selectivity, reactor 1 [%]	6.0	6.3	6.9
CH_4 selectivity, reactor 2 [%]	7.9	8.4	9.4
CH_4 selectivity, reactor 3 [%]	11.7	12.6	14.3

A lower steam to carbon ratio is favourable for C_{5+} production, as it gives a syngas with lower H_2/CO ratio, and therefore higher selectivity to higher hydrocarbons. Reducing the steam to carbon ratio from 0.6 to 0.3 gives an increase in production of 3.7 tonne/h. However, a low steam to carbon ratio can give carbon formation problems in the pre-reformer and soot formation in the ATR. Due to this and industrial experience of using a steam to carbon ratio of 0.6, this value is chosen for the final design. However, as it is beneficial to have a lower steam to carbon ratio, a lower value was used in the beginning of the work. In some parameter evaluations a steam to carbon ratio of 0.3 has therefore been used, which will be specified in the text.

4.2.4 ATR oxidant feed

In the beginning of the work an air-blown ATR was used, however, this was changed during the work to the use of enriched air. This section gives information about evaluation of the use of air, and enriched air.

4.2.4.1 Air

In a early stage of the work, the air feed temperature and amount to the ATR was evaluated. This evaluation was done only looking at the syngas production part of the process. Three different evaluations were performed: the effect of changing the air temperature, the amount of air at 250°C and the amount of air at 550°C.

For this evaluation pure air was fed to the ATR, the amount of natural gas feed was 22,000 kmole/h, with 85% to the ATR and 15% to the HER. The steam to carbon ratio before the ATR was adjusted to 0.3, and the hydrogen selective polymer membrane and Reactor A was used.

The inlet air temperature to the ATR was changed to evaluate what effect a higher air temperature would have on the syngas production. In this evaluation, the temperature out of the ATR was kept constant to 1,050°C by changing the amount of air feed. Table 4.22 gives gives the amount of air needed to reach the decided outlet temperature with different air inlet temperatures, the H_2/CO ratio for the syngas and the fraction of inert in the syngas, including CH_4, N_2

and CO_2.

Table 4.22: The effect of changing the temperature of the air feed to the ATR, on the amount of air needed to the ATR and the inert concentration to the FTS.

Air temperature [°C]	250	350	450	550
Air flow amount [kmole/h]	66,409	63,936	61,580	59,330
Fraction of inert to FTS	0.50	0.49	0.48	0.46
H_2/CO ratio [-]	1.91	1.92	1.94	1.95

A further evaluation was done for two of the air temperatures; 250°C and 550°C. In this evaluation the ATR outlet temperature was not set to a given value, and the effect of air feed amount was evaluated (Figure 4.12).

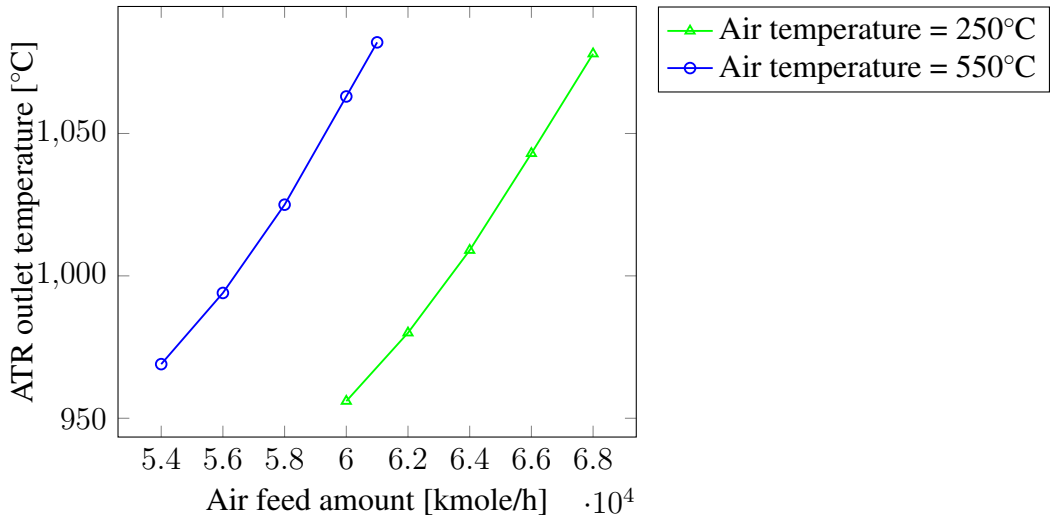

Figure 4.12: The ATR outlet temperature as a function of air feed amount, for air temperature of 250°C and 550°C

The result is as expected. A higher pre-heat temperature of the air, would reduce the amount of air needed in the process, to achieve the same amount of heat for the endothermic reaction.

To increase the selectivity towards higher hydrocarbon a low H_2/CO ratio is wanted, and therefore, as illustrated in Figure 4.13, a high ATR outlet temperature is favourable.

By pre-heating the air feed as much as possible, the amount of inert in the system is kept to a low value. However, for the ATR there are a material limitation for pre-heating. According to information from Syntroleums patent [59] and confirmation on material limitation from Haldor Topsøe [32], it was decided to pre-heat the air to 550°C.

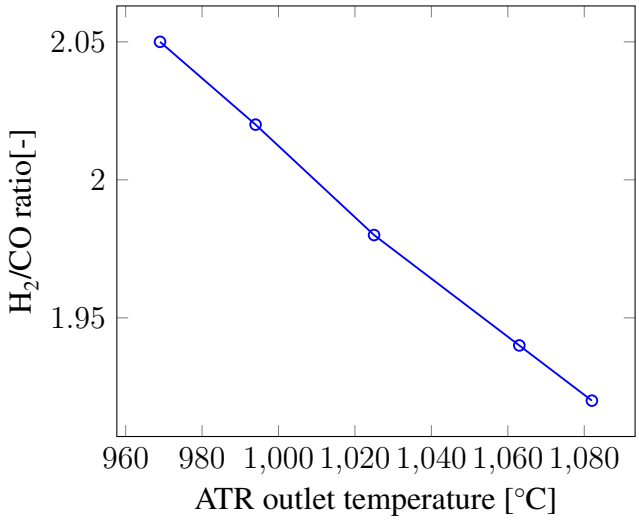

Figure 4.13: H_2/CO ratio as a function of ATR outlet temperature.

4.2.4.2 Comparison of Air, Enriched Air and Pure Oxygen

To reduce the amount of inert in the system, and improve the process design, the PRIMS membrane from Air Products was included to produce enriched air as feed to the ATR.

For the air membrane, performance are decided from the data sheet received form Air Product [43]. However, the membrane performance is changed with different feed pressures, and an evaluation was performed to decide the optimal operation of the membrane.

In the simulation the membrane is simulated as a component splitter and the information about calculation and the different split factors to be used with different air feed pressure are given in Appendix C.

The process design with 85% of the natural gas feed to the ATR and 15% to the HER, steam to carbon ratio of 0.3, hydrogen selective carbon membrane, and Reactor A was used in the evaluation of the air membrane. Different split factors for the component splitter and feed pressure to the air membrane was used.

A comparison between the use of air, pure oxygen and the different air membranes are given in Table 4.23. When using an air membrane the feed amount given in the table is the feed to the membrane. However, for the use of air or pure oxygen the feed is the amount fed to the ATR. The inert fraction in the syngas includes CH_4, N_2 and CO_2.

Table 4.23: The result from the simulations with the use of air, different air membranes and oxygen as feed to the ATR.

	Air	Enriched Air					O_2
Membrane feed pressure		15 barg	12 barg	9 barg	7 barg	5 barg	
Feed amount [kmole/h]	16,443	17,056	17,395	17,814	17,007	16,981	2,962
Inert fraction in syngas	0.47	0.31	0.31	0.32	0.32	0.34	0.06
H_2/CO ratio [-]	1.827	1.851	1.851	1.850	1.849	1.847	1.884
Total CO conversion [%]	94.1	94.6	94.6	94.5	94.5	94.5	93.1
C_{5+} product [tonne/h]	42.9	48.6	48.5	48.3	48.1	47.6	54.6

The result is as expected, with the highest production for pure oxygen feed and the lowest for air feed. The change in C_{5+} production for the different enriched air feed pressures are small. To decide the air feed pressure to use, the membrane capacity was evaluated.

A high feed pressure to the membrane reduces the number of membrane units needed (Table 4.24). However, the compression work before the membrane would be increased. The nitrogen rich tail gas from the membrane could be used in the gas turbine, and then the high pressure is favourable. It is therefore decided to use an air membrane with feed pressure of 15 barg. This is also the highest allowable feed pressure for the proposed membrane according to vendor [34].

Table 4.24: The capacity of the air membrane and number of membrane units needed for different air feed pressures.

Membrane feed pressure [barg]	15	12	9	7	5
Air feed capacity one unit [kmole/h]	2.27	2.12	1.53	1.15	0.77
Total membrane units [-]	6,278	8,056	11,119	14,831	22,049

The use of air in the ATR was tested with the final design giving an reduction in C_{5+} production of 3.6 tonne/h compare to the use of enriched air.

4.2.4.3 Enriched Air

It is expected that the trends for air feed amount and temperature would be the same for the new improvements of the process design with change in effectiveness factor, hydrogen selective carbon membrane and the use of enriched air. However, some evaluation was repeated to evaluate the effect of enriched air temperature on the C_{5+} production.

In this evaluation enriched air with oxygen content of 34.3% was fed to the ATR. The amount of natural gas feed was 6,000 kmole/h, with 90% to the ATR and 10% to the HER. The steam to carbon ratio before the ATR was adjusted to 0.6.

The result of changing the pre-heat temperature of the enriched air is given in Table 4.25 and illustrated in Figure 4.14. The outlet temperature of the ATR is kept constant to 1,060°C by adjusting the feed amount of enriched air.

Table 4.25: The effect of changing the temperature of the enriched air feed to the ATR, on the amount of enriched air needed to the ATR and production of C_{5+}.

Enriched air temperature [°C]	350	450	500	550
Enriched air amount [kmole/h]	10,363	10,146	10,039	9,933
C_{5+} production [tonne/h]	52.9	53.2	53.4	53.5

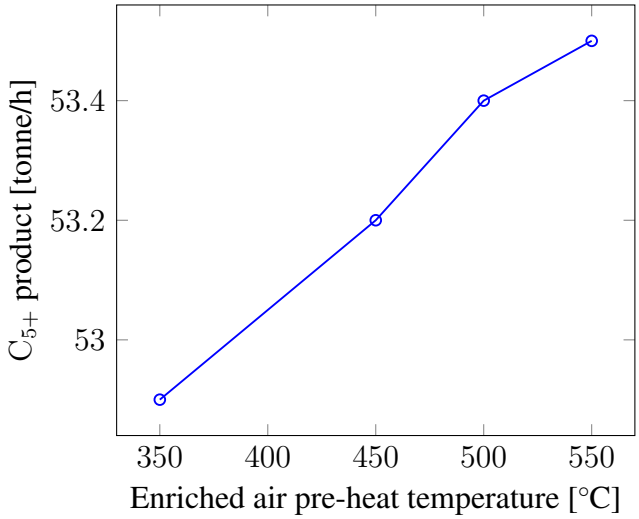

Figure 4.14: C_{5+} *production as a function of enriched air pre-heat temperature.*

The conclusion is the same as for the air evaluation and a pre-heat of the air feed to 550°C and a ATR outlet temperature of 1,060°C is used in the final design.

4.2.4.4 Cost Evaluation of Air Membrane

A simple cost evaluation of the use of an air membrane was done, for the results given in section 4.2.4.2. This was done in order to evaluate if the use of an air membrane is economical feasible. In this evaluation the cost of the membrane was compared with the extra income for the increased production.

The annual capital charge for the membrane was found from equation 4.2.1 with the use of the annual capital charge ratio (ACCR) equation 4.2.2 [40].

$$C_y = ACCR \cdot C_{inv} \tag{4.2.1}$$

$$ACCR = \frac{i(1+i)^n}{(1+i)^n - 1} \tag{4.2.2}$$

where i is the interest rate, n is the lifetime for the membrane, C_y is the annual capital charge, and C_{inv} is the investment cost of the membrane.

The lifetime for the membrane is set to 10 year by the vendor [34], and two different interest rate has been evaluated; 5% and 10%.

Three different crud oil prices ($/barrel) has been evaluated and it is assumed that the FT product price is 5% higher than the crude oil price. In addition, it is assumed 8,400 operating hours per year.

For these evaluations it is assumed that all the other equipment cost would be the same, that might not be correctly as the equipments size may increase as the amount of inert in the system is increased (Table 4.23, section 4.2.4.2). The extra power needed for compression of the air is not included in the calculation. In addition, the produced amount of power from the gas turbine is not evaluated. No conclusion can be made from these evaluations, however, it indicates that including an air membrane may be an economical solution (Figure 4.15).

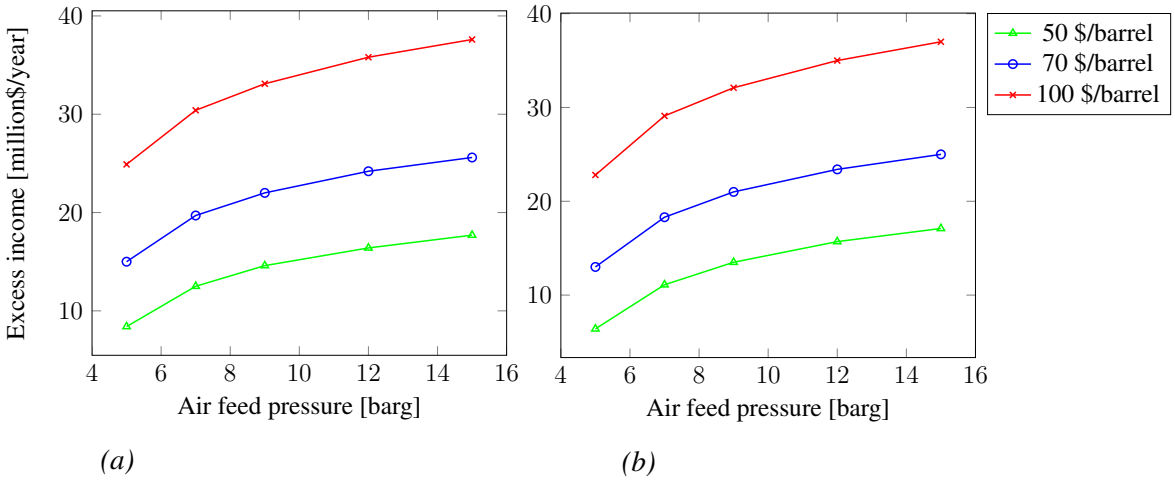

Figure 4.15: The total excess income with the use of different feed pressure to the air membrane, and three different crud oil prices. Fischer-Tropsch product price is assumed 5% higher than crude oil. (a) interest rate of 5% and (b) interest rate of 10%.

4.2.5 Hydrogen to Carbon Monoxide Ratio

For the process design it was decided to keep the same H_2/CO ratio for the inlet of each reactor. The amount of hydrogen added between the stages, was decided so the H_2/CO ratio was maintained.

When selecting operating conditions for temperatures, steam to carbon ratio and the distribution of natural gas to ATR and HER, a value for H_2/CO ratio is given.

A lower value for the H_2/CO ratio would probably have been preferred to increase the selectivity towards higher hydrocarbon, however the reaction rate would then be reduced. If a lower ratio should be obtained more CO_2 need to be recycled or a lower steam to carbon ratio need to be used.

4.2.6 Hydrogen Selective Carbon Membrane

The gas velocity and outlet pressure on the permeate side for the membrane, were evaluated to find a membrane design with a good separation of H_2 and CO_2.

First the flow velocity through the membrane was evaluated. The pressure of the feed (P_h) was 25.5 bar and the pressure of the permeate (P_l) was set to 2.55 bar to give a pressure ratio to 10. The pressure ratio is defined as the pressure of the feed over the pressure of the permeate. This value was decided as commercial membrane separation processes usually operates with a pressure ratio between 5-15 [60]. The feed amount to the membrane is 2,993 kmole/h with the composition given in Table 4.26.

Table 4.26: The composition of the feed to the membrane used for the evaluation of flow velocity and permeate pressure for the membrane.

Component	Mole fraction [-]
CO_2	0.1482
H_2	0.7776
CO	0.0682
H_2O	0.0019
CH_4	0.0040

To decide flow velocity the parameters that has been evaluated is the membrane area and H_2 fraction in the retentate. As indicated from Table 4.27, the amount of hydrogen in the retentate (CO_2 rich stream) is reduced with increased residence time. A higher residence time would also give an increased membrane area. Since the H_2 fraction in the retentate is only 0.117 with a flow velocity of 0.08 m/s it is decided to design the membrane with a velocity of 0.08.

Table 4.27: The MATLAB results of changing gas feed velocity with a pressure ratio of 10. Pressure of feed is 25.5 bar and the pressure of the permeate is 2.55 bar.

Velocity [m/s]	Membrane area [m^2]	H_2 fraction in retentate [-]
0.08	10,273	0.117
0.09	9,132	0.155
0.1	8,219	0.204
0.2	4,109	0.568
0.3	2,740	0.662
0.4	2,055	0.698
0.5	1,644	0.717
0.6	1,370	0.729
0.7	1,174	0.737
0.8	1,027	0.743
0.9	913	0.747
1	822	0.751

A high pressure ratio is recommended to give the best separation. However, with a low permeate pressure more duty is needed for compression of the hydrogen to be used in the FTS. As illustrated in Table 4.28 the hydrogen fraction in the retentate is increased with reduced pressure ratio. The decision for permeate pressure is therefore an economical evaluation.

Table 4.28: MATLAB results of changed permeate pressure with a gas velocity in the membrane of 0.08 m/s.

P_l [bar]	Pressure ratio [-]	H_2 fraction in retentate [-]
2.55	10	0.117
7	3.6	0.357
10	2.55	0.508

A evaluation between having a ratio of 10 with permeate pressure of 2.55 bar and a permeate pressure of 7 bar was done for the final design. By increasing the permeate pressure to 7 bar, the C_{5+} production will be reduce with 0.1 tonne/h (Table 4.29). However, it would also reduce the need for compression with 55.5%. From this evaluation it is decided to use a permeate pressure of 7 bar.

Table 4.29: Comparison of having a permeate pressure of 2.55 or 7 bar.

P_l [bar]	H_2 in retentate [kmole/h]	Compressor duty [MW]	C_{5+} product [tonne/h]
2.55	85	7.13	53.5
7	360	3.17	53.4

4.2.7 Number of Tubes in Heat Exchanged Reformer

For the evaluation of optimal operating conditions for the process the number of tubes in the heat exchanged reformer (HER) was set to 1,000. However, when the other parameters was decided a closer evaluation of the HER was done. Due to heat transfer in the HER the minimum temperature (ΔT_{min}) of hot inlet stream and cold outlet stream should be 10°C.

With 1,000 tubes in the heat exchanged reformer the ΔT_{min} was 0. To obtain the temperature difference required the number of tubes needs to be reduced to 280.

The design of the shell to the HER in the model is connected to the number of tubes. The shell diameter is calculated based on a given distance between each tube, referred to as pitch. With a low number of tubes, the cross section of the shell side will be small compared to the large volume flow passing through. For the HER used in this process design, a small stream is going through the tubes and a large flow in the shell, and to avoid a large pressure drop for the shell side, the pinch distance needs to be increased. However, as the HER model gives a reduction in the shell size when reducing the number of tubes the calculated pressure drop for the shell side is very high (Figure 4.16). As the pressure drop is not expected to be that high a compressor and cooler is included in the simulation to balance for the unrealistic high pressure drop.

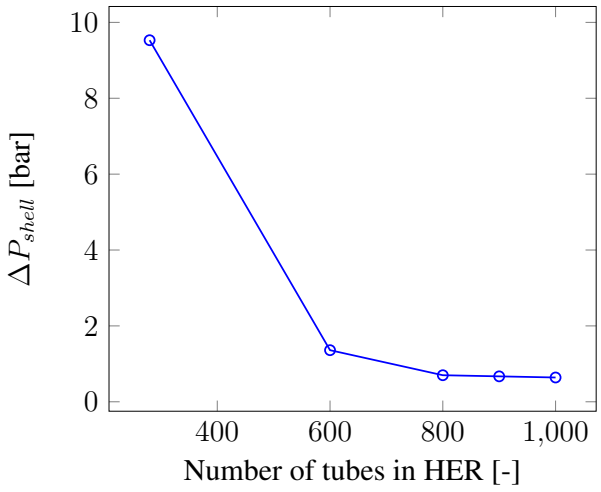

Figure 4.16: Illustrates the calculated pressure drop for the shell side of the heat exchanged reformer (HER) as a function of number of tubes.

4.2.8 Gas Turbine

After the last FT reactor the tail gas is sent to the gas turbine for power production. The nitrogen rich stream from the air membrane could also be sent to the gas turbine. An evaluation of the effect of using the nitrogen flow was performed. The amount of air feed to the gas turbine is adjusted to a give 15% more than stoichiometric consumption of oxygen.

The nitrogen is an inert component in the combustion for the gas turbine, and it was found that a large volume flow of inert helps reducing the gas turbine inlet (TIT) and outlet temperature (TOT) (Figure 4.17).

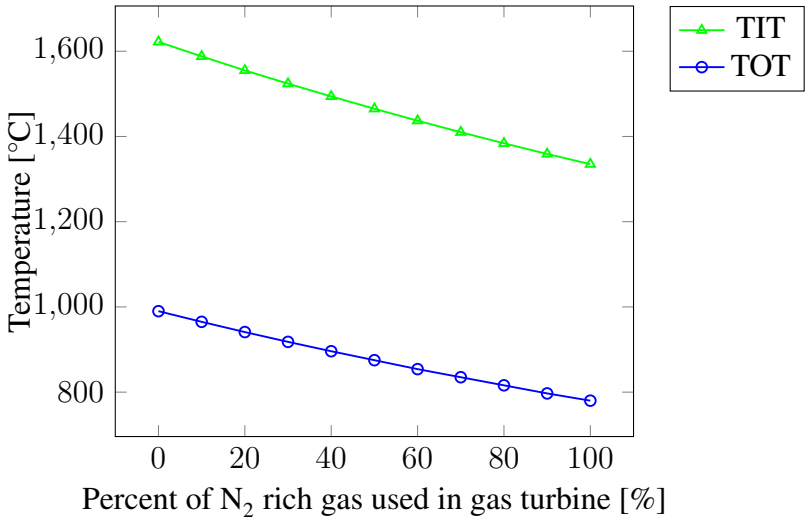

Figure 4.17: Illustrates how the gas inlet and outlet temperature is changed by adding N_2 rich stream from the air membrane.

The excess power production in the plant is increased with the amount of N_2 added (Figure 4.18). From this evaluation it is decided to include all the N_2 rich gas from the air membrane as it both increase the excess power production, but also reduces the inlet temperature for the gas turbine.

In the process the tail gas has a pressure around 19 bar, the nitrogen rich gas has a pressure of 16 bar. An evaluation for the gas turbine power production with respect to air pressure was done, with result given in Figure 4.19. As the nitrogen rich gas has a pressure of 16 bar, it is decided to use 16 bar as inlet for the gas turbine. The reason for this choice is that an higher pressure would have required more compressor units for compression of the tail gas and the N_2 rich gas. As the plant is to be placed on a FPSO, space is one important issue, when operating at 16 bar as high as possible pressure is used without the need of extra compressors.

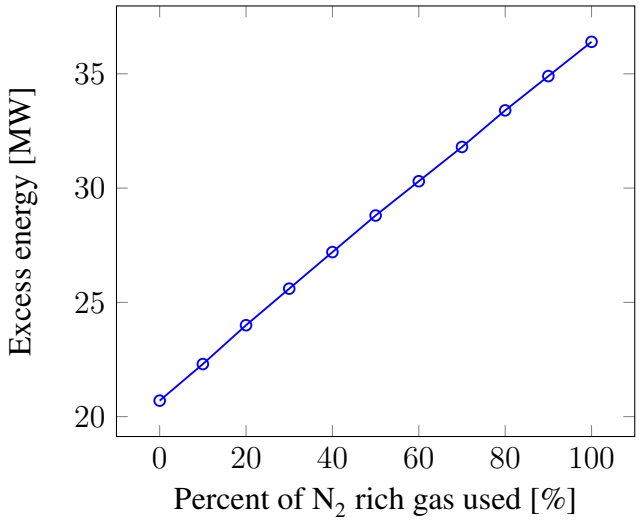

Figure 4.18: Excess power production in the plant as a function of addition of N_2 rich gas from the air membrane.

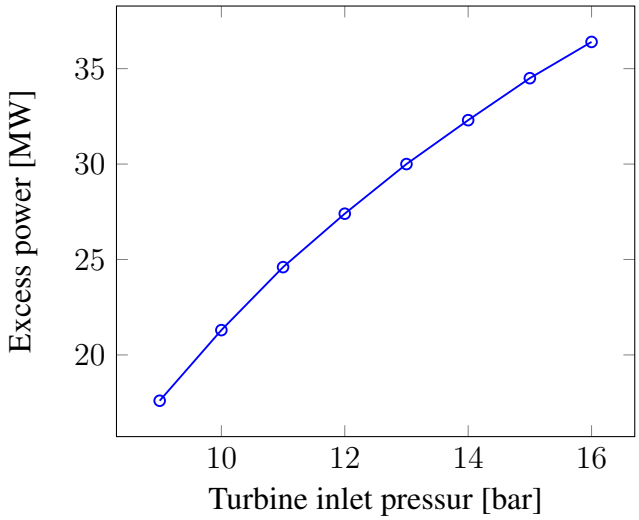

Figure 4.19: The excess power produced in the process as a function of gas turbine inlet pressure.

4.3 Evaluation of Assumptions

Parameters like constant H_2/CO ratio, natural gas feed pressure, natural gas composition, and catalyst effectiveness factor for the FT reactor are some parameters that has been assumed to be given values in the process. The H_2/CO ratio in the process has been adjusted to have the same value for each reactor inlet, the natural gas feed pressure is assumed to 30 bar and the effectiveness factor is assumed to 0.08. These assumptions has been evaluated to find out if the operation is optimal or if higher production could be obtained.

4.3.1 Hydrogen to Carbon Monoxide Ratio

The H_2/CO ratio is kept to a constant value (section 4.2.5) for the inlet of each reactor by adding H_2 between the steps. To investigate this assumption, an evaluation of different H_2/CO ratio for the three reactor inlets were done.

For this evaluation the size of the reactor was not changed when adding more or less hydrogen and only one reactor was evaluated at the time. For the second reactor the result is given in Table 4.30 and the changes in C_{5+} production as a function of H_2/CO is given in Figure 4.20.

Table 4.30: The effect of adding hydrogen to the feed before reactor two on CO conversion, CH_4 selectivity and C_{5+} production.

Amount of H_2 added [kmole/h]	0	25	50	100	150	200
H_2/CO ratio [-]	2.08	2.09	2.10	2.11	2.13	2.15
CO conversion [%]	53.0	52.9	53.9	52.8	52.7	52.6
CH_4 selectivity [%]	9.2	9.3	9.3	9.4	9.5	9.6
C_{5+} production [tonne/h]	18.53	18.50	18.47	18.40	18.33	18.25

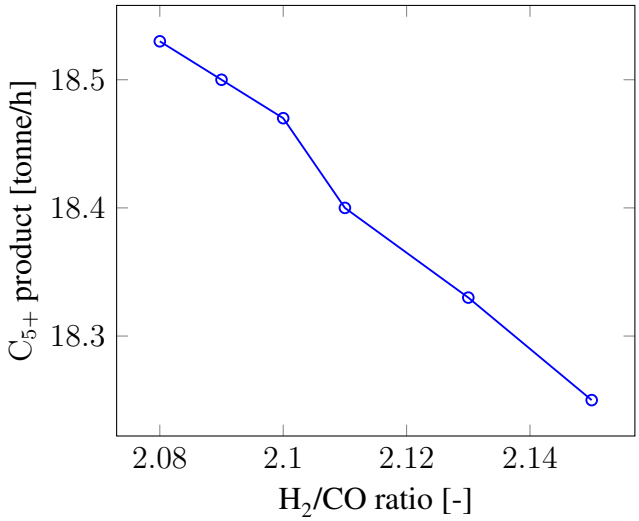

Figure 4.20: C_{5+} production as a function of H_2/CO ratio in the feed to Fischer-Tropsch reactor 2.

The highest production of C_{5+} is given when no hydrogen is added. Compared to the value used in the final process design 59 kg/h more C_{5+} product is produces when no hydrogen is added.

When evaluating the last reactor the optimal point for reactor 2 was used. The result is given in Table 4.31 and the changes in C_{5+} production as a function H_2/CO is given in Figure 4.21.

Table 4.31: The effect of adding hydrogen to the feed before reactor three on CO conversion, CH_4 selectivity and C_{5+} production, when no hydrogen is added before Fischer-Tropsch reactor 2.

Amount of H_2 added [kmole/h]	0	50	100	150	200	250	300
H_2/CO ratio [-]	2.01	2.05	2.08	2.11	2.15	2.18	2.22
CO conversion [%]	59.4	59.9	60.4	60.9	61.3	61.7	62.06
CH_4 selectivity [%]	13.3	13.6	13.9	14.3	14.6	14.9	15.3
C_{5+} production [tonne/h]	8.860	8.878	8.890	8.894	8.892	8.883	8.868

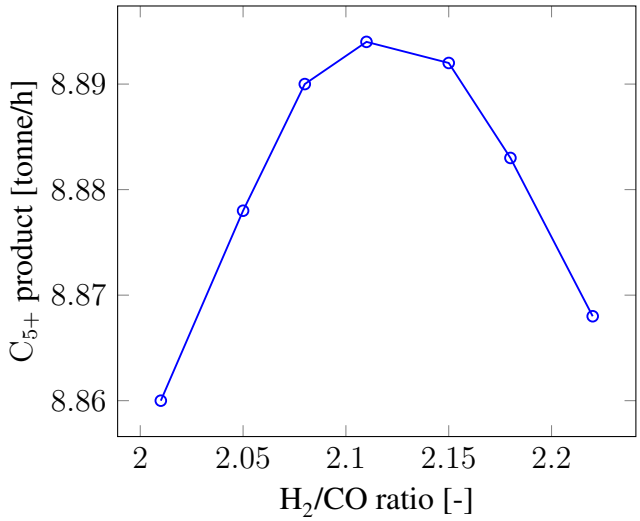

Figure 4.21: C_{5+} production as a function of H_2/CO ratio in the feed to Fischer-Tropsch reactor 3. In this evaluation no hydrogen is added before the second reactor.

A maximum point for C_{5+} production is given at a H_2/CO ratio of 2.148 (Figure 4.21). By increasing the H_2/CO ratio from 2.097 to 2.148 the C_{5+} production in the last reactor is decreased with 11 kg/h compared to the final process design where the H_2/CO is kept constant for each reactor inlet.

If the optimal H_2/CO ratios found above is used for the two last reactors, the C_{5+} production would have been increased with 49 kg/h compared to the final process design.
As the production of reactor 3 is reduced an evaluation with only changing the H_2/CO ratio before reactor 3 was done, with the result in Table 4.32. The H_2/CO ratio before reactor 1 and 2 is kept constant to 2.097.

Table 4.32: The effect of adding hydrogen to the feed before reactor three on CO conversion, CH_4 selectivity and C_{5+} production, when the ratio before the two first reactors are kept constant.

Amount of H_2 added [kmole/h]	0	50	100	150	200	250
H_2/CO ratio [-]	2.04	2.08	2.11	2.14	2.18	2.21
CO conversion [%]	59.8	60.3	60.8	61.2	61.6	62.0
CH_4 selectivity [%]	13.5	13.9	14.2	14.5	14.9	15.2
C_{5+} production [tonne/h]	8.889	8.901	8.907	8.905	8.898	8.883

When hydrogen is added only before the third reactor a maximum point for production of C_{5+} are found at a H_2/CO ratio of 2.11 (illustrated in Figure 4.22). By changing the H_2/CO ratio for the last reactor the C_{5+} production could be increased with 1 kg/h.

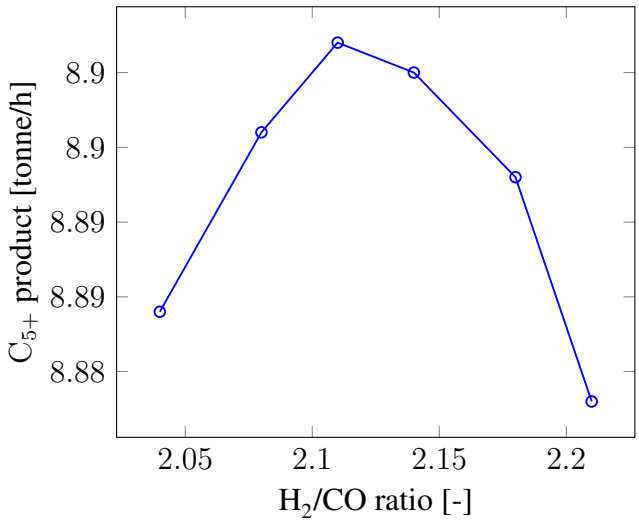

Figure 4.22: C_{5+} production as a function of H_2/CO ratio in the feed to Fischer-Tropsch reactor 3, when the ratio is kept constant for the two first reactors.

The assumption of keeping the ratio constant for each reactor inlet seems to be good as the increase of production is under 50 kg/h. However, this is based on the given natural gas feed, with a high H_2/CO ratio in the syngas.

4.3.2 Natural Gas Feed Pressure

The natural gas feed pressure is assumed to 30 bar. However, natural gas feed can be at higher pressure so the effect of changing the feed pressure on the C_{5+} production was evaluated.

For this evaluation the different component splits are used for the hydrogen selective membrane, as the pressure difference over the membrane is changed and membrane performance will be changed. The compression of air, and recycle streams are also changed with the same

ratio as the increase in natural gas feed pressure. In this evaluation heat integration was not included, and the stream from the ATR is cooled down to 30°C to knock out water instead of 99°C which is decided from the heat integration.

In the first evaluation the size of the reactor is kept constant. As the pressure is changed the density of the flow will also be changed giving different gas velocities trough the reactor.

When the pressure is increased from 30 bar to 40 bar with constant reactor size, the production is increased with 3.78 tonne/h (Table 4.33).

Table 4.33: The effect of changing the natural gas feed pressure on CO conversion, CH_4 selectivity and C_{5+} production, when the reactor size is kept constant.

Natural gas pressure [bar]	30	40
H_2/CO ratio [-]	2.097	2.077
CO conversion [%]	89.5	92.0
CH_4 selectivity [%]	9.0	7.1
C_{5+} production [tonne/h]	53.53	57.31

If the reactor size is changed when changing the natural gas feed pressure, to maintain the same gas velocity through the reactors the effect is opposite. Then the production is reduced with increased pressure, as given in Table 4.34.

Table 4.34: The effect of changing the natural gas feed pressure on CO conversion, CH_4 selectivity and C_{5+} production, when the reactor size is changed maintain constant residence time.

Natural gas pressure [bar]	30	40
H_2/CO ratio [-]	2.097	2.077
CO conversion [%]	89.5	78.3
CH_4 selectivity [%]	9.0	6.4
C_{5+} production [tonne/h]	53.53	49.35
Number of tubes reactor 1 [-]	48,500	35,100
Number of tubes reactor 2 [-]	38,200	30,500
Number of tubes reactor 3 [-]	30,500	25,900

This indicates that an increase in natural gas feed pressure would increase the C_{5+} production if no other changes is performed on the system. A natural gas feed with higher pressure would be favourable for the process.

4.3.3 Catalyst Effectiveness Factor

The cobalt catalyst has a small temperature operating region from 200-240°C, and an increase in temperature would increase the methane selectivity [61]. Because of the exothermic reac-

tions in the FTS the potential for catalyst sintering is relative high. Sintering is one of the reasons for deactivation of the cobalt catalyst [62]. To minimize deactivation and avoid hot-spot the CO conversion for once-through is limited to around 40%, for pure syngas [63].

As illustrated in Figure 4.23 the temperature is reduced faster for each reactor. A reason for this is the reduction of gas feed amount to the reactor and reduction in reaction rates along the reactor.

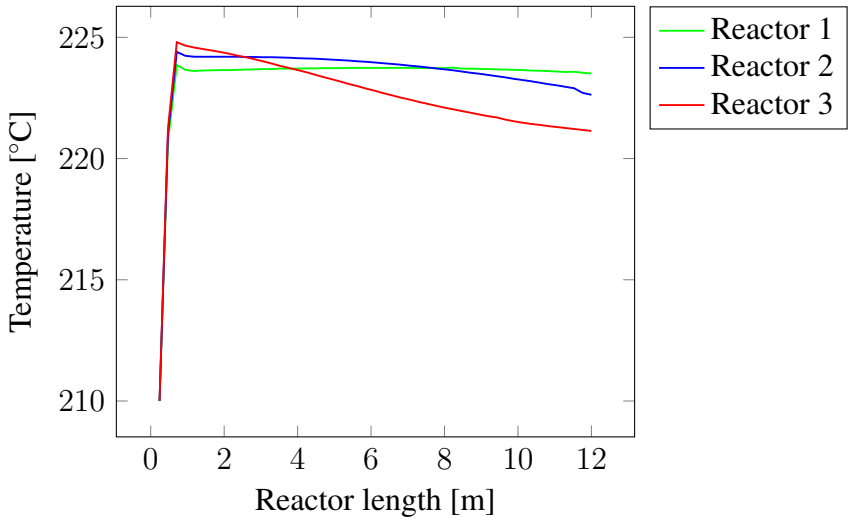

Figure 4.23: The temperature profile along the reactor for the three Fischer-Tropsch reactors with effectiveness factor of 0.08.

The temperature given in the profile is the average radial temperature. And the maximum temperature in radial direction is give by equation 4.3.1. The derivation of the temperature expression is given in Appendix K.

$$T_{max} = T_{average} + \frac{T_{average} - T_{cw}}{\frac{8\lambda}{UD}} \tag{4.3.1}$$

where T_{max} is the maximum temperature in radial direction, $T_{average}$ is the average radial temperature, T_{cw} is the temperature of the cooling water, λ is the effective radial conductivity, U is the overall heat transfer coefficient and D is the diameter.

For this process where enriched air is used in the ATR, nitrogen dilutes the syngas. The nitrogen helps keeping the temperature low, and therefore a higher CO conversion could possibly be achieved. An evaluation of increasing the effectiveness factor from 0.08 to 0.1 was done, and the result are given in Table 4.35. When the effectiveness factor is changed the volume of the two last reactors are reduced to keep constant gas velocity and residence time in the reactor.

Table 4.35: A comparison of the process with the two different effectiveness factors for the FT catalyst; 0.08 and 0.1.

Effectiveness factor [-]	0.08	0.1
CO conversion [%]	89.24	94.32
CH_4 selectivity [%]	9.06	9.60
C_{5+} production [tonne/h]	53.36	55.70
Total production [tonne/h]	53.85	56.31
T_{max} [°C]	227	229
Number of tubes reactor 1 [-]	48,500	48,500
Number of tubes reactor 2 [-]	38,200	34,200
Number of tubes reactor 3 [-]	30,500	26,600

As expected is the temperature increase in the reactor higher with the use of an effectiveness factor of 0.1 compared to 0.08 (Table 4.24). However, the highest temperature reached with effectiveness factor 0.1 is around 229°C, so it is reasonable to assume that the effectiveness factors actually could have been increased. If changing the effectiveness factor the CO conversion can be increased from 89.24% to 94.32% compared to the use of 0.08. The C_{5+} production is increased with 4.4% and the total reactor volume needed are reduced. The amount of FT product produced per catalyst volume is increased from 0.078 tonne/$(h \cdot m^3)$ to 0.087 tonne/$(h \cdot m^3)$ when changing the effectiveness factor from 0.08 to 0.1.

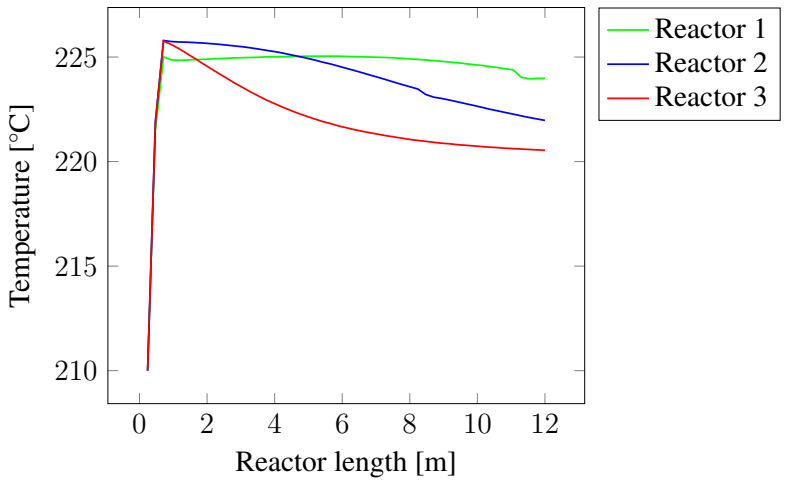

Figure 4.24: The temperature profile along the reactor for the three Fischer-Tropsch reactors with effectiveness factor of 0.1.

If the effectiveness factor is increased even further to 0.15 the maximum temperature reached is around 335°C. This temperature is in the upper range of the operating temperature for the catalyst. It would therefore not be recommended to increase the effectiveness factor to a value higher than 0.1.

4.3.4 Natural Gas Feed Composition

The simulation is based on a given natural gas feed (in this section named NG1) with a large amount of methane. With this natural gas feed the H_2/CO ratio in the syngas are close to the stoichiometric value. This gives a low reduction of the ratio along the reactor, and only a small amount of hydrogen needs to be added to maintain constant ratio for the reactor inlet. It is therefore a large amount of excess hydrogen in the process.

If a heavier natural gas feed was used with a larger amount of higher hydrocarbons or CO_2 it is expected that the H_2/CO ratio would be decreased. With a lower H_2/CO ratio the additional hydrogen amount required would be increased and the excess hydrogen in the process reduced.

An evaluation of changing the natural gas feed on the final design was done. The same natural gas feed distribution was used with the new natural gas feed (named NG2). However, the performance of the membrane is changed with another feed, so the split factors used in the membrane was changes. In addition was the reactor size changed to maintain the same gas velocity. The composition if NG2 has a higher content of heavier hydrocarbon and some CO_2 (Table 4.36) [27].

Table 4.36: Composition of the two different natural gas feeds.

Component	Mole fraction [-]	
	NG1	NG2
Methane	0.950	0.850
Ethane	0.020	0.067
Propane	0.015	0.033
n-Butane	0.010	0.022
n-Pentane	0.005	0.011
Carbon dioxide	0	0.017

As expected is the H_2/CO ratio decreased with the alternative natural gas feed and the production is increased (Table 4.37). The total CO conversion is almost the same, however, the selectivity towards methane is reduced. The reduction in methane selectivity is the explanation for the increased C_{5+} production with the same total conversion. The total production is increased with 6.96 tonne/h which gives an reduction in tail gas amount. From this it should be expected that the power production is reduced, however, the amount of air to the air membrane is increased giving more nitrogen rich gas to be used in the gas turbine.

With the alternative natural gas feed the steam demand is increased with 17.6 tonne/h. And the amount of enriched air is increased with 26.7 tonne/h. Because of this increase in feed amount the inert in the system is higher, and the reactor volume are increased.

Table 4.37: Comparison of using two different natural gas feeds in the process.

	NG1	NG2
Steam demand [tonne/h]	105.7	123.3
Enriched air feed [tonne/h]	291.8	318.5
H_2/CO ratio [-]	2.097	1.999
CO conversion [%]	89.24	88.82
CH_4 selectivity [%]	9.06	8.40
C_{5+} production [tonne/h]	53.36	60.26
Total product [tonne/h]	53.85	60.81
Number of tubes reactor 1 [-]	48,500	53,300
Number of tubes reactor 2 [-]	38,200	41,800
Number of tubes reactor 3 [-]	30,500	33,700
Excess H_2[tonne/h]	4.4	3.8
Excess power [MW]	36.4	36.5

This indicates that a heavier natural gas feed would give higher production, however, the size and feed amount is increased. More evaluation should have been done with the alternative natural gas feed to evaluate the effect as this might not be the optimal operation point. This result gives an indication of that a heavier natural gas feed could give more production, and may be more suitable for the proposed process design.

Chapter 5

Conclusion

In this master thesis a GTL process design for offshore applications was investigated. The process design was successfully simulated in Aspen HYSYS V 8.6. A MATLAB model for the carbon membrane was produced and the result was implemented in the simulation.

Based on the given natural gas feed composition and the kinetic model used for the FTS reactor, it is found that:

- The optimal distribution of natural gas feed between the autothermal reformer and the heat exchanged reformer is 90% to the ATR and 10% to the HER.
- The production of C_{5+} is increased with 0.5 tonne/h with the use of a HER compared to a process design without the HER. The heat exchanged reformer is used in the process to produce the hydrogen needed. In addition, it provides good heat integration and eliminates the use of a waste heat boiler after the ATR.
- A high temperature of the feed and outlet stream from the ATR is favourable, but the materials in the equipment will give limitations. It was found that pre-heating the enriched air feed to 550°C and adjusting the outlet temperature with enriched air to a temperature of 1,060°C, was optimal for the proposed process design.
- It is favourable to have the steam to carbon ratio in the natural gas feed to the ATR as low as possible. Due to carbon format in pre-reformer and soot formation in the ATR the lowest industrially proven value is 0.6.
- The total production from the process was found to be 53.9 tonne/h with a total CO conversion of 89.2%
- The methane selectivity in the process is increase with reduced pressure, due to lower growth probability factor predicted by the kinetic model. The total methane selectivity in the process is found to be 9.1%
- The carbon efficiency in the process is 57% and the energy efficiency is 45%.

- 501 tonne/h of medium pressure steam with a pressure of 19.07 bar and temperature of 210 °C is produced in the process.
- The tail gas in the process is used for power production and an excess power of 36.4MW is obtained.
- All the available heat was recovered by the use of heat integration in the process and no external heating is required. The external cooling duty needed for the process is reduced from 504.6 MW to 236.5 MW with the use of heat integration.
- The total weight of the equipments in the plant not including the heat exchangers is estimated to 1,965 tonne.
- The total capital cost of the plant is estimated to 278.1 million$, where 37.6% is related to the FTS. The total investment cost without considering the ship, buildings and structures, and the upgrading unit is estimated to 542.7 million$, which is less than existing projects.
- An increase in the natural gas feed pressure from 30 to 40 bar would increase the production with 3.8 tonne/h, if no other changes was performed on the system.
- The use of enriched-air in the process gives an synthesis gas diluted with nitrogen. This gives a possibility to achieve a higher CO conversion by increasing the effectiveness factor from 0.08 to 0.1. With this change the production is increased with 2.5 tonne/h.
- A heavier natural gas feed with a larger amount of higher hydrocarbons or CO_2 will give an syngas with a lower H_2/CO ratio. This gives a higher selectivity towards C_{5+}, and a reduced amount of excess hydrogen in the process.

5.1 Further Work

During the work with this master thesis, several topics for furter work are identified;

- The simulation results in this master thesis are based on that the kinetic model used are reliable. It could been interesting to evaluate the process design with the use of another kinetic model to compare the results.
- A simple simulation was performed with the use of another natural gas feed. It could be interesting to perform an evaluation in more detail where the process design was optimized for the new feed.
- The cooling water temperature for the Fischer-Tropsch reactors are assumed to be 220°C. This might not be the optimal value, and an evaluation of this should be done. It could also be an option to have different cooling temperatures for the three reactor stages, which also would lead to the need of different steam pressure levels. This can be evaluated further.

- The residence time in the reactors are kept constant for all the reactors. This might not be the optimal situation and it could be interesting to evaluate the effect of changing the residence time.
- The feed temperature to the hydrogen selective membrane may not be at the optimum value. A higher temperature may be required to avoid adsorption of components on the membrane surface, that would block the membrane pores. An evaluation of increasing the temperature before the membrane after water is knocked out could be done.

Bibliography

[1] Todic B, Ma W, Jacobs G, Davis BH, Bukur DB. CO-insertion mechanism based kinetic model of the Fischer-Tropsch synthesis reaction over Re-promoted Co catalyst. Catalysis Today. 2014;228:32–39.

[2] Todic B, Ma W, Jacobs G, Davis BH, Bukur DB. Corrigendum to: CO-insertion mechanism based kinetic model of the Fischer-Tropsch synthesis reaction over Re-promoted Co catalyst. Catalysis Today. 2015;242:386.

[3] Hillestad M. Modeling the Fischer-Tropsch product distribution and model implementation; Submitted for publication in Chemical Product and Process Modeling.

[4] Moulijn JA, Makkee M, Van Diepen AE. Chemical Process Technology. 2nd ed. Chichester: Wiley; 2013.

[5] World Bank Group. Regulation of Associated Gas Flaring and Venting: A Global Overview and Lessons from Internationla Experience [pdf]; 2010 [Accessed 27.05.2015]. Available from: http://www-wds.worldbank.org/external/default/WDSContentServer/WDSP/IB/2004/07/16/000012009_20040716133951/Rendered/PDF/295540Regulati1aring0no10301public1.pdf.

[6] Bamji Z. Zero Rutine Flaring by 2030 [online]; [Accessed 27.05.2015]. Available from: http://www.worldbank.org/en/programs/zero-routine-flaring-by-2030.

[7] Kim HJ, Choi DK, Ahn Si, Kwon H, Lim HW, Denholm D, et al. GTL FPSO - An Alternative Solution to Offshore Stranded Gas. Oil and Gas Facilities. 2014 Jun;3(03):41–51.

[8] Van Loenhout A, van Zeelenberg L, Roth G, van Sheehan E, Jannasch N. Commercialization of Stranded Gas With a Combined Oil and GTL FPSO; Offshore Technology Conference, 2006.

[9] Masanobu S, Kato S, Nakamura A, Sakamoto T, Yoshikawa T, Sakamoto A, et al. Development of Natural Gas Liquefaction FPSO; 23rd International Conference on Offshore Mechanics and Arctic Engineering, Volume 1, Parts A and B, 2004.

[10] Fonseca A, Bidart A, Rassarelli F, Nunes G, Oliviera R. Offshore gas-to-liquids: Modulare solution for associated gas with variable CO_2 content; Word gas conference, 2012.

[11] LeViness S, Tonkovich AL, Jarosch K, Fitzgerald S, Yang B, McDaniel J. Improved Fischer-Tropsch Economic Enabled by Microchannel Technology (white paper). Velocys; 2011.

[12] Bakkerud PK. Update on synthesis gas production for GTL. Catalysis Today. 2005 Oct;106(1-4):30–33.

[13] Dybkjaer I, Christensen TS. Syngas for Large Scale Conversion of Natural Gas to Liquid Fuels. Natural Gas Conversion VI. 2001;136:435–440.

[14] Rostrup-Nielsen JR. Syngas in perspective. Catalysis Today. 2002 Jan;71(3-4):243–247.

[15] Sharifnia S, Mortazavi Y, Khodadadi A. Enhancement of distillate selectivity in Fischer–Tropsch synthesis on a Co/SiO2 catalyst by hydrogen distribution along a fixed-bed reactor. Fuel Processing Technology. 2005 Aug;86(12-13):1253–1264.

[16] Rytter E. Gas to liquids plant with consecutive Fischer-Tropsch reactors and hydrogen make-up. US2010/0137458 A1; 2010.

[17] Dalane K. Modelling and optimization of a Gas-to-Liquid plant; 2014.

[18] Rafiee A, Hillestad M. Staging of the Fischer-Tropsch reactor with an iron based catalyst. Computers & Chemical Engineering. 2012 Apr;39:75–83.

[19] Thomsen SG, Han PA, Loock S, Ernst W. The First Industrial Experience with the Haldor Topsoe Exchanger Reformer. Ammonia Plant Safety and Related Facilities. 2006;47:259–266.

[20] Malhotra A, Macris A, Gonsnell J. Increase hydrogen production usin KBR's KRES Technology. National Petrochemical & Refiners Association. 2004;p. 1–14.

[21] Johnson Matthey Davy Technologies. Core Technologies: Reforming (ATR,GHR,SMR) [online]; [Accessed 05.27.2015]. Available from: `http://www.davyprotech.com/what-we-do/licensed-processes-and-core-technologies/core-technologies/refiningdistillation/specification/`.

[22] Abbott J, Crewdson BJ. Gas heated reforming imporves Fischer-Tropsch process. Oil&Gas. 2002;100(16).

[23] Hillestad M. Personal Communication. Norwegian University of Science and Technology (NTNU); 2015.

[24] Ostadi M. Personal Communication. Norwegian University of Science and Technology (NTNU); 2015.

[25] Falkenberg M, Hillestad M. Modeling, simulation and design of three different concepts for offshore methanol production; Submitted for publication.

[26] Wilhelm DJ, Simbeck DR, Karp AD, Dickenson RL. Syngas production for gas-to-liquids applications: technologies, issues and outlook. Fuel Processing Technology. 2001 Jun;71(1-3):139–148.

[27] Klerk AD. Fischer-Tropsch Refining. 1st ed. Weinheim: Wiley-VCH; 2011.

[28] Aasberg-Petersen K, Christensen TS, Stub Nielsen C, Dybkjaer I. Recent developments in autothermal reforming and pre-reforming for synthesis gas production in GTL applications. Fuel Processing Technology. 2003 Sep;83(1-3):253–261.

[29] Christensen TS. Adiabatic prereforming of hydrocarbons - an important step in syngas production. Applied Catalysis A: General. 1996 May;138(2):285–309.

[30] Aasberg-Petersen K, S NC, Dybkjaer I, J P. Large Scale Methanol Production from Natural Gas [pdf]. Haldor Topsoe; [Accessed 01.03.2015]. Available from: `http://www.topsoe.com/sites/default/files/topsoe_large_scale_methanol_prod_paper.ashx_.pdf`.

[31] Aasberg-Petersen K, Bak Hansen JH, Christensen TS, Dybkjaer I, Christensen PS, Stub Nielsen C, et al. Technologies for large-scale gas conversion. Applied Catalysis A: General. 2001 Nov;221(1-2):379–387.

[32] Winter-Madsen S. Personal Communication. Haldor Topsoe; 2015.

[33] Jess A, Popp R, Hedden K. Fischer-Tropsch-synthesis with nitrogen-rich syngas. Applied Catalysis A: General. 1999 Oct;186(1-2):321–342.

[34] Nodeland SG. Personal Communication. Air Products; 2015.

[35] Wesenberg MH. Gas Heated Steam Reformer Modelling [PhD Thesis]. Norwegian University of Science and Technology, NTNU. Trondheim; 2006.

[36] Barbosa Lima DF, Ademar FA, Kaminski ML, Matar PN. Modeling and Simulation of Water Gas Shift Reactor: An Industrial Case; Petrochemicals, 2012.

[37] Hagg MB. Personal Communication. Norwegian University of Science and Technology (NTNU); 2015.

[38] Chorkendorff I, Niemantsverdriet JW. Concepts of Modern Catalyssis and Kinetics. 2nd ed. Weinheim: Wiley-VCH; 2007.

[39] Spath PL, Dayton DC. Preliminary Screening - Technical and Economic Assessment of Synthesis Gas to Fuel and Chemicals with Emphasis on the Potential for Biomass Derived Syngas. National Renewable Energy Laboratory; 2003.

[40] Sinnott RK, Towler G. Chemical Engineering Design. 5th ed. Amsterdam: Elsevier; 2009.

[41] Smith R. Chemical Process Design and Integration. 1st ed. Chichester: Wiley; 2005.

[42] Xu J, Froment GF. Methane steam reforming, methanation and water-gas shift: I. Intrinsic kinetics. AlChE. 1989 January;35(1):88–96.

[43] Air Products. PRISM PA4050-N1-SS Stainless steel nitrogen membrane sepataor for severe-duty applications. 523-13-017-GLB [data sheet]; 2013.

[44] Godorr S. GTL Technology Advancements; World Pertoleum Conference - ORYX GTL site visit, 2011.

[45] Johansson TB, editor. Global Energy Assessment: Toward a Sustainable Future. Cambridge: Cambridge Unicersity Press; 2012.

[46] Dillon CP. Performance of tubular alloy heat eexchanger in seawater service in the chemical process industries; 1987. [Accessed 27.05.2015]. Available from: http://www.nickelinstitute.org/~/Media/Files/TechnicalLiterature/PerformanceofTubularAlloyHeatExchangersinSeawaterServiceintheChemicalP 12002_.pdf#page=.

[47] AK Steel. Product Data Sheet 304/304L Stainless Steel. T304/304L-S-8-01-07 [data sheet]; 2007.

[48] Walas SM. Chemical Process Equipment - Selection and Design. 1st ed. Boston: Butterworth-Heinemann; 1990.

[49] Peters MS, Timmerhaus KD. Plant Design and Economic for Chemical Engineers. 4th ed. New York: McGraw-Hill; 1991.

[50] OSHWIN OVERSEAS. Stainless Steel tube price [online]; [Accessed 20.05.2015]. Available from: http://www.oshwin.com/stainlesssteel-piping-tubing-pipes-tubes/stainless-steel-pipes-tubes/pipetube-price/.

[51] Worldsteelprices. Steel rates from around the World [online]; [Accessed 20.05.2015]. Available from: http://www.worldsteelprices.com/.

[52] Metalprices. Stainless Steel [online]; [Accessed 20.05.2015]. Available from: http://www.metalprices.com/metal/stainless-steel/stainless-steel-flat-rolled-coil-304.

[53] Bakkerud PK, Gol JN, Aasberg-Petersen K, Dybkjaer I. Preferred synthesis gas production routes for GTL. Natural Gas Conversion VII, Proceedings of the 7th Natural Gas Conversion Symposium. 2004;147:13–18.

[54] O'Brien E. Gas to Liquids Plant: Turning Louisiana Natural Gas into Marketable Liquid Fuels [pdf]. Louisiana Department of Natural Resources/Technology Assessment Division; 2013. [Accessed 29.05.2015]. Available from: `http://dnr.louisiana.gov/assets/TAD/newsletters/2013/2013-11_topic_1.pdf`.

[55] Salehi E, Nel W, Save S. Viability of GTL for the North America gas market. Hydrocarbon processing. 2013 January;p. 41–48.

[56] Choi GN, Karmer SJ, Tam SS, Fox JM, Carr NL, Wilson GR. Design/Economics of a Once-Through Natural Gas Fischer-Tropsch Plant With Power Co-Production. Coal Liquefaction & Solid Fuels Contractors Revie Conference, Pittsburg, Pennsylvania. September, 3-4, 1997;p. 1–7.

[57] Sogge J. Personal communication. Statoil; 2015.

[58] Fogler HS. Elements of Chemical Reaction Engineering. 4th ed. Upper Saddler River, N.J.: Prentice-Hall PTR; 2005.

[59] Agge aAMA Kenneth L, Weick LJ, Trepper EL. Synthesis gas production system and method. US2000/6085512; 2000.

[60] Huang Y, Merkel TC, Baker RW. Pressure ratio and its impact on membrane gas separation processes. Journal of Membrane Science. 2014 Aug;463:33–40.

[61] Khodakov AY, Chu W, Fongarland P. Advances in the Development of Novel Cobalt Fischer-Tropsch Catalysts for Synthesis of Long-Chain Hydrocarbons and Clean Fuels. Chemical Reviews. 2007 May;107(5):1692–1744.

[62] Tsakoumis NE, Ronning M, Borg O, Rytter E, Holmen A. Deactivation of cobalt based Fischer-Tropsch catalysts: A review. Catalysis Today. 2010 Sep;154(3-4):162–182.

[63] Rytter E, Holmen A. Deactivation and Regeneration of Commercial Type Fischer-Tropsch Co-Catalysts - A Mini-Review. Catalysts. 2015 Mar;5(2):478–499.

[64] Skogstad S. Prosessteknikk: masse- og energibalanser. 3rd ed. Trondheim: Tapir akademisk forlag; 2009.

[65] Slawinski. Production-Programme [data sheet]; [Accessed 06.05.2015]. Available from: `http://www.slawinski.de/fileadmin/user_upload/downloads/Slawinski-Datasheet-EN.pdf`.

[66] Monnery WD, Svrcek WY. Successfully Specify Three-Phase Separators. Chemical Engineering Progress. 1994;p. 29–39.

[67] Haryanto A, Fernando SD, Filip To SD, Steele PH, Pordesimo L. High Temperature Water Gas Shift Reaction over Nickel Catalysts for Hydrogen Production: Effect of Supports, GHSV, Metal Loading, and Dopant Materials. Journal of Thermodynamics & Catalysis. 2011;02(01).

[68] Halabi M, Decroon M, Van der Schaaf J, Cobden P, Schouten J. Modeling and analysis of autothermal reforming of methane to hydrogen in a fixed bed reformer. Chemical Engineering Journal. 2008 Apr;137(3):568–578.

[69] Velocys. Microchannel Fischer-Tropsch [pdf]; [Accessed 20.04.2015]. Available from: dbvjpegzift59.cloudfront.net/8721/8818-6Ip8q.pdf.

[70] Mulder M. Basic principles of membrane Technology. 2nd ed. Dordrecht: Kluwer; 1996.

[71] Linbraathen A. Personal Communication. Norwegian University of Science and Technology (NTNU); 2015.

[72] NTC. Gas Turbine Prices $ per kW [online]; [Accessed 11.05.2015]. Available from: http://www.gas-turbines.com/trader/kwprice.htm.

[73] ESMAP. Study of Equipment Prices in the Power Sector [pdf]; [Accessed 11.05.2015]. Available from: https://www.esmap.org/sites/esmap.org/files/TR122-09_GBL_Study_of_Equipment_Prices_in_the_Power_Sector.pdf.

[74] Farrar G. Nelson-Farrar Quarterly Costimating. Oil & Gas. 2013;111(7).

[75] Nelson-Farrar monthly cost indexes. Oil & Gas. 2014;112(9).

Appendix A

Paper

The result from the work in this master thesis has been used in a paper to compare the process design with the use of a fixed bed reactor with a microchannel reactor.

My contribution to the paper are;

1. All the results for the process design with use of multitubular fixed bed reactor.
2. My HYSYS model has been used in the paper (first author have had full access to all simulation files).
3. Discussion related to structure and content of paper.
4. Discussion related to the documented findings.
5. Provided all information and results about the two membranes used in the process design.

The paper is planed submitted to Fuel and Processing Technology.

In this appendix a draft version of the paper is given.

Conceptual design of an autonomous once-through gas-to-liquid process - comparison between fixed bed and microchannel reactors

Mohammad Ostadi, Kristin Dalane, Erling Rytter, Magne Hillestad*

Department of Chemical Engineering, Norwegian University of Science and Technology (NTNU), Sem Sælandsvei 4, N-7491 Trondheim, Norway

Abstract

A novel process concept is proposed for converting natural gas to liquid Fischer-Tropsch products. An autothermal reformer with enriched air as oxidant is applied for synthesis gas (syngas) production, and because of the inert nitrogen a once-through Fischer-Tropsch synthesis is the preferred option. In order to maximize the syngas conversion and the production of heavy hydrocarbons, a staged reactor path with distributed hydrogen feed and product withdraw is proposed. The hydrogen is produced by steam methane reforming in a heat exchange reformer (gas heated reformer), heat integrated with the hot effluent stream from the autothermal reformer. Tail gas from the last Fischer-Tropsch stage is sent to a gas turbine for power production. The hot exhaust gas from the gas turbine is used for natural gas preheating. The process is autonomous in the sense that it is self sufficient with power and water, and therefore well suited for production in remote locations such as a floating production unit. The process concept is simple and inexpensive since cryogenic air separation and fired heaters are not required. For the Fisher-Tropsch synthesis, both the conventional shell and tube fixed bed reactors and microchannel reactors are considered and compared.

Keywords: Gas-to-Liquid, Fischer-Tropsch, Autothermal reformer, Heat exchange reformer, Fixed bed reactor, Microchannel reactor, Distributed hydrogen feed, Autonomous, FPSO, Remote gas

*Corresponding author.
Email address: magne.hillestad@chemeng.ntnu.no (Magne Hillestad)

1. INTRODUCTION

Due to the depletion of easily accessible oil, and steadily increasing energy consumption worldwide, focus is turned on untapped resources that are unused for technical or economic reasons, such as associated and stranded gas reserves. One of the biggest challenges in exploiting remote gas reserves is transportation of the gas. Converting natural gas to liquid fuels, gas-to-liquids, is one possibility to bring remote natural gas reserves to the market.

If a floating production vessel is to be used for gas-to-liquid processing, there are several requirements that are not necessarily equally restrictive for an onshore plant. There are restriction with respect to space and the total weight of equipment. The floating production vessel need to be autonomous in the sense that all production utilities, such as water and power, need to be available onboard the unit. Due to safety issues a cryogenic air separation unit may be problematic onboard a floating production vessel because of the possibility of presence of pure oxygen in the vicinity of hydrocarbons. Also high columns with liquid inventory on board a rolling vessel may create problems.

There has been some investigations looking at the feasibility of installing a gas-to-liquid (GTL) process on a floating production storage and offloading (FPSO) vessel. Daewoo Shipbuilding & Marine Engineering together with RES Group Incorporated, have completed conceptual design package of GTL process for FPSO application producing 20000 bbl/day of a Fischer-Tropsch liquid syncrude product. They considered steam-CO_2 combined reforming for syngas production and slurry bubble column as Fischer-Tropsch (FT) synthesis Kim & al. (2014b). Velocys, which is one of the pioneers of commercializing microchannel technology, propose the use of microchannel technology on FPSO (Leviness & al. , 2011; Tonkovich & al. , 2008). Velocys together with Toyo Engineering and Mitsui Ocean Development & Engineering Co are working on commercializing Micro-GTL technology which is applicable for small scale gas reserves. CompactGTL is another leading company in modular small scale GTL. Together with Petrobras, they built a fully integrated small scale GTL facility using associated gas. SBM Offshore together with CompactGTL is cooperating on offshore projects to increase productivity and to reduce flaring. The concept utilizes CompactGTL technology for conversion of associated gas into syncrude. Loenhout & al. (2006) proposed to use air instead of pure oxygen in the reforming step. Three-phase slurry bubble column reactors were used for the two stages of the FT reaction. Use of air in the reformer resulted in very large equipment downstream the reformer. Masanobu & al. (2004) proposed to use oxygen blown autothermal reformer (ATR), which requires an air separation unit onboard the ship. Syntroleum Corporation has developed an offshore gas-to-liquid conversion process that uses air in a reforming process step to produce syngas (Hutton & Holmes , 2005). The feasibility assessment of utilizing associated gas and converting it into Fischer-Tropsch liquids on the FPSO was studied by Chevron Research and Technology in cooperation with Fluor Daniel, Inc. and Air Products and Chemical (Lowe & al. , 2001).

Fonseca & al. (2012) used steam methane reformer to produce syngas. In their design, they considered microchannels for the steam methane reforming and FT reactors. Kim & al. (2014a) considered process design and simulation of a methanol plant on an FPSO. They used steam-CO_2 reforming and plug flow reactor model in their design. The overall process was set in a high pressure environment to comply with the spatially constrained off-shore condition. Tonkovich & al. (2008) considered methanol production on an FPSO using multiple microchannel unit operations. These unit operations include reactors, phase separation, and distillation.

In our proposed design, the FT reactor path is staged with distributed hydrogen feed and products withdrawal between the stages. The selectivity to higher hydrocarbons is increased by lowering the H_2/CO ratio, however, the total rate will decrease. A slightly under-stoichiometric H_2/CO will increase the production of C_{5+} products. To compensate for the consumption, hydrogen is added between the stages. The hydrogen is produced by the use of a heat exchange reformer (HER), a high temperature shift reactor and a membrane units to separate H_2 from CO_2. Part of the hydrogen will be used for product upgrading. Syngas is produced by an autothermal reformer with enriched air as as oxidant. High once-through conversion over the FT reactors, more than 90%, is possible even with inert nitrogen in the syngas. The tail gas, being unconverted syngas, nitrogen, and lighter hydrocarbons, is used as fuel for the gas turbine for necessary power production. Furthermore, the use of enriched air instead of air to the ATR will increase the production of C_{5+} enough to compensate for the extra investment of an air membrane and extra compressors. A comparison between conventional fixed bed reactors and microchannel reactors is made. With fixed bed reactors three stages are applied, while with microchannel reactors two stages are sufficient to obtain high CO conversion with a once-through configuration. A comparison of the two reactor types indicates that microchannel will require less space, but the total weight is larger.

The selected capacity of the proposed GTL plant utilizes 120 MMscfd of natural gas and produces about 58 tonne/h or more than 12000 bbl/day of hydrocarbon products. Natural gas specifications are given in Table 1. The natural gas NG1 is used throughout the paper as the base case, while NG2 is only applied to see the effect of a heavier natural gas. The wax products need to be upgraded by hydrocracking in order to keep the oil liquified and prevent the product viscosity from becoming too high, but also to saturate the alkenes. If the GTL plant is integrated with oil production, the products may be blended with the conventional oil. A simplified block flow diagram of the proposed process concept is shown in Figure 1.

2. THE PROPOSED PROCESS CONCEPT

A more detailed process flow diagram of the proposed GTL process concept is shown in Figure 2. The main areas shown here are syngas production, hydrogen production, Fischer-Tropsch synthesis, in addition to gas turbine power generation, while the product upgrading process and the steam utility system are not

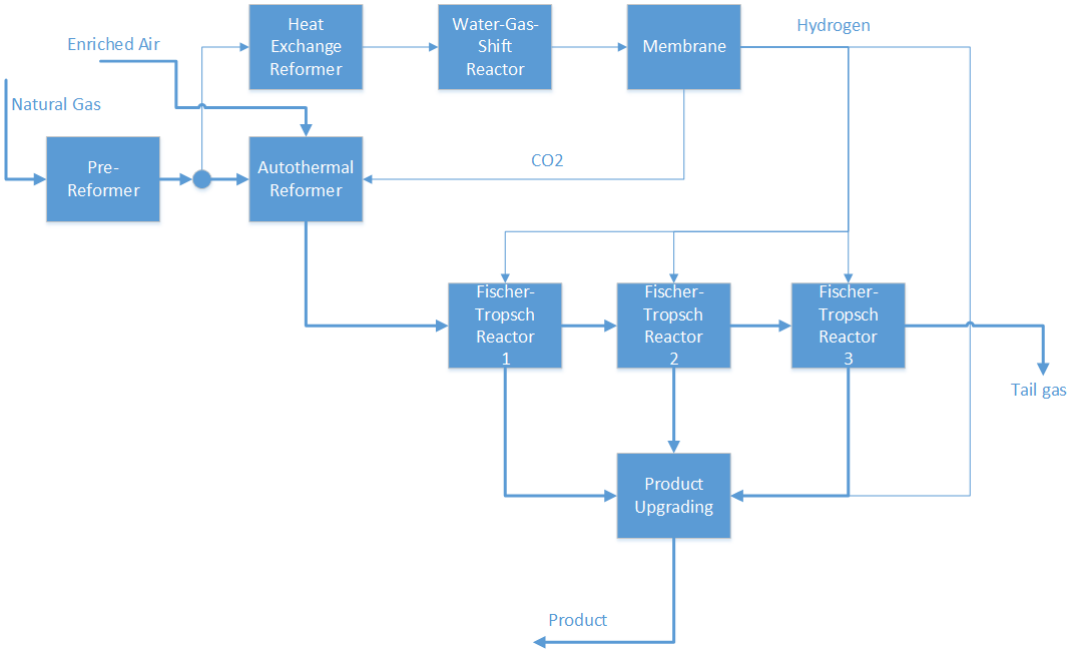

Figure 1: Block flow diagram of the proposed process concept; water and steam are not shown.

shown. After sulfur removal, the natural gas is mixed with steam and preheated to 480 °C before entering the pre-reformer. The outlet of the pre-reformer is further heated to ca 650 °C. These heat exchangers will be located inside the exhaust gas duct from the gas turbine. Stream 100 is split into two streams, 101 and 102, the former to the ATR and the latter to the HER. The energy required for the steam reforming reactions in the HER is provided by the hot outlet stream from the ATR. The outlet of the HER is cooled down to 350 °C before entering the high temperature water gas shift (WGS) reactor, shifting CO to CO_2 and H_2. After the WGS reactor, the stream is cooled to ca 30 °C and water is knocked out before entering the membrane unit for separation of H_2. The hydrogen rich stream with 99 % purity is then compressed and distributed between the Fischer-Tropsch stages. The CO_2 rich stream, which also contains some H_2, CO and CH_4, is compressed and recycled to the ATR. By adding this stream the H_2/CO ratio out of the ATR will be reduced, which is beneficial for the FT synthesis. The effluent stream from ATR after heat exchanged with the HER, is further cooled to 30 °C to knock out water from the syngas. Without further compression the syngas stream is heated to 210 °C before entering the first Fischer-Tropsch stage. The approximate inlet pressure to the first stage is about 26 bar. In order to increase the rate of the FT reactions, and also suppress catalyst deactivation, the gas outlet from FT reactors are cooled down and partly condensed where water and hydrocarbon products are separated from the gas. The tail gas, consisting of unconverted syngas, nitrogen and light gas components produced in the Fischer-Tropsch reactors, is used as fuel in the gas turbine to supply power to consumers.

Simulations were carried out using HYSYS V8.6 process simulator. Modeling of Fischer Tropsch reactor

and HER are done using Aspen Custom Modeler. The other reactors (WGS, Pre-reformer and ATR) are simulated using the Gibbs reactor model present in HYSYS. Soave-Redlich-Kwong (SRK) equation of state is used as the thermodynamic model to calculate thermodynamic properties. All chemical properties were provided by Aspen Properties V8.6.

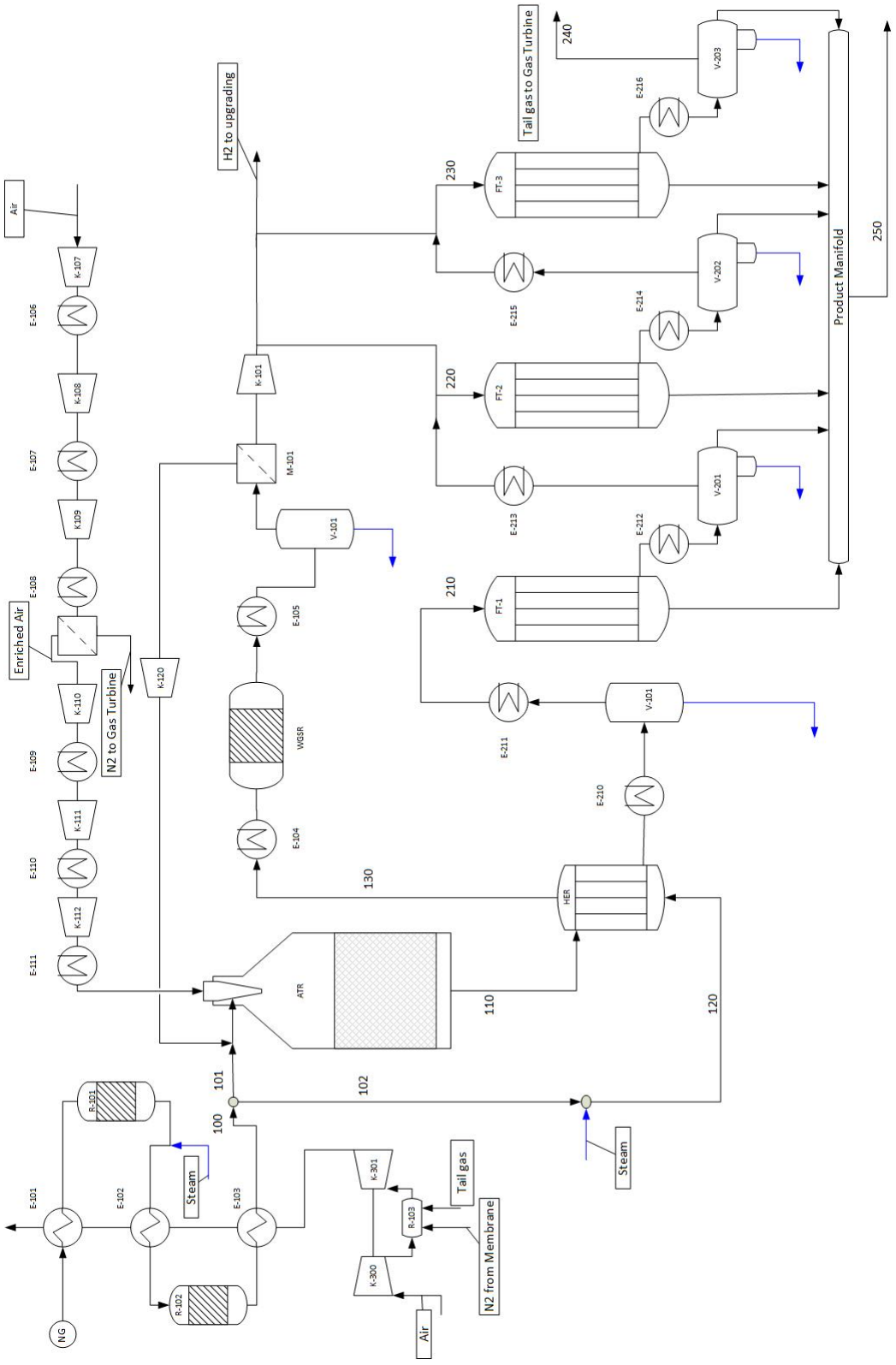

Figure 2: Process flow diagram of the proposed GTL plant. Heat integration and the steam system are not shown here.

Table 1: Specifications of the natural gas feeds; NG1 is used for all the results produced here, while NG2 is used to see the effect of heavier natural gas.

	NG1	NG2
Temperature [°C]	50	50
Pressure [bar]	30	30
Flow [MMscfd]	120.2	120.2
Molar flow [kmol/h]	6000	6000
Mole fraction		
CH_4	0.95	0.85
C_2H_6	0.02	0.067
C_3H_8	0.015	0.033
$n-C_4H_{10}$	0.01	0.022
$n-C_5H_{12}$	0.005	0.011
CO_2	0	0.017

2.1. Syngas production

An autothermal reformer is selected for syngas production. The main reasons are that the H_2/CO ratio can be adjusted to be close to the optimal ratio and the ease of scalability. The ATR is a relatively simple piece of equipment with a burner and a catalyst bed in a brick-lined pressure vessel (Rostrup-Nielsen , 2002). A pre-refomer is recommended in front of the ATR to prevent coke formation on the ATR catalyst (Chen & al. , 2003). Pre-reforming is usually operated adiabatically at $400 - 550°C$, and almost all higher hydrocarbons are converted to methane and carbon oxides.

With an air-blown ATR, it is practically impossible to recycle the unconverted syngas because of very high nitrogen concentrations. This is also the case with enriched air, and a once-through synthesis scheme is the only option to avoid high accumulation of nitrogen. However, by using enriched air instead of air, an increased production of 7.8 and 15.5 % can be obtained with fixed bed and microchannel reactors, respectively. PRISM membrane separators from Air Products are considered (Air Products , 2015). With these membranes, enriched air with oxygen concentrations ranging from 25 to 50% can be obtained. Considering the large air flow through the membrane and therefore avoiding a very large membrane modules, a PRISM membrane is chosen to have 34% oxygen purity. Long durability and simple startup of the separator are highlighted by the producer. Air is fed to the membrane at 16 bar and 100 °C. The enriched air is on the permeate side at a pressure of 1 bar, and needs to be re-pressurized before entering the ATR.

On the other hand, pure oxygen from cryogenic air separation poses significant safety challenges offshore,

in addition to large investment costs.

2.2. Hydrogen production

As demonstrated here, slightly under-stoichiometric H_2/CO ratios to the Fischer-Tropsch reactors result in higher C_{5+} production. With under-stoichiometric H_2/CO feed ratios, this ratio will naturally decrease along the reactors. The stoichiometric consumption H_2/CO ratio can be calculated as described by Hillestad (2015). There are four reactions to take into account, but the predominant reaction is the formation of alkanes. When the product distribution follows the Anderson-Schulz-Flory distribution, the consumption ratio is $3 - \alpha$, where α is the propagation probability. The propagation probability will change with the H_2/CO ratio and the temperature, but a typical value of α is 0.94 giving a stoichiometric H_2/CO consumption ratio of 2.06. When H_2/CO ratio is slightly under-stoichiometric, more C_{5+} products can be obtained (Rafiee & Hillestad , 2012; Rytter , 2010) and in order to compensate for the consumption, hydrogen is added between the stages.

Steam reforming with the use of a heat exchange reformer is applied to produce hydrogen with H_2/CO ratios of more than three. Heat exchange reformers are now commercially available and the technology is becoming mature. Kellogg Brown and Root (KBR) started using this technology in 1994 (Malhotra & al , 2004), Haldor Topsøe in 2003 (Thomsen & al. , 2001), and Johnson Matthey/Davy Technologies has solid experience with this technology (Carson & al. , 2008). Apart from being a hydrogen generator, the HER provides efficient heat integration and avoids the use of a waste heat boiler. Here, the steam to carbon ratio (S/C) of the feed to the HER is chosen to be two. The heat exchange reformer is counter current and consists of 1000 steam reformer tubes of 10 cm diameter and 10 m long. Modelling of the heat exchange reformer is described in detail by Falkenberg & Hillestad (2015).

The remaining CO is converted to CO_2 by the use of a water gas shift reactor. The CO reacts with water to produce CO_2 and H_2. For simulation purposes chemical equilibrium (Gibbs reactor) is assumed at the outlet of the WGS and the operating conditions are 450°C and 28 bar. The WGS inlet gas is cooled to approximately 350°C in E-104. The WGS effluent is cooled down to 30°C to remove most of the water before entering the membrane.

With the use of a membrane, a hydrogen rich and a CO_2 rich stream are produced. 85.5 % of the H_2 is separated and ends up in the hydrogen rich stream. The CO_2 rich stream is recycled back to the ATR to decrease the H_2/CO ratio at the outlet of the ATR. The membrane used here is a carbon membrane. It is ceramic tubes covered with membrane surface and tailored pores so that mainly hydrogen will pass through. The permeance of hydrogen is 200 GPU and for CO_2 it is 2 GPU, while for methane it is negligible (He , 2011). The membrane is countercurrent and there is no sweep gas on the permeate side. This will produce very pure hydrogen on the permeate side.

2.3. Fischer-Tropsch Synthesis

Cobalt catalysts are more selective to higher hydrocarbons, more active at lower temperatures, considerably less shift active and less selective to alkenes than iron catalysts and is therefore chosen for this process. On the other hand, the cost ratio between cobalt and iron catalysts is 230 (Rao & al , 1992) based on the relative price of metals. Although a number of kinetic models have been proposed in the literature, we have chosen to apply a rigorous kinetic model developed by Todic & al. (Todic & al. , 2015, 2014). The model is based on experiments done in a stirred tank slurry reactor with cobalt catalyst over a range of operating conditions which fits to our design conditions. The production of alkanes and alkenes are described by two chain growth probabilities and both increases slightly with the carbon number. The selectivities of methane and ethene are given by specific rate constants. A method for handling infinite number of reactions and components, suggested by Hillestad (2015) is used, where lumps of components and their average molecular weight are accurately described without violating the element balances. The method provides an accurate description of the overall consumption of CO and H_2 without calculating very many individual reaction rates. We have chosen to model alkane components individually up to C_{10} and a lump C^{p}_{11+} describing the tail distribution. While for alkenes, with less heavier components, we have chosen to model individual components up to C_4 and a lump C^{o}_{5+}. The reason for having that many individual components is to get the phase equilibrium calculations more accurate. For the sake of brevity the lumps C^{p}_{5+} and C^{o}_{5+} are reported here, but they are made by adding individual components and the modeled lumps. The molecular weight of the lumps C^{p}_{11+} and C^{o}_{5+} will change as the propagation probability changes. However, components in a process simulation system are normally described by constant molecular weights, so also in Hysys. A way of handling this is to let a lump with varying molecular weight be represented by two lumps with constant but different molecular weight. This is described in detail by Hillestad (2015).

The Fischer-Tropsch synthesis is staged with product withdrawal and hydrogen addition between the stages. This enables high conversion of syngas and high selectivity to higher hydrocarbons. The Fischer-Tropsch reactors are shell and tube fixed bed or microchannel fixed bed reactors. Since water is the main byproduct, the partial pressure of water vapor increases along the reactor. This can cause hydro-thermal sintering of many FT catalysts (Baxter , 2010; Tsakoumis & al. , 2010). Once through conversion in one stage is limited to 80% to have the maximum C_{5+} selectivity and also preserve catalyst life (Schanke & al. , 2001). Studies of the effect of low amounts of water during FTS for cobalt catalysts show that a low partial pressure of water ($p_{H_2O}/p_{H_2} < 1$) may have a positive kinetic and selectivity effect during FTS (Lögdberg & al. , 2011). However, at high water partial pressures, oxidation of some cobalt to irreducible oxidized cobalt compounds may occur (Schanke & al. , 1995).

Studies on the kinetics of FT synthesis show that nitrogen only dilutes syngas and therefore has no influence on the kinetics if the partial pressures of carbon monoxide and hydrogen are kept constant (Jess & al. , 1999). Moreover, nitrogen plays an important role in the operation of multi-tubular reactors by

facilitating removal of generated heat.

2.3.1. Fixed bed reactor

Considering the robustness against marine motion, and in particular inclination and inertia effects, fixed bed reactors are considered a good option for installation on a FPSO. Slurry bubble column reactors, having many favorable properties such as better heat transfer properties, have large volumes of liquid inventory and may be sensitive to wave motion. For the fixed bed reactor we assume a two-dimensional homogeneous reactor model with no axial dispersion. Boiling water is used as the coolant and its temperature is assumed to be constant along the axial direction. Table 2 shows the chosen design parameters of the fixed bed model.

Table 2: Design parameters of fixed bed and microchannel reactors.

	Fixed bed	Microchannel
Catalyst bulk density [kg/m^3]	1200	1200
Catalyst particle diameter [mm]	3	0.2
Catalyst void fraction	0.40	0.40
Cooling water temperature [°C]	220	220
Diameter of tube / channel side [mm]	25	2×2
Length of tube / channel [m]	12	2

Due to diffusion, there are concentration gradients, and to some extent a temperature gradient, inside a pellet. The effectiveness factor of a pellet, defined as the ratio between the integrated reaction rate over the pellet volume and the rate at bulk gas conditions, is normally less than unity. For a catalyst pellets of 3 mm diameter with homogeneous distribution of active sites, and with a kinetic model as applied here (Todic & al. , 2015, 2014), the effectiveness is calculated to be 0.20-0.25 on average along the reactor for the main reaction formation of alkanes. Due to different diffusion rates of reactants, a pellet will affect the selectivity compared to the intrinsic kinetics. Here, however, we assume the catalyst pellets have a thin layer of active catalyst sites only on the external surface. On the external surface we may neglect the diffusion resistance. The volume fraction of active layer on a pellet is here chosen to be 8 %. The catalyst loading can be increased beyond 8 % without running into problems of temperature runaway since the syngas consists of more than 27 % nitrogen, which helps mitigate temperature profile. Even with a homogeneous distribution of active sites throughout the pellet and with our diluted syngas, the calculations indicate that the temperature peak will be moderate. By increasing the catalyst loading on the pellet to 100 %, an effectiveness factor of 0.20-0.25 has to be applied. However, in the sequel we have assumed 8% catalyst loading and no diffusion resistance.

2.3.2. Microchannel reactor

Microchannel technology, with numerous parallel channels of small dimensions, enhances heat transfer because the specific heat transfer area is much larger. With microchannel technology heat transfer rates are accelerated 10 to 1000 times (Leviness & al. , 2011). Reactors with microchannels are suited for reactions that are highly exothermic or highly endothermic. Channels filled with FT catalyst powder and channels with coolant water are arranged in a cross flow configuration. Our simulations are based on channels with a dimension of 2×2 mm^2 and a length of 2 meter. Considering the thickness of the channel wall, the outer dimensions of each channel will be 3×3 mm^2. An illustration of a repeating unit of microchannels is shown in Figure 3. The reactor consists of several thousands of these repeating units. We assumed a two-dimensional homogeneous model with no axial dispersion. Boiling water is used as coolant and its temperature is assumed to be constant along the axial direction. Particles with diameter of 0.2 mm are applied in the reaction channels. Because of the small diameter a reasonable assumption is that there will be no mass transfer limitation inside the particles, equivalent to setting the effectiveness factor equal to unity for all reactions (Rytter & al. , 2007). All catalyst sites are exposed to the syngas, and that is why system volumes can be reduced up to 10 times compared to conventional reactors (Leviness & al. , 2011). Table 2 shows the design parameters of the microchannel reactor model.

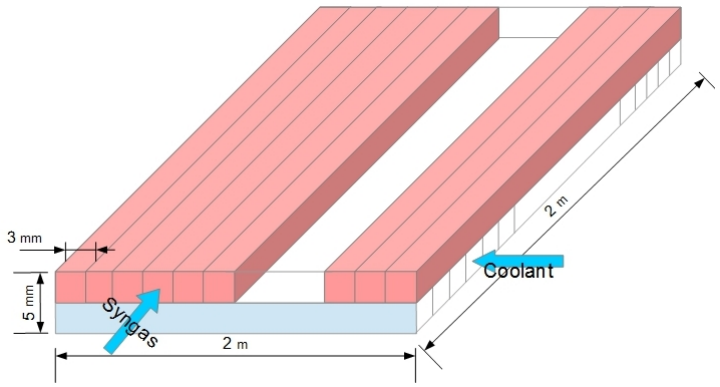

Figure 3: A repeating unit of a microchannel reactor.

Isothermal behavior of microchannel FT reactors has been demonstrated by Tonkovich et al. (Tonkovich & al. , 2008). The hot cooled microchannel reactors are isothermal to within $\pm 1^\circ$ C (Deshmukh & al. , 2010). This is also verified with our reactor model. With very high heat removal capability, single pass conversions near 80% can be realized. Unlike the fixed bed case, only two microchannel FT reactor stages are required due to the high CO conversion at each stage. The tail gas out of the second stage contains large amounts of nitrogen, 75 %, which makes it uneconomical to use a third stage. The tail gas is sent to the gas turbine for power generation.

2.4. Gas turbine for power production

The tail gas from the last Fischer-Tropsch stage is used as fuel to the gas turbine for power production. This gas consists of unconverted syngas, nitrogen, and lighter components formed in the synthesis reactors. The retenate stream from the air separation membrane is used as feed to the gas turbine. This stream is very useful as a feed to the gas turbine for several reasons; it does not need to be pressurized because the pressure is 16 bar, it keeps the turbine inlet temperature low, it contains nitrogen for cooling of the turbine blades, and since it contains 10 % oxygen less air needs to be compressed. The amount of oxygen to the gas turbine is adjusted to 15% more than the stoichiometric consumption, and there is about 1.3 % excess oxygen in the exhaust gas. If the inlet pressure to gas turbine is increased more power can be produced. However, to avoid two extra compressors, 16 bar pressure is chosen for power generation. With the high conversion obtained with microchannel reactors, the tail gas contains 73% nitrogen and 13% CO_2. This gas does not contain enough energy and in this case 20% of the excess hydrogen is added to the tail gas as fuel to gas turbine. Still there is more than sufficient amount of hydrogen for product upgrading. With the fixed bed reactors the conversion is lower and the tail gas contains enough energy to produce sufficient power. The power production is sufficient to provide power for all the consumers accounted for in this process. Approximately 22.7 MW and 9.3 MW of excess power is produced with fixed bed and microchannel reactors, respectively. The temperature of the exhaust gas, after heat exchanged, is approximately 240° C.

3. RESULTS AND DISCUSSION

To obtain a CO conversion of more than 90%, three fixed bed stages or two microchannel stages are required for the FT synthesis. The number of tubes or channels in each stage are selected so as to have approximately the same superficial gas velocity profile in all stages. The lengths are not changed. The simulations are done for both air-blown and enriched air-blown ATR, but only the results with enriched air are shown here. It is found that by using enriched air instead of air, on average 7.8% and 15.5% more C_{5+} can be produced in fixed bed and microchannel reactors, respectively.

In all simulations, the ATR outlet temperature is kept at 1060 °C and the steam-to-carbon ratio to the ATR is 0.6, while to the HER the steam-to-carbon ratio is 2.0. The feed composition to each stage is adjusted by hydrogen addition so that the H_2/CO ratios are the same and equal to the ratio from the ATR. Equal H_2/CO ratios to each stage need not be optimal, but is here chosen to be the case for convenience. Also the coolant temperatures are chosen the same for all stages, 220 °C, and furthermore the gas residence times at each stage are chosen the same. These parameters need not be optimal, and there is a potential of reducing the FT reactor volume without losing production. This will be studied further, and a methodology for systematic staging of reactor paths, described by Hillestad (2010), will be applied to find the optimal conditions for all parameters.

3.1. The effect of the split ratio between ATR and HER

As the split ratio to ATR is increased, more natural gas is sent to ATR and less to HER. Less gas to HER means less H_2 and CO_2 production, and therefore less CO_2 recycle to ATR inlet. This causes the H_2/CO ratio to increase. In all simulations, methane selectivity is higher in the next FT stage than in the previous one. The reason is that the applied kinetic model (Todic & al. , 2015, 2014) predicts that the growth factor decreases with decreasing pressure, and consequently more production of lighter hydrocarbons.

The effect of the split between the ATR and the HER for both FT synthesis reactor types are shown in Tables 3 and 4. The overall CO conversions for both microchannel and fixed bed simulations increases as the split ratio is increased. The reason for this trend is attributed to the kinetic model that dictates enhanced rates at increasing H_2/CO ratios. On the other hand, the chain growth probability, and thus the selectivity to higher hydrocarbons, decreases with increasing H_2/CO ratios. In Tables 3 and 4 the production rates of C_{5+} for both microchannel and fixed bed are seen to have a maximum, though relative flat for the fixed bed. For the microchannel case the maximum is at 85 % split and therefore this is chosen as the optimum split, while for the fixed bed 90% is chosen as the optimum split in terms of C_{5+} production. The optimum split will certainly depend on many parameters including temperature, the natural gas feed composition and steam-to-carbon ratio.

Table 3: Simulations with fixed bed model and with different feed gas split ratios to ATR and S/C=0.6.

Split ratios to ATR	0.85	0.9	0.92	0.95	0.97	1.0
H_2/CO ratio to first stage	2.00	2.09	2.13*	2.18*	2.22*	2.28*
CO Conversion [%]	88.9	89.5	89.9	90.5	91.0	90.6
C_{5+} production [tonne/h]	53.3	53.5	53.5	53.3	53.2	52.8
CH_4 Selectivity in first stage [%]	6.4	6.9	7.1	7.4	7.6	7.7
CH_4 Selectivity in second stage [%]	8.7	9.3	9.7	10.4	10.8	11.0
CH_4 Selectivity in third stage [%]	13.1	14.2	14.9	16.9	18.4	19.4

* H_2/CO ratio increased over the reactor

3.2. Steam-to-carbon ratio

The effect of the feed steam-to-carbon (S/C) ratio and the split ratio to the ATR on the H_2/CO ratio is shown in Figure 4. As the S/C ratio is increased, the H_2/CO ratio out of ATR increases. The effect of S/C ratio and the split ratio to the ATR on the C_{5+} production rates in both fixed bed and microchannel are shown in Figure 5. Lowering the S/C ratio, the H_2/CO ratio of the syngas becomes lower, and the production of C_{5+} has a maximum at a H_2/CO ratio which is slightly under-stoichiometric. By reducing

Table 4: Simulations with microchannel model and different feed gas split ratios to ATR and S/C=0.6.

Split ratio to ATR	0.82	0.85	0.87	0.9	0.92	0.95	0.97	1.0
H_2/CO ratio to first stage	1.97	2.00	2.04	2.09	2.13	2.18*	2.22*	2.28*
CO Convesion [%]	95.6	96.0	96.5	97.1	97.5	99.0	99.9	100.0
C_{5+} production [tonne/h]	57.2	57.3	57.2	57.1	57.0	56.5	55.8	55.3
CH_4 Selectivity in first stage [%]	7.0	7.3	7.7	8.3	8.8	9.5	10.0	10.7
CH_4 Selectivity in second stage [%]	14.0	14.9	15.9	17.6	18.7	26.8	36.3	44.9

* H_2/CO ratio increased over the reactor

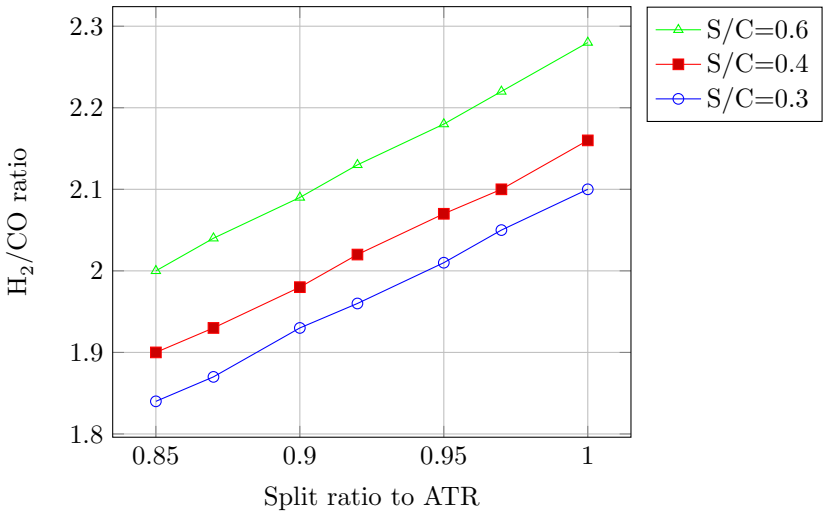

Figure 4: H_2/CO ratio out of the ATR as function of the split feed flow ratio to the ATR.

the S/C ratio from 0.6 to 0.3, about 4 tonnes/h more C_{5+} products can be produced. Although a low S/C ratio is beneficial, a S/C ratio of 0.6 is chosen here because this ratio is industrially tested and proven. The risk of coke formation and catalyst deterioration increases with lower S/C ratios.

3.3. Design at the optimal split

The optimal ATR split with fixed bed FT synthesis reactors is 0.9 at a steam-to-carbon ratio of 0.6. At these conditions, a summery of the the result of the chosen design is given in Table 5. Similarly, the optimal ATR split with the microchannel FT synthesis reactors is 0.85 at the the same S/C ratio, and a summary of the results of the chosen design is given in Table 5. In the microchannel case, as much as 87.5% of the C_{5+} products are produced in the first stage.

At these split ratios, an overview of some important process streams are given in Tables 6 and 7 for the fixed bed and the microchannel reactors. The stream numbers are referred to the process flow diagram in

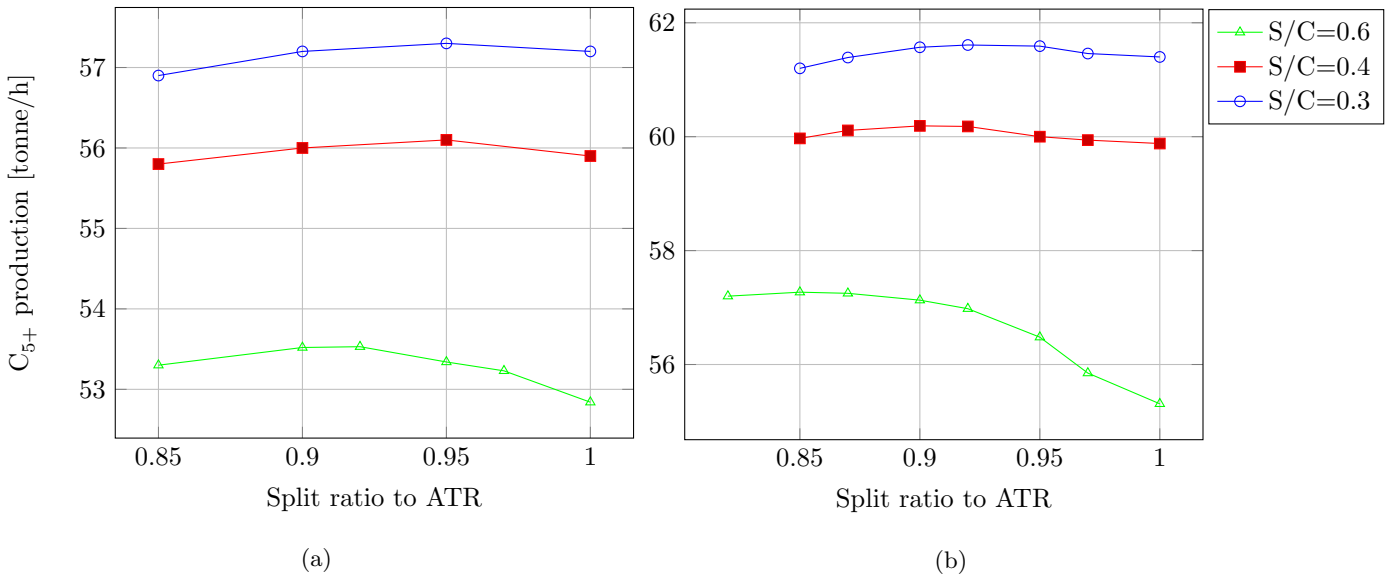

Figure 5: The production of C_{5+} with different S/C ratios and split ratios to the ATR, a) Fixed bed model b) Microchannel model

Figure 2. Temperature, pressure, mass flows in addition to mass fractions of the important components are chosen to be shown. Stream 110 is the hot outlet stream from the ATR, while 120 and 130 are the feed and effluent streams on the tube side of the heat exchange reformer. Streams 210, 220 and 230 are the feed streams to stage 1,2 and 3 of the FT reactors, while stream 240 is the tail gas and 250 is the total product stream.

3.4. Water and power

If the process concept is to be deployed on a FPSO, it need to be self sufficient with water and power. With the proposed process concept, there is no need to desalinate seawater or burn extra natural gas. Table 8 shows the water balance for the two reactor concepts. Water retrieved from the product may contain some oxygenates and small amounts of hydrocarbons but the water is perfect to be used as feed to the ATR or HER. These components will be reformed in the pre-reformer. Water retrieved from the syngas is much cleaner, mainly small amounts of CO_2 is present, and the water can easy be purified.

Table 9 shows the power balance. With fixed bed reactors the tail gas contains enough energy, whereas with the microchannel reactors 20 % of the hydrogen is added to the tail gas to obtain sufficient energy. In that respect the plant is autonomous in the sense that it produces more power and water than consumed.

Table 5: Fixed bed model results with a split to ATR of 0.9 and microchannel model with split to ATR of 0.85 and with S/C=0.6 for both cases.

	Fixed bed				Microchannel		
Stages	1	2	3	Total	1	2	Total
Catalyst volume [m^3]	286	225	179	690	96	64	160
CH_4 selectivity [%]	6.9	9.3	14.2	9.0	7.3	14.9	8.5
CO conversion [%]	42.5	53.2	60.9	89.5	81.3	79.0	96.1
C_{5+} production [tonne/h]	26.3	18.4	8.8	53.5	50.1	7.1	57.3

Table 6: Important stream information in the simulation with fixed bed model; the split to ATR is 0.9 and S/C = 0.6.

Stream	110	120	130	210	220	230	240	250
Temperature (°C)	1060	441	1050	210	210	210	30	175
Pressure (bar)	28.50	28.50	26.49	27.00	24.60	22.12	19.99	19.99
Mass flow (tonne/h)	485.31	42.44	42.44	407.74	339.63	291.39	266.53	54.02
Mass fractions								
CO	0.312	0	0.345	0.371	0.256	0.140	0.060	0.001
H_2	0.047	0.003	0.095	0.056	0.039	0.021	0.008	0
H_2O	0.161	0.726	0.425	0.002	0.001	0.001	0.001	0.002
CH_4	0.002	0.237	0.005	0.003	0.011	0.021	0.031	0
C_2-C_4	0	0	0	0	0.006	0.014	0.022	0.002
C_{5+}^{p} (alkanes)	0	0	0	0	0.005	0.008	0.010	0.891
C_{5+}^{o} (alkenes)	0	0	0	0	0	0	0	0.100
CO_2	0.100	0.033	0.130	0.119	0.143	0.167	0.182	0.003
N_2	0.377	0	0	0.449	0.538	0.627	0.686	0.002

Table 7: Important stream information in the simulation with microchannel model; the split to ATR is 0.85 and S/C = 0.6.

Stream	110	120	130	210	220	240	250
Temperature (°C)	1060	441.2	1052	210	210	30	178.5
Pressure (bar)	28.50	28.50	28.10	26.93	22.80	19.15	19.15
Mass flow (tonne/h)	476.90	63.89	63.89	399.10	270.90	249.40	58.10
Mass fractions							
CO	0.314	0	0.343	0.375	0.104	0.024	0
H_2	0.045	0.003	0.095	0.054	0.015	0.002	0
H_2O	0.165	0.727	0.428	0.002	0.001	0.001	0.004
CH_4	0.002	0.236	0.005	0.003	0.023	0.032	0
C_2-C_4	0	0	0	0	0.017	0.027	0.002
C^{p}_{5+} (alkanes)	0	0	0	0	0.007	0.009	0.857
C^{o}_{5+} (alkenes)	0	0	0	0	0	0	0.130
CO_2	0.107	0.033	0.129	0.128	0.189	0.205	0.005
N_2	0.366	0	0	0.438	0.645	0.700	0.002

Table 8: Water balance.

Water Stream [tonne/h]	Fixed Bed	Microchannel
Steam demand	105.7	119.1
Retrieved water from syngas	89.8	96.4
Retrieved water from product	87.5	92.8
Excess water	71.5	70.1

Table 9: Power balance.

Category	Power source/ sink	Fixed bed [MW]	Microchannel [MW]
Power sinks	Aircompression	139	134.2
	H_2 compression	3.0	4.5
	CO_2 recycle to ATR	0.2	0.2
Power sources	Gas Turbine	164.9	148.2
Excess power production		22.7	9.3

3.5. Comparing fixed bed and microchannel reactors

The principal results for the two reactor types are given in Table 10. The reactor productivity in terms of catalyst volume, the microchannel reactor has 4.6 times larger productivity than the fixed bed. On the other hand, the total weight of the microchannel reactors are calculated to be greater that the fixed bed. Including the catalyst weight the microchannel reactors are 17 % heavier than with fixed bed reactors. The total weight includes cylindrical pressure shells that the microchannel modules are kept in.

Table 10: Comparison between processes with fixed bed and microchannel reactors

	Fixed bed	Microchannel
Optimum feed split ratio to ATR	0.90	0.85
Total CO Conversion [%]	89.47	96.08
Total Methane Selectivity [%]	9.05	8.46
Carbon efficiency [%]	57.15	61.71
Catalyst volume [m^3]	690	160
Size of reactors [m^3]	3053	2115
Weight of empty reactors [tonne]	2141	3293
Weight of catalysts [tonne]	828	192
Reactor Productivity [tonne/(h m^3)]	0.078	0.358
Surplus hydrogen [tonne/h]	4.4	4.7

The carbon efficiency is defined as the fraction of the carbon of components in the feed ending up as carbon of components in the product stream. Figure 6 shows the carbon distributions with the two synthesis reactor types. With fixed bed, the carbon efficiency is about 57 %, while with microchannel synthesis reactors is is about 62 %. The main reason is that higher conversion, and thus less CO in the tail gas, is obtained with microchannel reactors. The rest of the carbon ends up in different components in the tail gas, including CO_2 produced in the ATR and lighter hydrocarbons produced in the Fischer-Tropsch synthesis reactors.

The carbon distribution is an important process descriptor, but energy distribution through the process is even more important. In the literature energy efficiency can be calculated different ways so they may be difficult to compare. Here we look at the fraction of the total NG1 feed LHV that is converted to LHV of the product and hydrogen streams, in addition to power export, energy of steam and finally lost energy. The tail gas and eventually some hydrogen are combusted to produce power that covers the compressor demands. The compressors are not included as input energy since their power demand is covered by the gas turbine. The excess power from the gas turbine, adjusted with the Carnot efficiency to be comparable to thermal energies, is reported as "power export". Lost energy includes external cooling and thermal energy

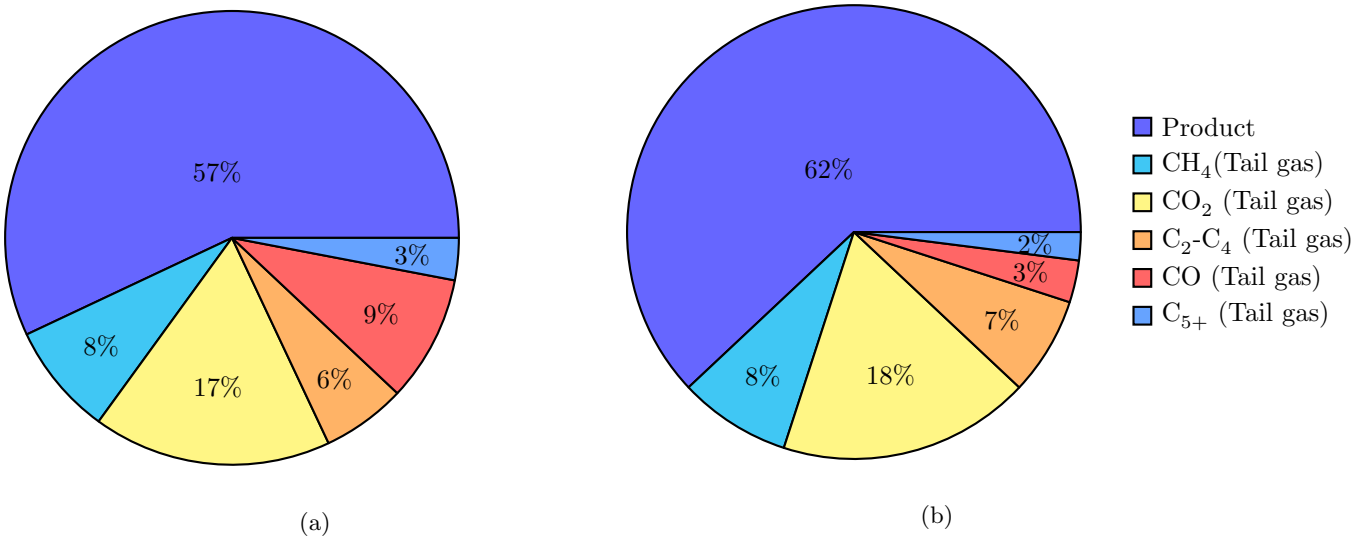

(a) (b)

Figure 6: The relative distribution of carbon between the products stream and the tail gas, with a) fixed bed reactor and with b) microchannel reactors.

of the exhaust gas from the gas turbine, in addition to pressure losses and loss of energy in compressors and turbine. Figure 7 gives a picture of the energy distribution with the two different synthesis reactor types. We should also bear in mind that part of the hydrogen energy will be transferred to the product after the product upgrading.

With fixed bed reactors 45 % of the natural gas LHV ends up in the product, while 9 % ends up as LHV of excess hydrogen, 26 % is steam produced from the FT reactors and hot syngas, 4 % is power export, while 16 % is lost energy. With the microchannel alternative, 50 % (slightly less) of the natural gas LHV ends up in the product stream, while 9 % ends up as LHV of excess hydrogen. Less energy in steam production mainly due to less energy in the hot syngas, and less power export and slightly less lost energy.

Reaction heat generated in the Fischer-Tropsch reactors will used for medium pressure steam production. This steam can be used in other parts of the process, however not considered here. The amount of steam from the FT reactors are estimated to be 289.5 and 311.4 tonnes/h for the fixed bed and microchannel reactors. The sensible heat generated from the FT reactors is calculated by integrating the heat transfer along the tubes, and the amount of steam generated is calculated by heating and evaporating water from 20 °C and 23.19 bar. However, there will be more steam produced with the fixed bed alternative, because of the higher spit and thus the hot syngas after HER contains more energy.

3.6. The effect of heavier natural gas

The natural gas used so far, NG1 in Table 1, is relatively light. If the natural gas is somewhat heavier, as NG2 in Table 1, what will be the consequences? Notice that 6000 kmol/h of NG2 contains more carbon

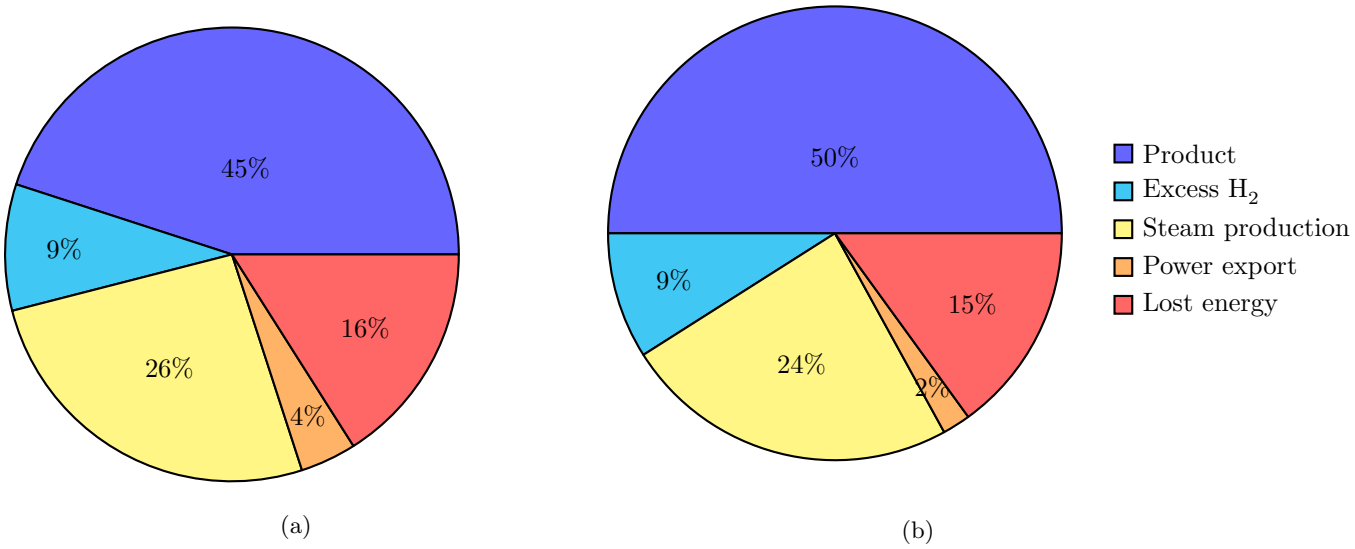

Figure 7: The relative distribution of energy content of the natural gas in different products streams of the GTL plant with a) fixed bed reactors and b) microchannel reactors.

that NG1. Notice also that the split parameter is not optimized in the case.

With fixed bed reactors and with NG2 as the feed and the same conditions as described in Table 5, i.e same split and S/C ratio, the production of C_{5+} is increased to 60.3 tonnes/h, while the CO conversion is about the same, and the methane selectivity is decreased to 8.4 %. More hydrogen is distributed between the stages and excess hydrogen has dropped to 3.8 tonnes/h, while the excess power is about the same. The same tendency is also found with microchannel reactors. The methane selectivity drops to 7.6 %, the CO conversion drops to 93.6 %, while the C_{5+} production increases to 63.7 tonnes/h. There is a slight drop in the carbon efficiency, 61 %. The amount of distributed hydrogen is increased so the excess hydrogen is lower.

3.7. Cost Estimation

The purchased cost for the fixed bed reactors is estimated based on different methods. One is to estimate the cost of the pressure shells and tubes and the cost of assembling the reactor be equal to the material costs. There are 48500 tubes distributed in two shells at the first stage, 38200 tubes distributed in two shells at the second stage and 30500 tubes in one shell at the third stage. Installed costs include piping, equipment erection, instrumentation and control, electrical and lagging and paint. Note that civil, structure, buildings and the ship are not included. If the process is to be on a FPSO the upgrading process will be relatively simple because the oil need to be refined onshore. The cost of upgrading is not part of the cost estimate. The total fixed capital investment including offsites, design and engineering and contingency add up to approximately 500 million USD.

Table 11: Breakup of equipment cost estimates for the plant with fixed bed reactors. Factors associated with civil, structures, buildings and the ship are not included.

	Equipment cost [million USD]	
Equipment	Purchased	Installed
Pre-reformer	1.3	2.8
ATR	8.7	20.4
Air compressors	8.7	28.3
Air membrane	18.8	37.5
HER	2.1	6.6
WGS reactor	0.3	0.7
Separators	1.2	3.1
H2 membrane	2.6	2.6
H2 compressor	0.5	1.6
Recycle compressor	0.1	0.3
Fixed bed FT reactors	42.6	100.9
Steam drum	0.7	1.8
Three Phase separators	0.7	1.8
Heat exchangers	2.9	9.3
Steam production	1.4	4.4
Coolers	3.2	10.4
Gas Turbine	40.4	43.1
Total ISBL	136.2	275.6

4. CONCLUSION

A novel process concept is proposed for converting natural gas to liquid hydrocarbon products. Syngas is produced in an enriched air-blown ATR at a slightly under-stoichiometric H_2/CO ratio. There is a H_2/CO ratio and temperature conditions that give a maximum production of higher hydrocarbons in the Fisher-Tropsch synthesis. The synthesis section is staged and hydrogen is fed between the stages to make up for the hydrogen consumption. Products and water are removed between the stages. This enables a high CO conversion in a once-through configuration. The process produces syngas and hydrogen in two parallel paths. Hydrogen is produced in a heat exchange reformer, heat integrated with the hot outlet from the ATR. The process does not require cryogenic air separation or fired heaters. With the proposed configuration, high once-through CO conversion, in the order of 90 % and more, is achieved.

Conventional fixed bed and microchannel reactor models for the FT synthesis are developed and tested separately in process simulations. The carbon efficiencies for a once-through synthesis are calculated to be 57 and 62 % for the fixed bed and microchannel reactors, respectively. The part of the energy that ends up in the product is 45 and 50 % for the fixed bed and microchannel reactors. However, the fixed bed alternative produces more energy as steam and power for export.

The effect of using a natural gas with heavier gas gives more products and less excess hydrogen. As long as there is sufficient excess hydrogen for upgrading, the heavier natural gas NG2 gives a more favorable energy distribution.

The process is autonomous as it is self-sufficient with power and water. The total investment of a 12000 bbl/day plant without considering the ship, buildings and structures or the upgrading unit is estimated to approximately 500 million USD with fixed bed reactors. Even when everything is not counted in the total cost, the proposed process concept is less expensive than existing projects. The main reason for the low cost is that cryogenic air separation and the costly steam methane reformer are avoided.

Acknowledgements

The authors gratefully acknowledge financial support from the Research Council of Norway through the GASSMAKS program.

References

Air Products, Stainless steel nitrogen membrane separator (white paper), (2015).

Baxter, I, Modular GTL as an Offshore Associated Gas Solution, *Deep Offshore Technology International*, (2010), pp. 1–19.

Carson, N, Hawker, P, Whitley, N, Wright, A, Dunleavy, J, & Tomlinson, D, Presentation to Analysts/ Investors, (white paper), Johnson Matthey, (2008), pp. 139–148.

Chen, Z, Yan, Y, & Elnashaie, S S E H, Modeling and optimization of a novel membrane reformer for higher hydrocarbons, *AIChE Journal*, vol. **49** , (2003), pp. 1250–1265.

Deshmukh, S R, Tonkovich, A L Y, Jarosch, K T, Schrader, L, Fitzgerald, S P, Kilanowski, D R, Lerou, J J, Mazanec, T J, Scale-up of microchannel reactors for Fischer-Tropsch synthesis, *Industrial and Engineering Chemistry Research*, vol. **49** , (2010), pp. 10883 –10888.

Falkenberg, M, Hillestad, M, Modeling, simulation and design of three different concepts for offshore methanol production, *Submitted for publication.*

Fonseca, A, Bidart, A, Passarelli, F, Nunes, G & Oliveira, R, Offshore gas-to-liquids : Modular solution for associated gas with variable CO2 content, *World gas conference*, (2012), pp. 1–15.

He, X Developement of hollow fiber carbon membranes for CO_2 separation, PhD Thesis, Norwegian University of Science and Technology, Department of Chemical Engineering, 2011.

Hillestad, M, Systematic staging in chemical reactor design, *Chemical Engieering Science*, **65**, (2010), pp. 3301–3312.

Hillestad, M, Modeling the Fischer-Tropsch product distribution and model implementation, *Chemical Product and Process Modeling*, **xx**, (2015), pp. yyy–yyy.

Hutton, W. J., & Holmes, J., Floating Gas to Liquids - A Solution to Offshore Stranded Gas, *18th World Petroleum Congress.*

Jess, A, Popp, R & Hedden, K, FischerTropsch-synthesis with nitrogen-rich syngas: fundamentals and reactor design aspects, *Applied Catalysis A: General*, vol. **186** , (1999), pp. 321–342.

Kim, W S, Yang, D R, Moon, D J & Ahn, B S, The process design and simulation for the methanol production on the FPSO (floating production, storage and off-loading) system, *Chemical Engineering Research and Design*, vol.**92**, (2014), pp. 931–940.

Kim, H J, Choi, D K, Ahn, S I, Kwon, H, Lim, H W, Denholm, D, Park, T & Zhang, L, OTC 24113 GTL FPSO : An Alternative Solution to Offshore Stranded Gas, *Oil and Gas Facilities*, June 2014, pp. 41–51.

Leviness, S, Tonkovich, A, Mazanec, T, & Jarosch, K, Improved Fischer-Tropsch economics enabled by microchannel technology (white paper), (2011), pp. 1–7.

Loenhout, V, Zeelenberg, L, Gerritse, A, Roth, G, Sheehan, E & Jannasch, N, Commercialization of Stranded Gas With a Combined Oil and GTL FPSO, *Offshore Technology Conference*, (2006).

Lowe, C., Gerdes, K., Stupin, W., Hook, B., Marriott, P., Impact of syngas generation technology selection on a GTL FPSO, *Studies in surface science and catalysis*, (2001), pp. 57-62.

Lögdberg, S, Boutonnet, M, Walmsley, J C, Jaras S, Holmen, A, & Blekkan E A, Effect of water on the space-time yield of different supported cobalt catalysts during FischerTropsch synthesis, *Applied Catalysis A: General*, vol. **393** , (2011), pp. 109–121.

Malhotra, A, Macris, A, & Gosnell, J, Increase Hydrogen Production Using KBRs KRES Technology, *National Petrochemical and Refiners Association*, (2004), pp. 1–14.

Masanobu, S, Kato, S, Nakamura, A, Sakamoto, T, Yoshikawa, T, Sakamoto, A, Uetani, H, Kawazuishi, K, Sao, K, Development of Natural Gas Liquefaction FPSO, *23rd internationa conference on offshore mechanics and arctic engineering*, (2004), pp. 1–10.

Rafiee, A & Hillestad M, Staging of the Fischer Tropsch reactor with an iron based catalyst, *Computers and Chemical Engineering*, vol. **39**, (2012), pp. 75 - 83.

Rao, V U S, Stiegel, G J, Cinquegrane, G J, Srivastava, R D, Iron-based catalysts for slurry-phase Fischer-Tropsch process: Technology review, *Fuel processing technology*, vol. **30**, (1992), pp. 83–107.

Rostrup-Nielsen, J R, Syngas in perspective, *Catalysis Today*, vol. **71**, (2002), pp. 243–247.

Rytter, E, Eri, S, Skagseth, T H, Schanke, D, Bergene, E, Myrstad, R, Lindvåg, A, Catalyst Particle Size of Cobalt/Rhenium on Porous Alumina and the Effect on FischerTropsch Catalytic Performance, *Industrial & Engineering Chemistry Research*, vol. **46**, (2007), pp. 9032-9036.

Rytter, E, Gas to liquids plant with consecutive fischer-tropsch reactors and hydrogen make-up, Patent US 2010/0137458 A1, (2010).

Schanke, D, Hilmen, A.M, Bergene, E, Kinnari, K, Rytter, E, Adnanes, E. & Holmen, A. Study of the deactivation mechanism of Al_2O_3-supported cobalt Fischer-Tropsch catalysts, *Catalysis Letters*, vol. **34**, (1995), pp. 269–284.

Schanke, D, Lian, P, Eri, S, Rytter, E, Sannaes, B H & Kinnari, K J, Optimisation of Fischer-Tropsch reactor design and operation in GTL plants, *Studies in Surface Science and Catalysis*, vol. **136**, (2001), pp. 239-244.

Thomsen, SG, Han, PA, Loock, S & Ernst, W, The first industrial experience with the Haldor Topsøe exchange reformer, *Ammonia Plant Safety and Related Facilities*, vol. **47**, (2006), pp. 259–266.

Todic, B., Ma, W.P., Jacobs, G., Davis, B.H. & Bukur, D.B., CO-isertion mechanism based kinetic model of the Fischer-Tropsch synthesis reaction over Re-promoted Co catalyst, *Catalysis Today*, vol. **228**, (2014), pp. 32–39.

Todic, B., Ma, W.P., Jacobs, G., Davis, B.H. & Bukur, D.B., Corrigendum to: CO-insertion mechanism based kinetic model of the FischerTropsch synthesis reaction over Re-promoted Co catalyst, *Catalysis Today*, vol. **242**, (2015), pp. 386.

Tonkovich, A L, Jarosch, K, Arora, R, Silva, L, Perry, S, McDaniel, J, Daly, F & Litt, B, Methanol production FPSO plant concept using multiple microchannel unit operations, *Chemical Engineering Journal*, vol. **135**, (2008), pp. 2–8.

Tsakoumis, N E,Rnning, M, Borg, , Rytter, E, Holmen, A, Deactivation of cobalt based Fischer-Tropsch catalysts: A review, *Catalysis Today*, vol. **154**, (2010), pp. 162-182.

Wilhelm, D J, Syngas production for gas-to-liquid applications:technologies, issues and outlook, *Fuel processing technology*, vol. **71**, (2001), pp. 139–148.

Appendix B

Simulation Flow Sheet

This appendix include picture of the simulation flow sheet for the main process design, without heat integration (Figure B.3), the heat integration network design (Figure B.1) and the steam cycle (Figure B.2).

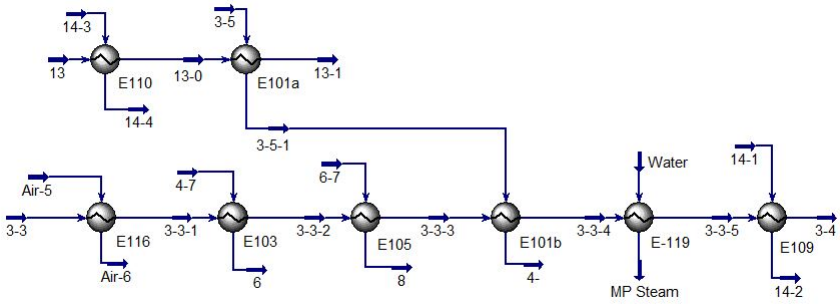

Figure B.1: HYSYS flow sheet for the simulation of the heat integration network.

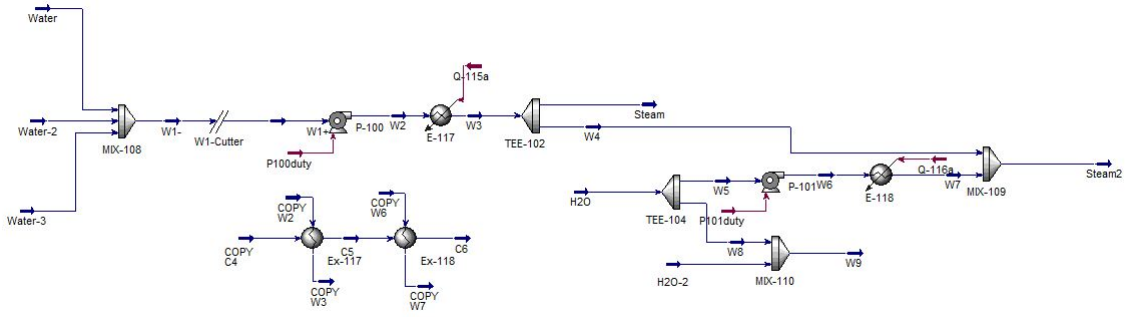

Figure B.2: HYSYS flow sheet for the simulation of the steam cycle and the heat integration with the effluent gas from the gas turbine after pre-heating the natural gas.

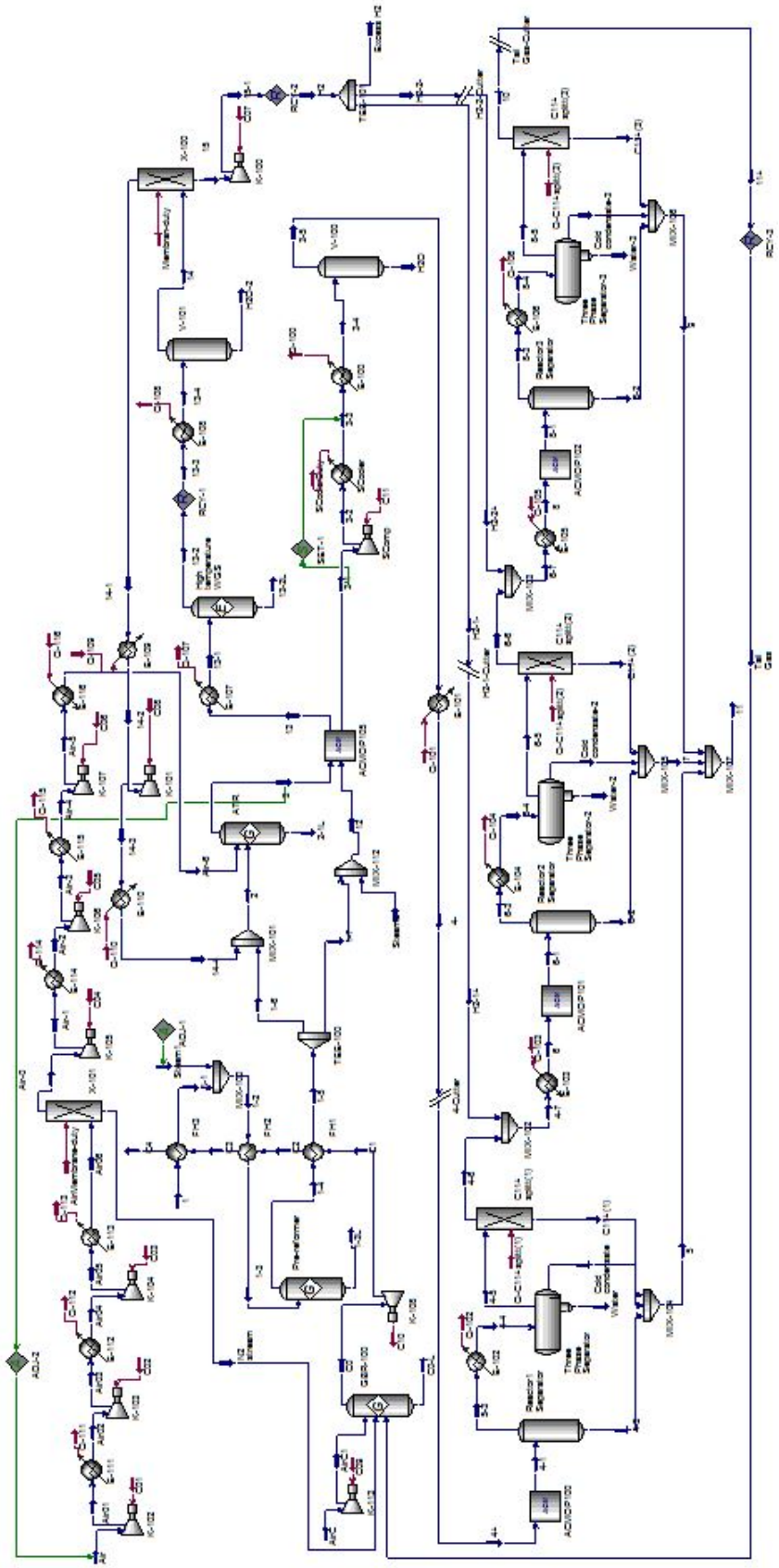

Figure B.3: HYSYS flow sheet of the main process.

Appendix C

Air Membrane

In the simulation the Air Membrane is simulated as a component splitter and in this appendix the calculation for the split fraction to be used in the component splitter is given. A received data sheet for a PRISM membrane from Air Product is used as basis for the calculation [43]. The flow of nitrogen stream (permeate), and the air feed flow in Nm^3/h from the data sheet is given in Table C.1.

Table C.1: Information about normal cubic meter per hour flow of nitrogen product and air feed from PRISM membrane data sheet [43].

N_2 purity	99.5%		99.0%		98.0%		97.0%		96.0%		95.0%	
	Air	N2	Air	N2	Air	N2	Air	N2	Air	N2	Air	N2
5 barg	12.3	1.7	13.1	2.4	14.5	3.6	15.7	4.7	16.9	5.8	18.2	7.0
7 barg	17.8	2.8	19.1	4.0	21.2	5.8	23.1	7.5	25.0	9.3	27.1	11.2
9 barg	23.3	4.0	25.1	5.5	28.0	8.1	30.7	10.5	33.4	12.9	36.2	15.5
12 barg	31.7	5.7	34.2	8.0	38.4	11.6	42.2	15.0	46.1	18.5	50.1	22.2
15 barg	40.1	7.5	43.4	10.4	48.9	15.2	53.9	19.7	58.9	24.2	64.2	29.1

The molar volume with a temperature of 15°C and pressure of 1 atm is calculated using Eq.C.0.1. The flows given in Nm^3/h is converted to kmole/h by dividing with the molar volume.

$$\frac{V}{n} = \frac{RT}{P} \tag{C.0.1}$$

where $\frac{V}{n}$ is the volume per mole, R is the gas constant, T is the temperature, and P is the pressure.

It is assumed that the composition of air is 21% oxygen and 79% nitrogen. From this information the composition of the enriched air is calculated and the mole fraction of oxygen is given in Table C.3.

Table C.2: Mole fraction of oxygen in enriched air with different membrane conditions.

N2 purity	99.5%	99.0%	98.0%	97.0%	96.0%	95.0%
5 barg	0.243	0.255	0.273	0.287	0.299	0.310
7 barg	0.248	0.263	0.282	0.297	0.311	0.323
9 barg	0.252	0.266	0.287	0.304	0.317	0.330
12 barg	0.255	0.271	0.292	0.309	0.324	0.337
15 barg	0.257	0.273	0.296	0.314	0.329	0.343

As the table illustrates is the amount of oxygen in the enriched air increased with feed pressure and with less purity of the nitrogen stream (permeate). From this evaluation is it decided to use the membrane with 95% purity of nitrogen, however, the pressure is dependent on compression energy for the air. The split fraction for the component splitter with different feed pressure are given below.

Table C.3: The split fraction to be used for a component splitter in the simulation for different operation pressure.

Pressure [barg]	Retentate (Enriched Air)	
	O_2	N_2
5	0.9084	0.5375
7	0.9016	0.5030
9	0.8981	0.4851
12	0.8945	0.4671
15	0.8921	0.4549

Appendix D

Hydrogen Selective Carbon Membrane

This appendix contain the MATLAB script used to decide the split factors used for the component splitter in HYSYS for the hydrogen selective carbon membrane.

```
%Main Script

clear all
clc

%Membran model for one tube
global k Pf Pp

n=20;
[x, A, B, q] = colloc(n ,1 ,1);

nK = 5;                              %Number of components [CO2,H2,CO,H2O,CH4]
Y=ones(n+2,2*nK);                    %initial guess

Lmembran = 1;                         %Length of membrane [m]
v = 0.08;                             %Velocity [m/s]

d = 0.004;                            %Tube diameter [m]
aph = 4/d;                            %[m2/m3]
S = pi*(d/2)^2;                       %Tube cross section area [m2]

R = 8.314472;                         %Gas constant [m3*kPa/K*kmole]
T = 30+273.15;                        %Temperature [K]
V_n = (R*275.15)/100;                 %Molar volume [m3/kmole]

k(1) = (2*2.7*10^-3)/(V_n*3600);  %Permeance CO2 [kmole/m2*s*bar]
k(2) = (200*2.7*10^-3)/(V_n*3600);%Permeance H2  [kmole/m2*s*bar]
k(3) = 0;                             %Permeance CO  [kmole/m2*s*bar]
k(4) = 0;                             %Permeance H2O [kmole/m2*s*bar]
k(5) = 0;                             %Permeance CH4 [kmole/m2*s*bar]

Pf = 25.5;                            %Pressure feed side [bar]
```

```
Pp = 7;                                %Pressure permeate side [bar]
                                       %Ph/Pl = 10

Cf = (100*Pf)/(R*T);                  %Total concentration feed side [kmole/m3]
Flow = Cf*v*S;                        %total flow [kmole/s]

%Molar flow in feed - start conditions
nR0(1) = 0.1482*Cf*v;                  %CO2(x_CO2*Cf*v)[kmole/m2*s]
nR0(2) = 0.7776*Cf*v;                  %H2 (x_H2*Cf*v) [kmole/m2*s]
nR0(3) = 0.0682*Cf*v;                  %CO (x_CO*Cf*v) [kmole/m2*s]
nR0(4) = 0.0019*Cf*v;                  %H2O(x_H2O*Cf*v) [kmole/m2*s]
nR0(5) = 0.0040*Cf*v;                  %CH4(x_CH4*Cf*v) [kmole/m2*s]

%Molar flow in permeate - start conditions
nP0(1) = 0;                            %CO2 [kmole/m2*s]
nP0(2) = 0;                            %H2  [kmole/m2*s]
nP0(3) = 0;                            %CO  [kmole/m2*s]
nP0(4) = 0;                            %H2O [kmole/m2*s]
nP0(5) = 0;                            %CH4 [kmole/m2*s]

opt=optimset('Display','iter','MaxFunEval',1000000,'MaxIter',1000);
%Function F
Y=fsolve(@(Y) mem(Y, A, n, nR0, nP0, aph, Lmembran, nK),Y);

%Calculation of split for permeate
for i = 1:5
Split_P(i) = Y(1,nK+i)/(Y(1,nK+i)+Y(n+2,i)); %Split factor
end
Split = Split_P

%Fraction of H2&CO2 in retentate
FracR_H2 = Y(n+2,2)/sum(Y(n+2,1:5));
FracR_CO2 = Y(n+2,1)/sum(Y(n+2,1:5));

%Total flow amount from one tube (sum(nR)*S) [kmole/s]
Feed      = sum(Y(1,1:nK))*S;
Retentate = sum(Y(n+2,1:nK))*S;
Permeate  = sum(Y(1,nK+1:2*nK))*S;

%Total feed to the membrane [kmole/h]
Feed_tot = 2993;

%Number of tubes needed
Ntubes = (Feed_tot/3600)/Feed
```

```
function F = mem(Y, A, n, nR0, nP0, aph, Lmembran, nK)
global k Pf Pp
nR = Y(:,1:nK);
nP = Y(:,nK+1:2*nK);
FR = zeros(n+2,nK);
FP = zeros(n+2,nK);
```

```
7
8  %boundary z=0
9  for j=1:nK
10     FR(1,j)=nR0(j)-nR(1,j);
11     J(j)=k(j)*((Pf*(nR(1,j)/sum(nR(1,:))))-...
12         (Pp*(nP(1,j)/sum(nP(1,:)))));
13     FP(1,j)=(A(1,:)*nP(:,j))+(J(j)*aph*Lmembran);
14 end
15
16 %internal collocation points
17 for i = 2:n+1
18     for j=1:nK
19         J(j)=k(j)*((Pf*(nR(i,j)/sum(nR(i,:))))-...
20             (Pp*(nP(i,j)/sum(nP(i,:)))));
21         FR(i,j)=(A(i,:)*nR(:,j))+(J(j)*aph*Lmembran);
22         FP(i,j)=(A(i,:)*nP(:,j))+(J(j)*aph*Lmembran);
23     end
24 end
25
26 %boundary z=1
27 for j=1:nK
28     J(j)=k(j)*((Pf*(nR(n,j)/sum(nR(n,:))))-...
29         (Pp*(nP(n,j)/sum(nP(n,:)))));
30     FR(n+2,j)=(A(n+2,:)*nR(:,j))+(J(j)*aph*Lmembran);
31     FP(n+2,j)=nP0(j)-nP(n+2,j);
32 end
33 F=[FR FP];
34 end
```

Appendix E

Stream Composition in Mass Fraction

A flow sheet of the process is given in Figure E.1 and a table with the operating conditions and the composition in mass fraction is given in Table E.1.

A flow sheet of the processes and a table with operating conditions and composition in mole fraction is given in the section 3.1 in the main report. In the report the composition is given in mole fraction, as the molar flow is more useful; i.e. if it is wanted to look at the conversion. However, for the higher hydrocarbons more information is given when looking at the mass fraction, these tables is therefore included here.

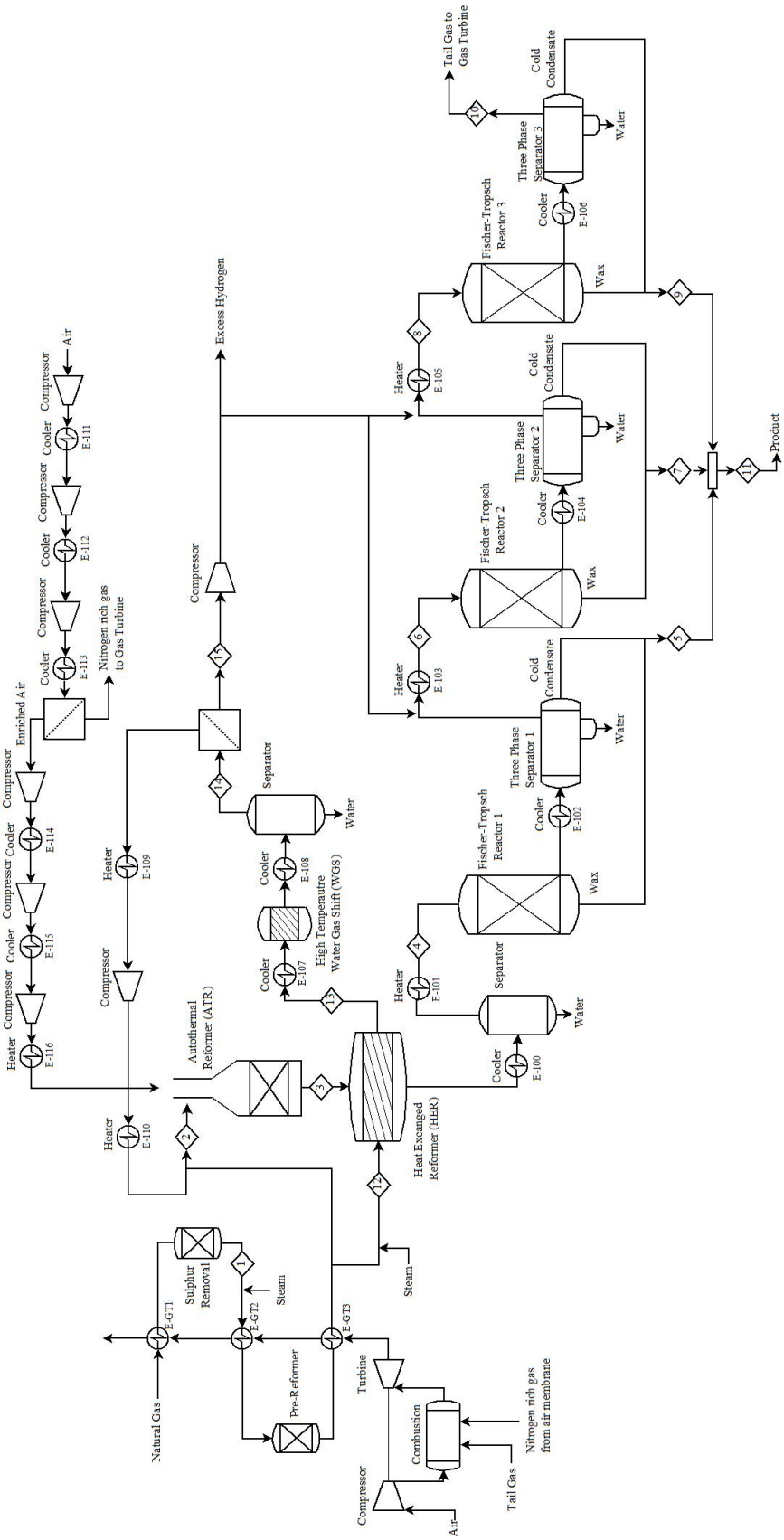

Figure E.1: Flow sheet of the GTL-FPSO process, with synthesis gas production and Fischer-Tropsch synthesis

Table E.1: Specification of temperature, pressure, molar flow and mass flow for the numbered streams in the process flow sheet. The compositions is given in mass fraction.

Stream Number	1	2	3	4	5	6	7	8	9	10	11	12	13	14
Temperature [°C]	350.0	649.9	1,060.1	210.0	189.9	210.0	171.4	210.0	135.6	30.0	174.7	440.5	1,050.0	30.0
Pressure [bar]	30.0	28.5	28.5	27.0	25.1	24.6	22.6	22.1	19.9	19.9	19.9	28.5	26.5	25.5
Molar Flow [kmole/h]	6,000	11,084	28,787	24,681	80	17,668	68	12,735	42	10,038	190	2,440	3,671	2,993
Mass Flow [tonne/h]	104.7	193.5	485.3	411.3	26.2	340.5	18.7	292.1	9.0	266.9	53.9	42.4	42.4	30.2
Mole fraction [-]														
Carbon monoxide	0	0.030	0.312	0.368	0.001	0.258	0	0.142	0	0.061	0	0	0.345	0.189
Hydrogen	0	0.010	0.047	0.056	0	0.039	0	0.021	0	0.009	0	0.003	0.095	0.155
Water	0	0.328	0.161	0.011	0.002	0.001	0.002	0.001	0.001	0.001	0.002	0.726	0.425	0.003
Carbon dioxide	0	0.162	0.100	0.118	0.002	0.143	0.004	0.167	0.006	0.182	0.003	0.033	0.130	0.646
Nitrogen	0	0	0.377	0.445	0.001	0.537	0.002	0.626	0.003	0.685	0.002	0	0	0
Methane	0.874	0.469	0.002	0.003	0	0.011	0	0.021	0	0.031	0	0.237	0.005	0.006
Ethane	0.034	0	0	0	0	0.001	0	0.001	0	0.002	0	0	0	0
Ethylene	0	0	0	0	0	0.001	0	0.003	0	0.005	0	0	0	0
Propane	0.038	0	0	0	0	0.001	0	0.002	0	0.003	0	0	0	0
Propylene	0	0	0	0	0	0.001	0	0.003	0.001	0.005	0	0	0	0
n-Butane	0.033	0	0	0	0	0.001	0.001	0.002	0.001	0.003	0.001	0	0	0
1-Butene	0	0	0	0	0	0.001	0.001	0.003	0.002	0.004	0.001	0	0	0
n-Pentane	0.021	0	0	0	0	0.001	0.002	0.002	0.005	0.003	0.002	0	0	0
n-Hexane	0	0	0	0	0.002	0.001	0.006	0.002	0.014	0.003	0.005	0	0	0
n-Heptane	0	0	0	0	0.004	0.001	0.014	0.002	0.028	0.002	0.012	0	0	0
n-Octane	0	0	0	0	0.009	0.001	0.023	0.001	0.038	0.001	0.019	0	0	0
n-Nonane	0	0	0	0	0.015	0	0.027	0	0.038	0	0.023	0	0	0
n-Decane	0	0	0	0	0.019	0	0.027	0	0.036	0	0.025	0	0	0
C^{p}_{11+}	0	0	0	0	0.859	0	0.790	0	0.685	0	0.806	0	0	0
C^{o}_{5+}	0	0	0	0	0.085	0	0.100	0	0.142	0	0.100	0	0	0

Appendix F

Total Mass and Energy Balance

In this appendix the total mass and energy balance from the HYSYS simulation are given. This is important to control that the overall mass and energy balance is conserved in the process.

F.0.1 Mass Balance

The mass balance equation for a steady state process is given in equation F.0.1. To control that mass is conserved in the process the mass flow into the system is compared with the mass flow out of the system, given in Table F.1. All the values are taken from the HYSYS simulation.

$$\dot{m}_{in} = \dot{m}_{out} \tag{F.0.1}$$

where $\dot{m}$ is the mass flow.

Table F.1: Mass balance over the process.

Inlet streams	$\dot{m}$ [kg/h]	Outlet streams	$\dot{m}$ [kg/h]
Natural gas	104,673	Product	53,851
Air to ATR	524,162	Knockout water 1	73,963
Air to Gas Turbine	387,407	Knockout water 2	12,209
Steam in 1	81,942	Water out 1	44,791
Steam in 2	23,780	Water out 2	29,930
		Water out 3	16,139
		Flue gas	886,680
		Excess hydrogen	4,403
Sum	1,121,964	Sum	1,121,965

The relative imbalance in the process is -0.00004% and is calculated according to equation F.0.2. The small imbalance in the process can be connected to the recycle loops in the process, and assumed to be acceptable.

$$Im\% = \frac{\dot{m}_{in} - \dot{m}_{out}}{\dot{m}_{in}} \cdot 100 \tag{F.0.2}$$

F.0.2 Energy Balance

The energy balance equation for a steady state process is given in equation F.0.3.

$$Q_{in} = W_{out} - \dot{Q}_{in} = W_{in} - \dot{Q}_{out} = Q_{out} \tag{F.0.3}$$

where Q is the total heat flow in and out of the system, W_{out} is the work done by the system, W_{in} is the work done to the system and $\dot{Q}$ is the heat in the streams in and out of the system.

All values are taken from HYSYS simulation and are given in Table F.2.

Table F.2: Energy balance over the process.

Inlet streams	Q [MW]	Outlet streams	Q [MW]
Natural gas	-126.0	Product	-26.2
Air to ATR	-2.2	Knockout water 1	-319.5
Air to Gas Turbine	-1.7	Knockout water 2	-53.7
Steam in 1	-299.8	Water out 1	-197.2
Steam in 2	-87.0	Water out 2	-131.7
		Water out 3	-71.0
		Flue gas	-368.5
		Excess hydrogen	1.2
Compressors	142.6	Gas Turbine	179.0
Heaters	108.4	Coolers	504.6
Membrane	0.1	FT reactor	217.6
Hypo-duty	40.7	Hypo-duty	40.8
Sum	-224.9	Sum	-224.7

The relative imbalance in the process is 0.053% and is calculated according to equationF.0.4. There is a small energy imbalance in the process, which can be connected to the recycle loops in the process, and assumed to be acceptable.

$$Im\% = \frac{Q_{in} - Q_{out}}{Q_{in}} \cdot 100 \tag{F.0.4}$$

Appendix G

Energy Efficiency Calculation

This appendix will give the values used for the calculation of the energy efficiency in the process.

The heat of combustion values for the different components, are taken from HYSYS and given in Table G.1

Table G.1: The heat of combustion for the different components.

Components	Heat of combustion [kJ/kmole]
CO	-283,000
H_2	-241,942
H_{20}	0
CO_2	0
O_2	0
N_2	0
Methane	-802,703
Ethane	-1,428,510
Ethylene	-1,323,570
Propane	-2,044,970
Propylene	-1,927,350
Butane	-2,652,850
Butene	-2,543,740
Pentane	-3,265,570
Hexane	-3,888,500
Heptane	-4,503,500
Octane	-5,188,500
Nonane	-5,733,550
Decane	-6,348,600

By plotting the heat of combustion value as a function of carbon number for the alkanes and the alkenes an expression for the heat of combustion as a function of carbon number was made

with the use of linear regression. The heat of combustion for the alkanes lumps are given from equation G.0.1 and for the alkenes from equation G.0.2.

$$\Delta H_{c,\text{alkanes}}(x) = -615,702x - 192,363 \tag{G.0.1}$$
$$\Delta H_{c,\text{alkenes}}(x) = -610,085x - 101,298 \tag{G.0.2}$$

where x is the number of carbon atoms.

The exact number of carbons in the lumps can be calculated from equation G.0.3-G.0.6 [3] with the given values for low and high α value (Table G.2).

$$\mathrm{C}_{11+}^{PH} : n_c = 11 + \frac{\alpha_{1H}}{1-\alpha_{1H}} \tag{G.0.3}$$
$$\mathrm{C}_{11+}^{PL} : n_c = 11 + \frac{\alpha_{1L}}{1-\alpha_{1L}} \tag{G.0.4}$$
$$\mathrm{C}_{5+}^{OH} : n_c = 5 + \frac{\alpha_{2H}}{1-\alpha_{2H}} \tag{G.0.5}$$
$$\mathrm{C}_{5+}^{OL} : n_c = 5 + \frac{\alpha_{2L}}{1-\alpha_{2L}} \tag{G.0.6}$$
$$\tag{G.0.7}$$

Table G.2: Overview over high and low α value for alkanes and alkenes.

α_{1H}	0.97	α_{2H}	0.74
α_{1L}	0.84	α_{2L}	0.60

The excess power is converted to thermal energy with the use of the Carnot efficiency (η) given in equation G.0.8 [64].

$$\eta = 1 - \frac{T_C}{T_H} \tag{G.0.8}$$

where T_C is the turbine outlet pressure and T_H is the inlet temperature.

The relation between thermal energy (E) and mechanical energy (P) are given in equation G.0.9.

$$E = \frac{P}{\eta} \tag{G.0.9}$$

Appendix H

Heat Integration

In this appendix the statement of no heat recovery pinch in the process is explained.

Due to the keeping the heat exchanger size small for an FPSO, it is desired to have a high temperature difference. Because of this some hot streams are more favourable to use for the heat integration. Figure H.1 gives an overview over the two hot streams and six cold stream included in the heat integration, together with temperatures and energy in each stream. All the values given in the figure is taken from the HYSYS simulation.

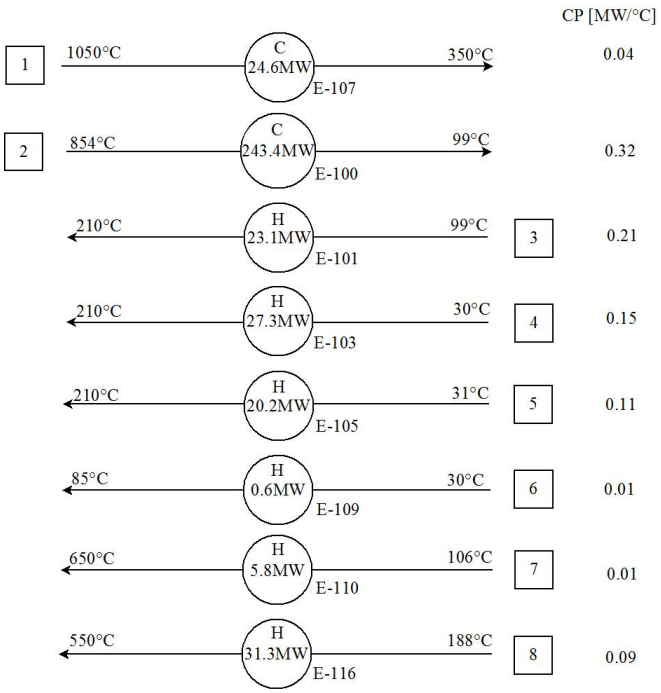

Figure H.1: The initial heat (H) and cooling (C) demand for the streams included in the heat integration network.

To produce the composite curves of the hot and the cold streams the temperature are arranged

in rising order. The heat capacities to the different streams in a temperature interval is added together (Table H.1).

Table H.1: The interval temperatures to produce the composite curve together with the total heat capacity in each interval and energy in the interval.

Hot stream				
Temp interval [°C]	ΔT_i [°C]	Stream in interval	Total CP [MW/°C]	ΔH_i [MW]
1050 - 854	196	1	0.04	6.9
854 - 350	504	1+2	0.36	180.2
350 - 99	251	2	0.32	80.9
Cold stream				
Temp interval [°C]	ΔT_i [°C]	Stream in interval	Total CP [MW/°C]	ΔH_i [MW]
650-550	100	7	0.01	1.1
550-210	340	7+8	0.10	33.1
210-188	22	3+4+5+7+8	0.57	12.3
188-106	82	3+4+5+7	0.48	39.7
106-99	8	3+4+5	0.47	3.6
99-85	14	4+5	0.26	3.7
85-31	53	4+5+6	0.28	14.7
31-30	1	4+6	0.17	0.2

The composite curves (Figure H.2) indicates a threshold problem. A threshold problem means that only either hot or cold utility are needed in the process. For this process the two hot streams has sufficient heat to heat up the cold streams, giving the need of only cold utility. For a threshold problems there are no heat integration pinch point and the heat integration design is made from the most constrained end. A utility pinch can be included in the process if several utilities are used.

If "The Problem Table Algorithm" explained in section 2.5 in the main report is used for a threshold problem a ΔT_{min} value below or above the threshold value will give the need for both utilities. Due to this the composite curve was used for the pinch evaluation giving no pinch in the system.

From Figure H.2 there is a need for external cooling in the system, however if medium pressure steam production is included as a cooling medium, other cooling medium are not needed, as illustrated in Figure H.3, for a MP steam at 210°C and 19.07 bar.

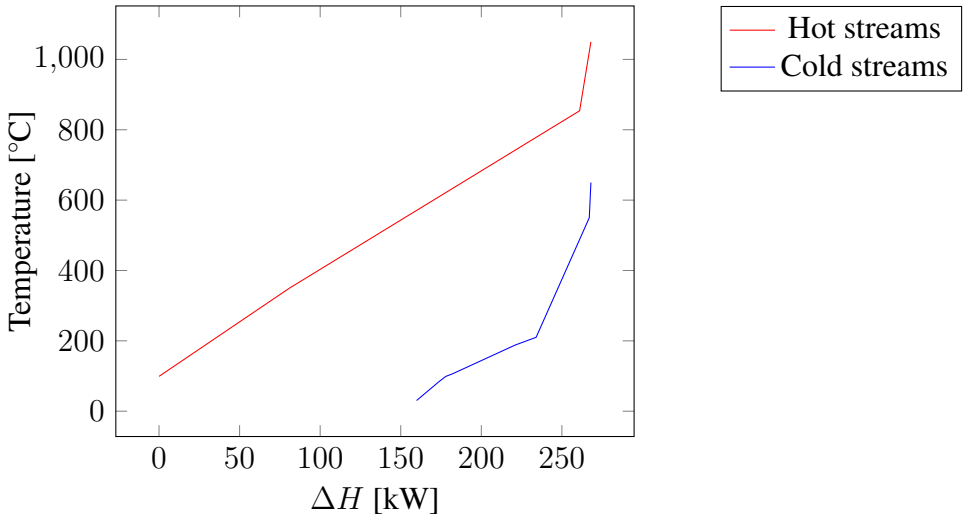

Figure H.2: The Composite Curves for the hot and cold streams included in the heat integration network.

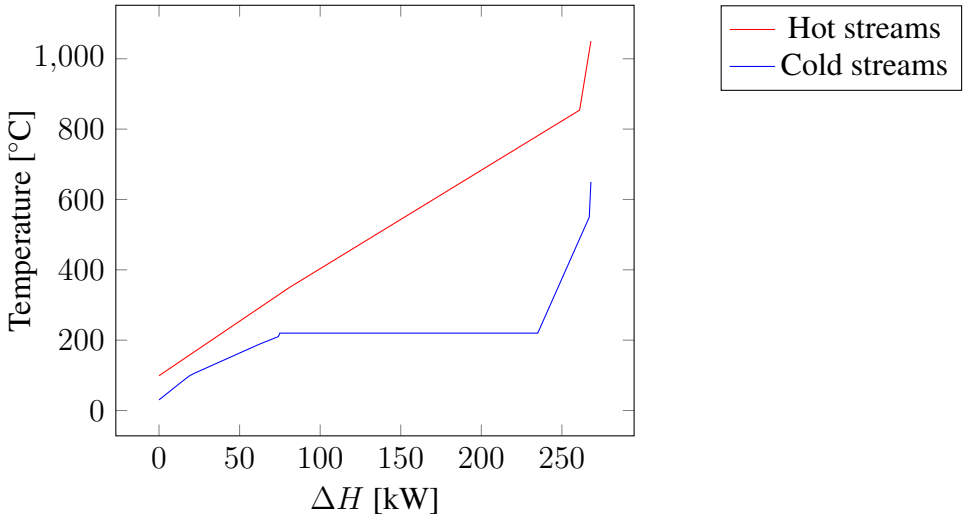

Figure H.3: The Composite Curves for the hot and cold streams included in the heat integration network, with steam production.

Appendix I

Equipment Size Calculations

This appendix gives the calculations used for equipment sizing. The outer size dimensions and weight values given in tables in this appendix are the same values as given in Table 4.13 in the main report. All the equipments are assumed to be made of stainless steel.

I.1 Pressure Vessel

The main equipments are modelled as pressure vessel. The calculation method to decide the dimension of the pressure vessel are different for the different equipments. However, for the weight and outer volume calculations the same method are used. In this section the method used for weight and volume calculation are given before more detailed information about how the dimensions of the equipments was calculated.

I.1.1 Weight Calculation

To calculate the wall thickness, t_w, of for the pressure vessel the equation below is used [40].

$$t_w = \frac{PD}{2SE - 1.2P} \tag{I.1.1}$$

where P is the design pressure, D is the vessel diameter, S is the allowable stress, and E is the welded-joint efficiency. The design pressure is set to 10% above operating pressure. The allowable stress value was found in Sinnott and Towler, Table 13.2 [40]. And the welded-joint efficiency was assumed to 1.

The surface area of the cylinder is calculated with equation I.1.2

$$A_s = \pi DH \tag{I.1.2}$$

where A_s is the surface ara and H is the vessel height.

The head of the pressure vessel is assumed to be elliptical head. The wall thickness is calculated from equation I.1.3 [40].

$$t_{w_{head}} = \frac{PD}{2SE - 0.2P} \tag{I.1.3}$$

The largest wall thickness is used for the pressure vessel shell and head.

The surface area of the head is:

$$A_h = 1.09D^2 \tag{I.1.4}$$

To calculate the weight of material in pressure vessel the equation below is used:

$$m = \rho_m t_w \left(A_s + 2A_h\right) \tag{I.1.5}$$

where m is the material weigh and ρ_m is the density of stainless steel given to 8000 kg/m^3 [47].

I.1.2 Outer Volume Calculation

To calculate the outer volume of the pressure vessel the height of the elliptical head needs to be found. Equation I.1.6 is used for the calculation [65].

$$H_h = 0.25D_v + 3S.F + t_w \tag{I.1.6}$$

where H_h is the outer height of the head and S.F is the straight flange set to $3t_w$.

The outer dimensions for the pressure vessel is then calculated from equations I.1.7 - I.1.8.

$$D_{outer} = D_v + 2t_w \tag{I.1.7}$$

$$H_{outer} = H + 2 * H_h \tag{I.1.8}$$

where D_{outer} is the outer diameter and H_{outer} is the total height/length of the vessel.

The outer volume of the pressure vessel is found from equation I.1.11.

$$V_{shell} = \frac{\pi D_{outer}^2 H_{outer}}{4} \tag{I.1.9}$$

$$V_{head} = \frac{\pi D_{outer}^3}{24} + \frac{\pi D_{outer}^2 S.F}{4} \tag{I.1.10}$$

$$V_{tot} = V_{shell} + V_{head} \tag{I.1.11}$$

I.1.3 Vertical Separators

The two separators to knock out water are modelled as vertical pressure vessels. The size is found with the use of the method given in Sinnott and Towler [40].

The settling velocity, u_s for the vertical pressure vessel is calculated with the use of equation I.1.12.

$$u_s = 0.07\sqrt{\left(\frac{\rho_L - \rho_v}{\rho_v}\right)} \tag{I.1.12}$$

where ρ_L is the liquid density and ρ_v is the vapour density.

The minimum diameter (D_v) the vessel can have to ensure that droplets will settle out can be calculated from Eq. I.1.13

$$D_v = \sqrt{\frac{4\dot{V}_v}{\pi u_s}} \tag{I.1.13}$$

where $\dot{V}_v$ is the gas/vapour volumetric flow.

To decide the height of the vessel the height of liquids (h_L) need to found. The hold-up time (t) is assumed to 10 min.

$$h_v = \frac{\dot{V}_L t}{A_c} = \frac{\dot{V}_L t}{0.25\pi D_v^2} \tag{I.1.14}$$

where $\dot{V}_L$ is the liquid volumetric flow, and A_c is the cross section area of the vessel.

The high of the pressure vessel, H, is calculated using equation I.1.15.

$$H = h_v + \frac{D_v}{2} + D_v + 0.4 \tag{I.1.15}$$

Values used for the calculation is taken from the HYSYS simulation. The values used for the calculation and the result is given in Table I.1.

Table I.1: Values used for size calculation of the separators and the result from the calculation.

	Separator syngas	Separator membrane
ρ_L [kg/m^3]	996.9	996.8
ρ_v [kg/m^3]	14.7	10.1
$\dot{V}_v$ [m^3/s]	7.8	0.8
$\dot{V}_L$ [m^3/s]	0.022	0.003
P [bar]	30.3	28.0
S [ksi]	15.0	20.0
D_{outer} [m]	4.3	1.5
H_{outer} [m]	10.3	4.7
V_{tot} [m^3]	137.1	8.1
m [tonne]	70.6	2.9

I.1.4 Horizontal Separators

The steam drum and three phase separator was modelled as horizontal pressure vessel and the size was calculated based on the residence time, as illustrated in this section. The size of the three phase separator was also calculated using the sizing method for a three phase separator with wire given by Monnery and Svercek [66]. The two different methods for size calculations gave the same result.

Assumptions made for calculations are listed below with values given in Table I.2.

- The ratio between the length of the vessel (L_v) and the vessel diameter (D_v) is set to a given value [40].
- The liquid volume in the vessel (V_L) is given as a fraction of the total vessel volume (V_{tot}).
- A residence time was assumed to a given value based on information from literature.

Table I.2: Overview of assumptions made when calculating the size of the three phase separators and the steam drum.

Assumption	Three phase separator	Steam drum
L_v/D_v [-]	4	4
V_{tot}/V_L [-]	3	2
Residence time [min]	20 [48]	5 [48]

The volume of the liquid phase (V_L) in the pressure vessel is calculated from equation I.1.16.

$$V_L = \dot{V} \cdot \tau \tag{I.1.16}$$

where $\dot{V}$ is the liquid flow and τ is the residence time.

For the three phase separator where there are two liquid streams the liquid flow is calculated with equation;

$$\dot{V} = \dot{m}_1 \rho_1 + \dot{m}_2 \rho_2 \tag{I.1.17}$$

where $\dot{m}_i$ is the mass flow of fluid i and ρ_i is the density of fluid i.

The total volume (V_{tot}) is calculated based on the given assumptions. The vessel diameter (D_v) is found from equation I.1.18.

$$D_v = \left(\frac{V_{tot}}{\pi} \right)^{(1/3)} \tag{I.1.18}$$

From the assumption the length of the pressure vessel is found as four times the vessel diameter.

The weight calculations was performed as given in section I.1.1 and the volume calculations as given in section I.1.2.

The values used for the calculation of the size for the three phase separators and the steam drum and the result is given in Table I.3.

Table I.3: Values used when calculating the size of the three phase separators and the steam drum, and the results.

	Three phase separator 1	Three phase separator 2	Three phase separator 3	Steam Drum
ρ_1 [kg/m^3]	996.8	996.7	996.6	840.4
$\dot{m}_1$ [tonne/h]	44.8	29.9	16.1	422.0
ρ_2 [kg/m^3]	763.1	753.0	759.0	-
$\dot{m}_2$ [tonne/h]	3.4	4.2	3.4	-
P [bar]	27.5	25.3	22.0	25.5
S [ksi]	20.0	20.0	20.0	12.9
D_{outer} [m]	2.6	2.3	1.9	3.1
H_{outer} [m]	11.5	10.3	8.6	13.8
V_{tot} [m^3]	54.1	39.0	22.7	88.5
m [tonne]	18.5	12.5	6.2	46.3

I.1.5 Pre-reformer, Autothermal Reformer and Water Gas Shift Reactor

The size of the pre-reformer, autothermal reformer and water gas shift reactor is calculated based on values for gas hourly space velocity (GHSV) found in literature (Table I.4). GHSV is defined as the gas feed volume in standard cubic feet per hour (SCFH), divided by the volume of catalyst, in cubic feet (ft^3).

Table I.4: GHSV values used for calculating reactor size.

Equipment	GHSV
Pre-reformer	5,000 [67]
Autothermal reformer	3,000 [48, 68]
Water gas shift reactor	8,000 [67]

The catalyst volume is then calculated from equation I.1.19.

$$V_c = \frac{\dot{V}}{GHSV} \tag{I.1.19}$$

where V_c is the catalyst volume and $\dot{V}$ is the gas feed flow.

It is assumed that the catalyst volume for the pre-reformer and WGS reactor counts for 80% of the total volume. And for the ATR the catalyst volume is assumed to 50% of the total volume. From this assumptions the total reactor volume can be calculated.

It is assumed that the ratio between the length of the reactor and the diameter is 1.5. The reactor diameter is then found from equation I.1.20.

$$D = \left(\frac{8V_{tot}}{3\pi}\right)^{1/3} \tag{I.1.20}$$

The weight and the outer volume of the reactors are calculated with the method given in section I.1.1 and I.1.2. Values used in the calculations and the result are given in Table I.5.

Table I.5: Values used in size calculation for the pre-reformer, autothermal reformer and the water gas shift reactor, and the results from the calculations.

	Pre-reformer	Autothermal reformer	Water gas shift reactor
$\dot{V}$ [MMSCFD]	211.4	421.2	73.6
P [bar]	31.9	31.4	28.6
S [ksi]	11.7	10.8	10.8
D_{outer} [m]	3.9	6.8	2.3
H_{outer} [m]	5.6	9.8	3.4
V_{tot} [m^3]	86.4	455.1	18.4
m [tonne]	62.2	307.7	11.2

I.1.6 Fischer-Tropsch Reactor and Heat Exchanged Reformer

When sizing the Ficher-Tropsch reactor and the heat exchanged reformer an existing design configuration was used as basis. Information about the existing design is given in Table I.6 [69].

Table I.6: Information about existing Fischer-Tropsch reactor design [69].

Parameter	Value
Shell length [m]	20
Shell diameter [m]	7
Tube length [m]	20
Tube diameter [m]	0.025
Number of tubes [-]	29,000

From these values the cross section area of the shell space around the tubes ($S_{empty,existing}$) for the existing reactor is found from equation I.1.21.

$$S_{empty,existing} = \frac{\pi D_{s,existing}^2}{4} - \frac{\pi D_{t,existing}^2}{4} = S_{s,existing} - S_{t,existing} \tag{I.1.21}$$

where $D_{s,existing}$ is the diameter of the shell, $D_{t,existing}$ is the diameter of the tube, $S_{s,existing}$ are the cross section area of the shell and $S_{t,existing}$ are the cross section area of the tube.

From this value a fraction of empty space (f) for the use in the design of the new reactors are calculated by;

$$f = \frac{S_{empty,existing}}{S_{t,existing}} \tag{I.1.22}$$

To decide the design of the reactors the total cross-section area of the tubes is needed. When the tube cross-section area (S_t) is calculated with equation I.1.23 the cross-section area of the shell (S_s) can be calculated from equation I.1.24.

$$S_t = \frac{\pi D_t^2 N}{4} \tag{I.1.23}$$

$$S_s = S_t(1 + f) \tag{I.1.24}$$

where D_t is the tube diameter and N is the total number of tubes in the reactor.

From the shell cross-section area the shell diameter (D_s) is found.

$$D_s = \sqrt{\frac{4S_s}{\pi}} \tag{I.1.25}$$

The total outer height of the FT reactor is decided to be 20 meter and for the HER it is decided to 18 meter. The calculation of the outer volume and weight of the reactor shell is calculated as given in section I.1.2 and I.1.1. However, as the elliptical heads are included in the total height, the cylinder high used for the volume and weight calculations are determined from equation I.1.26.

$$H = H_{tot} - (2(0.25D_s + 4t_w)) \tag{I.1.26}$$

For the weight calculation of the reactors it is important to remember the weight of the reactor tubes. The wall thickness of the tubes are calculated with the same formula used for a pressure vessel. The total weight (m_{tot}) for the reactor is calculated with equation I.1.27.

$$m_{tot} = \rho_m \left(t_{w,shell}(A_s + 2A_h) + t_{w,tube}A_t N\right) \tag{I.1.27}$$

where $t_{w,tube}$ is the wall thickness of the tube and A_t is the surface area of the tube.

The total weight including catalyst can be found. The catalyst weight is calculated based on the catalyst bulk density (ρ_b). The catalyst volume (V_c) is calculated from equation I.1.28, and the weight of the catalyst from equation I.1.29.

$$V_c = \frac{\pi D_t^2 N L_t}{4} \tag{I.1.28}$$

$$m_c = V_c \rho_b \tag{I.1.29}$$

where L_t is the length of the tubes.

Values used for the calculations and the results are given in Table I.7

Table I.7: Values used in size calculation for the Fischer-Trosch reactor and the Heat Exchanged reformer and the result from the calculation.

	FT reactor 1a/b	FT reactor 2a/b	FT reactor 3	HER
D_t [m]	0.025	0.025	0.025	0.1
N [-]	24,250	19,100	30,500	280
ρ_b [kg/m^3]	1,200	1,200	1,200	2,355.2
P_{shell} [bar]	25.3	25.3	25.3	31.4
S [ksi]	12.9	12.9	12.9	10.8
P_{tube} [bar]	29.7	29.7	29.7	31.4
D_{outer} [m]	6.6	5.8	7.4	2.9
V_{tot} [m^3]	593.4	475.2	733.0	111.9
$m_{\text{empty reactor}}$ [tonne]	367.9	290.5	460.3	96
$m_{\text{with catalyst}}$ [tonne]	539.3	425.5	675.9	148

I.2 Heat Exchangers

The heat transfer across a surface is described by

$$Q = U A \Delta T_m \tag{I.2.1}$$

where Q is the heat transferred per unit time, U is the overall heat transfer coefficient, A is the heat transfer area, and ΔT_m is the mean temperature difference.

To decide the heat transfer area needed for the heat exchangers equation I.2.1 was used. Temperatures and the heat transfer amount (Q) was taken from the HYSYS simulation. The overall heat transfer coefficient was found in Table 12.1 in Sinnott and Towler [40].

The mean temperature difference is calculated based on a true temperature different with the use of the logaritmic mean temperature (ΔT_{lm}). The temperature is then multiplied with a correction factor (F_t) as the heat exchangers is not true counter-current flow the [40].

$$\Delta T_m = F_t \Delta T_{lm} \tag{I.2.2}$$

The logarithmic mean temperature is calculated from equation I.2.3 [40].

$$\Delta T_{lm} = \frac{dT_1 - dT_2}{ln(dT_1/dT_2)} \tag{I.2.3}$$

$$dT_1 = T_{H,in} - T_{C,out} \tag{I.2.4}$$

$$dT_2 = (T_{H,out} - T_{C,in}) \tag{I.2.5}$$

$$\tag{I.2.6}$$

where H denotes the hot stream and C the cold stream.

The correction factor is given by [40];

$$F_t = \frac{\sqrt{(R^2+1)}ln\left[\frac{(1-S)}{(1-RS)}\right]}{(R-1)ln\left[\frac{2-S[R+1-\sqrt{(R^2+1)}]}{2-S[R+1+\sqrt{(R^2+1)}]}\right]} \tag{I.2.7}$$

where R and S are defined be equation I.2.8 and I.2.9.

$$R = \frac{T_{H,in} - T_{H,out}}{T_{C,out} - T_{C,in}} \tag{I.2.8}$$

$$S = \frac{T_{C,out} - T_{C,in}}{T_{H,in} - T_{C,in}} \tag{I.2.9}$$

The used values for the calculation and the calculated heat transfer area for the different heat exchangers are given in Table I.8.

Table I.8: The parameters used for the calculation of the heat transfer area for the heat exchangers and the result.

		ΔT_m [°C]	Q [MW]	U [W/m^2°C]	A [m^2]
Process-Process heat exchangers	E-101a	418.7	18.8	50	900
	E-101b	356.2	4.3	50	243
	E-103	564.0	27.3	50	967
	E-105	475.0	20.2	50	852
	E-109	35.3	0.6	100	163
	E-110	544.8	5.8	50	214
	E-116	398.7	31.3	50	1,570
Coolers	E-102	68.7	64.6	300	3,138
	E-104	68.4	45.6	300	2,222
	E-106	68.1	30.8	300	1,507
	E-108	118.0	22.1	300	624
	E-111	49.4	17.3	300	1,166
	E-112	57.4	22.1	300	1,282
	E-113	57.5	7.1	300	410
	E-114	65.7	14.8	300	752
	E-115	57.3	12.1	300	702
Steam cycle heat exchangers	E-117	198.2	67.4	100	3,402
	E-118	50.7	9.8	100	1,944
Steam production	E-119	175.7	159.7	300	3,030
	E-120	63.4	217.6	2,000	1,715
GasTurbine	E-GT1	306.6	24.8	100	807
	E-GT2	216.6	27.5	100	1,271
	E-GT3	146.4	34.4	100	2,347

I.3 Membranes

I.3.1 Air Membrane

The unit size of the air membrane given from the membrane data sheet is given in the table below.

Table I.9: Air membrane unit size information from membrane data sheet [43].

Dimension	Value
Length [m]	1.628
Width [m]	0.141
Height [m]	0.168
Weight [kg]	31.6

To simplify the calculations the membrane unit is assumed to have a cylindrical shape with the diameter as the largest value of the height and width. The volume of air membrane is the found from equation I.3.1.

$$V_{tot} = \frac{\pi D^2 L N}{4} \tag{I.3.1}$$

Where N is the number of units needed in the process. This value is calculated based on the air feed flow to the membrane, $\dot{n}_{\text{air feed}}$, and the capacity of one membrane unit ,$\dot{n}_{\text{air capacity}}$, according to equation I.3.2. For the air membrane used in the process the air feed capacity of one unit is given to 2.7 kmol/h.

$$N = \frac{\dot{n}_{\text{air feed}}}{\dot{n}_{\text{air capacity}}} \tag{I.3.2}$$

The total weight of the air membrane is found from equation I.3.3.

$$m_{tot} = N m_{unit} \tag{I.3.3}$$

where m_{unit} is the weight of one membrane unit.

The number of membrane units needed in the process is given in Table I.10 together with the total volume and weight for all the membrane units.

Table I.10: Overview of the total number of membrane units needed together with the total volume and weight of all the units.

Parameter	Value
Number of membrane units [-]	6,700
Total volume [m^3]	241.8
Total weight [tonne]	211.7

I.3.2 Hydrogen Selective Carbon Membrane

The membrane module is design as a pressure vessel with the ceramic tubes packed inside. The packing density for modules containing capillaries are about 600-1,200 m^2/m^3 [70]. For the calculation a packing density of 900 m^2/m^3 is assumed. It is also assumed that the membrane module diameter is 0.3 m [71]. As the membrane module is a pressure vessel the wall thickness is design according to operating temperature and pressure. If the diameter is increased the wall thickness needed is increased, this is also a reason for keeping the module diameter small.

When the volume of the module (V_{module}) is calculated with equation I.3.4 the total membrane area for the module ($A_{m,module}$) can be found with the use of packing density (a) according to equation I.3.5.

$$V_{module} = \frac{\pi D_{module}^2 L}{4} \tag{I.3.4}$$

$$A_{m,module} = aV_{module} \tag{I.3.5}$$

The total number of tubes (N_t) in each membrane module is given from equation I.3.6.

$$N_t = \frac{A_{m,module}}{A_{m,\text{one tube}}} \tag{I.3.6}$$

In the process the total number of ceramic membrane tubes needed are 817,520. The number of membrane units needed in the process (N) is then found with equation I.3.7.

$$N = \frac{N_{t,tot}}{N_t} \tag{I.3.7}$$

The outer volume of the membranes and the weight of the module, without the ceramic tubes are calculated as described in section I.1.2 and I.1.1. The values used for the calculation and the results are given in Table I.11.

Table I.11: Values used when calculating the size of the hydrogen selective carbon membrane and the results.

Parameter	Value
$N_{t,tot}$ [-]	817,520
P [bar]	287.1
S [ksi]	20.0
$D_{outer,unit}$ [m]	0.31
$H_{outer,unit}$ [m]	1.2
V_{tot} [m^3]	13.24
$m_{\text{tot,module vessel}}$ [tonne]	5.2

Appendix J

Cost Calculations

This appendix will give information about the equipment cost calculations and the calculation of the total investment cost of the plant. It is assumed that all the equipment is made by stainless steel.

J.1 Equipment Cost

The purchased equipment cost (C_e) for most of the equipments is calculated with the use of equation J.1.1 [40]. For the Fischer-Tropsch reactor several methods was used for cost estimation. To calculate the cost of the heat exchanged reformer method one given for FT cost calculations was used. However, the cost was multiplied with a factor of 2, due to more complex material design than for a normal heat exchanger.

$$C_e = a + bS^n \tag{J.1.1}$$

where a and b are constant values, n is the exponent for the type of equipment and S is the size parameter. The value used a, b, and c are found in Sinnott and Towler [40] and are listed in Table J.1. The cost calculated with the use of these correlation is given in 2007 basis.

Table J.1: The constant values used in the cost correlation for different equipments.

Equipment	Size unit	a	b	n
Heat exchangers	heat transfer area, m^2	24,000	46	1.2
Compressors[1]	driver power, kW	8,400	3,100	0.6
Vertical Pressure vessel	shell mass, kg	15,000	68	0.85
Horizontal Pressure vessel	shell mass, kg	11,000	63	0.85

1 - Cost basis year is 2006

The separators, pre-reformer, WGS reactor, and ATR are modelled as vertical pressure vessels. While the three phase separator are modelled as horizontal pressure vessels. The cost of the

ATR is multiplied with a factor of 2 as it contains a burner and other materials and to use a pressure vessel model underestimates the cost.

The purchased equipment cost calculated for heat exchangers and compressors are given for equipments made of carbon steel. The installed cost of the equipments is then calculated with the use of equation J.1.2. For pressure vessel the purchase equipment cost is calculated for equipments made of stainless steel and the installed cost is therefore calculated from equation J.1.3.

$$C = \sum_{i=1}^{n} C_{e,i,CS} \left[(1 + f_p)f_m + (f_{er} + f_{el} + f_i + f_l)\right] \tag{J.1.2}$$

$$C = \sum_{i=1}^{n} C_{e,i,A} \left[(1 + f_p) + (f_{er} + f_{el} + f_i + f_l)/f_m\right] \tag{J.1.3}$$

where $C_{e,i,CS}$ is the purchased equipment cost of equipment i in carbon steel, while $C_{e,i,A}$ is the cost for equipment i in alloy.

Explanation and values for the different f-factors are given in Table J.2. For this process installations factors like civil, and structure and buildings are not included as it is assumed to be a part of the ship.

Table J.2: Installed equipment cost calculation factors.

Parameter	Estimates	Value
f_p	Piping	0.8
f_m	Material factor, Stailness steel 304	1.3
f_{er}	Equipment erection	0.3
f_{el}	Electrical	0.2
f_i	Instrumentation and control	0.3
f_l	Lagging and paint	0.1

Cost calculations of the gas turbine was based on price of an existing gas turbine. The cost is related to the capacity according to equation J.1.4.

$$C_2 = C_1 \left(\frac{S_2}{S_1}\right)^n \tag{J.1.4}$$

where C_2 is the ISBL capital cost of the plant with capacity S_2 and C_1 is the ISBL capital cost of the plant with capacity S_1. The inside battery limits (ISBL) investment is the cost of the plant itself including the cost of procuring and installing. The exponent n has usually a value in the range of 0.4-0.9, with a value of 0.7 as a good estimate for this process [40].

For the gas turbine two different values of existing equipment was used. The values used and the result are given in Table J.3.

Table J.3: Values used for cost calculations for the gas turbine and the results.

	Existing 1[1] [72]	Existing 2[2] [73]
C_1 [million$]	32.2	34.6
S_1 [MW]	173.7	144
S_2 [MW]	179.0	179.0
C_2 [million$]	32.9	40.2
$C_{2,2014}$ [million$]	32.9	45.6

1 - Existing cost at 2014 basis

2 - Existing cost at 2008 basis

In the process it is assumed that the pre-heat of the natural gas is done by heat exchanging with the effluent gas from the gas turbine. It is assumed that these exchangers are included in the gas turbine cost. The gas turbine cost reported in the main report is the average value calculated from the existing gas turbines with the cost for the heat exchangers.

At last the cost is corrected for inflation, with the use of indexes according to equation J.1.5. In this theses all the cost estimates are given at 2014 basis.

$$C_{2014} = C_i \frac{I_{2014}}{I_i} \tag{J.1.5}$$

where C_i is the cost at year i, $I_{2014}$is the cost index in year 2014, and I_i is the cost index for year i. In this master thesis the Nelson-Farrar Refinery Inflation Indexes (NF-Indexes) are used. A list of the used values are given in Table J.4.

Table J.4: Nelson-Farrar Refinery Inflation Indexes used for cost calculations from 2003 [74], 2006 [74], 2007 [40] and 2014 [75].

Year	NF-Index
1990	1,225.7
2003	1,710.4
2006	2,008.1
2007	2,059.1
2014	2,553.7

The cost of the air membrane was calculated based on information given from Air Products [34]. The cost of one membrane unit is given to 2,800 $. For the carbon membrane the cost per membrane area was assumed to 250 $/m^2 [71]. The installation factor for the membrane are assumed to be 2.

J.1.1 Fischer-Tropsch reactor

The cost calculation for the Fischer-Tropsch reactor was performed with the use of several different methods. In this section the different methods will be explained and the correlations used are given.

J.1.1.1 Method 1 - Heat Exchanger

The first method used for calculating the FT reactor cost was to use the total heat integration area of the tubes and use cost correlations for a heat exchanger. The correlations used are given in equation J.1.6 to J.1.10 [48].

$$C_e = 1.218 f_d f_m f_p C_b \tag{J.1.6}$$
$$f_d = exp[-1.1156 + 0.0906 ln(A)] \tag{J.1.7}$$
$$f_m = 0.8603 + 0.23296 ln(A) \tag{J.1.8}$$
$$f_p = 1.0305 + 0.07140 ln(A) \tag{J.1.9}$$
$$C_b = exp[8.821 - 0.30863 ln(A) + 0.0681 ln(A)^2] \tag{J.1.10}$$

where A is the heat transfer area.

The cost year basis for this calculation was 1985 with chemical engineering plant cost index basis. The values used is given in Table J.5.

Table J.5: The chemical engineering plant cost index used for cost calculations from 1985 and 2014.

Year	Chemical Engineering Plant Cost Index (CEPCI)
1985	325
2014	580

J.1.1.2 Method 2 - Heat Exchanger U-tube

The second method used was the correlation for an U-tube shell and tube heat exchanger given in equation J.1.11 [40].

$$C_e = 24,000 + 24 S^{1.2} \tag{J.1.11}$$

where S is the heat transfer area.

The cost basis is year 2007, and the NF-indexes given in Table J.4 is used to calculate the 2014 cost.

J.1.1.3 Method 3 - Pressure vessel with tubes

In method 3 the reactor are assumed to be a pressure vessel with tubes inside. The cost of the tubes are calculated with two different methods; 3a and 3b.

The pressure vessel cost is calculated with the correlation given in equation J.1.12 [40].

$$C_e = 15,000 + 68S^{0.85} \tag{J.1.12}$$

where S is the shell mass.

The cost basis is year 2007, and the NF-indexes given in Table J.4 is used to calculate the 2014 cost.

J.1.1.3.1 Method 3a - Tube cost by length In this method the cost of the heat exchanger tubes was found from a correlation in literature [49]. For a tube with the diameter of 0.025 the price was found to approximately 0.5 $/feet of tube (1991 price). The total length of tube is calculated with equation J.1.13.

$$L = L_t N_t \tag{J.1.13}$$

where L_t is the length of one tube and N_t is the total number of tubes in the reactor. The indexes used to get cost at 2014 are given in Table J.4.

J.1.1.3.2 Method 3b - Tube cost by weight In this method the cost of the heat exchanger tubes was based on mass of tube needed. A cost value of the tubes was found to 4,000 $/tonne [50].

J.1.1.4 Method 4 - Material cost

The last cost method evaluated for the FT reactor was the simplest calculation only looking at the total mass needed in for the reactor. Two different steel prices was found and used in the evaluation; 2,762 $/tonne [51] and 2,899 $/tonne [52]

J.1.2 Catalyst

The total cost given for the different reactor are including the catalyst cost. For all the reactors the catalyst price is assumed to 100 NOK/liter. For the Pre-reformer, the ATR and the WGR reactor the catalyst void fraction is assumed to 0.4. For the FT reactor the void fraction is 0.4 and for the HER it is 0.545. Table J.6 gives the catalyst volume and the total cost of the catalyst. The currency is given to 1 $ = 7.9 NOK.

Table J.6: Catalyst volume and cost for the different reactors.

Used in	Catalyst volume [m^3]	C_{2014} [million/$]
Pre-reformer	49.9	0.25
ATR	165.7	0.84
WGS	10.8	0.05
HER	22.0	0.07
FT reactor	690.4	3.5

J.2 Total investment cost

The total investment cost is the sum of the total fixed capital cost and the working capital. Working capital is the cost needed to start up and run the plant before it produces it own income and is set to 15% of the fixed investment cost [40]. The fixed capital cost can be found from equation J.2.1.

$$C_{fc} = C(1 + OS)(1 + D\&E + X) \tag{J.2.1}$$

where C_{fc} are the fixed capital cost, C is the ISBL cost, OS is the offsite with a value of 0.3, $D\&E$ is the design and engineering with a value of 0.3 and X is the contingency with a value of 0.1 [40].

Appendix K

Maximum Radial Reactor Temperature

The radial temperature profile in the reactor tubes can be explained with a second order polynomial:

$$T(r) = a + br + cr^2 \tag{K.0.1}$$

The boundary conditions for the polynomial are given in equation K.0.2-K.0.3.

$$\text{Boundary condition 1:} \qquad r = 0 \quad \left(\frac{dT}{dr}\right)_0 = 0 \tag{K.0.2}$$

$$\text{Boundary condition 2:} \qquad r = R \quad \left(\frac{dT}{dr}\right)_R = \frac{U'(T_R - T_{cm})}{-\lambda} \tag{K.0.3}$$

where U' is the heat transfer through the wall, T_{cw} is the temperature of the cooling water, T_R is the temperature at the wall, R is the tube radius, and λ is the effective radial conductivity.

From these equation parameter b and c are found.

$$b = 0 \tag{K.0.4}$$

$$c = \frac{U'(T_R - T_{cw})}{-2R\lambda} \tag{K.0.5}$$

From boundary condition 1, it is also found that $T(0) = a = T_{max}$. This gives the polynomial given below:

$$T(r) = T_{max} + \frac{U'(T_R - T_{cw})}{-2R\lambda} r^2 \tag{K.0.6}$$

The average radial temperature is define as given in equation K.0.7.

$$T_{average} = T_R + \frac{T_{max} - T_R}{2} \tag{K.0.7}$$

Solving equation K.0.6 for $r = R$ with insertion of expression found for T_R from equation K.0.7 gives:

$$T_{max} = T_{average} + \frac{T_{average} - T_{cw}}{\frac{8\lambda}{UD}} \tag{K.0.8}$$

Where: (K.0.9)

$$\frac{1}{U} = \frac{D}{8\lambda} + \frac{1}{U'} \tag{K.0.10}$$